2017

Role of mitochondrial beta-oxidation in ethanol response: A candidate gene study using Caenorhabditis elegans

Harini Pallikarana Tirumala
Virginia Commonwealth University

Role of mitochondrial beta-oxidation in ethanol response: A candidate gene study using *Caenorhabditis elegans*

A thesis submitted in partial fulfillment of the requirements for the degree of Master of Science in Human Genetics at Virginia Commonwealth University.

By

Harini Pallikarana Tirumala
Master of Science in DNA Profiling from University of Central Lancashire, UK
2012

Directed by Jill C. Bettinger, Ph.D.,
Associate Professor of Pharmacology and Toxicology

Virginia Commonwealth University
Richmond, Virginia
June, 2017

ACKNOWLEDGEMENTS

I would like to thank my thesis advisor, Dr. Jill Bettinger for helping me grow as a scientist and for encouraging me to think out of the box. She has been immensely supportive during the course of my research project and has been a great mentor to me. I would like to thank my committee members, Dr. Andrew Davies, Dr. Laura Mathies and Dr. Rita Shiang. Their valuable inputs during committee meetings have helped me formulate and shape this project better. I would also like to thank all the members of the Davies-Bettinger lab, particularly Gina Blackwell, who has been a pillar of support from my first day in the lab and has patiently answered the umpteen questions I had. I would like to extend thanks to all the Human Genetics students, particularly Saranya Regupathy, Megan Hept and Javeria Aijaz for their support and confidence in me.

I would also like to thank all my family members and friends for their support during these two years. To my parents who always believed in me and gave me the confidence to pursue my dreams. A final thank you, to my husband, Swaminathan Balasubramanian, for listening to me talk endlessly about my worms and, for his constant love and support.

TABLE OF CONTENTS

LIST OF TABLES

LIST OF FIGURES

LIST OF ABBREVIATIONS AND ACRONYMS

AA	Arachidonic acid
ACAD/ACDH	Acyl CoA dehydrogenase
ACAT	Acetyl-CoA acetyltransferase
ACS	Acyl CoA synthase
ACSF	Acyl CoA synthetase family member
ACSL	Acyl CoA synthetase, long chain
ACSM	Acyl CoA synthetase, medium chain
ACSS	Acyl CoA synthetase, short chain
ACOX	Acyl CoA oxidase
AFT	Acute Functional Tolerance
AGPAT	Acylglycerolphosphate acyltransferase
ALD	Alcoholic liver disease
ATP	Adenosine triphosphate
AUD	Alcohol Use Disorder
BAC	Blood Alcohol Concentration
BLAST	Basic Local Alignment Search Tool
CACT	Carnitine-acylcarnitine translocase
CGC	*Caenorhabditis* Genetics Center
CoA	Coenzyme A
CPT	Carnitine palmitoyl transferase
DAG	Diacyl glycerol
DIOPT	DRSC Integrative Ortholog Prediction Tool
dNTP	deoxy Nucleoside Triphosphate

DRSC	*Drosophila* RNAi Screening Center
DSM	Diagnostic and Statistical Manual of Mental Disorders
ECH	Enoyl CoA hydratase
ECHS	Short-chain enoyl CoA hydratase
EHHADH	Enoyl-CoA hydratase and 3-hydroxyacyl CoA dehydrogenase
EMS	Ethyl methanesulfonate
EPA	Eicasapentanoic Acid
ER	Endoplasmic Reticulum
ETC	Electron Transport Chain
FA	Fatty acids
FA-CoA	Fatty acyl CoA
FAD	Flavin adenine dinucleotide
FDA	Food and Drug Administration
FFA	Free fatty acids
GABA	Gamma- aminobutyric acid
gf	Gain-of-function
GFP	Green fluorescent protein
GPAT	Glycerol-3-phosphate acyltransferase
GTP	Guanosine triphosphate
HACD/ HADH	Hydroxy acyl CoA dehydrogenase
HADHA	Hydroxy acyl CoA dehydrogenase alpha-subunit
HADHB	Hydroxy acyl CoA dehydrogenase beta-subunit
IPTG	Isopropyl β-D-1-thiogalactopyranoside
iVD	Isovaleryl-CoA dehydrogenase

KAT	Keto acyl CoA thiolase
Kb	kilobyte
KEGG	Kyoto Encyclopedia of Genes and Genomes
LB	Lysogeny Broth
LCAD	Long chain acyl CoA dehydrogenase
LCHAD	Long-chain hydroxy acyl CoA dehydrogenase
LC-PUFA	Long chain polyunsaturated fatty acid
LDTg	Laterodorsal tegmental nucleus
lf	Loss-of-function
LKAT	Long-chain ketoacyl-CoA thiolase
LR	Level of Response
LYHD	Long-chain enoyl CoA hydratase
MCAD	Medium chain acyl CoA dehydrogenase
MCHAD	Medium-chain L-3-hydroxyacyl-CoA dehydrogenase
MKAT	Medium-chain 3-ketoacyl-CoA thiolases
MMP	Million Mutation Project
MOM	Mitochondria Outer Membrane
MTP	Mitochondrial Trifunctional Protein
nAChR	Nicotinic acetylcholine receptor
NAD	Nicotinamide adenine dinucleotide
NCBI	National Center for Biotechnology Information
NGM	Nematode growth media
NIAAA	National Institute on Alcohol Abuse and Alcoholism
NPY	Neuropeptide Y
NSDUH	National Survey on Drug Use and Health

PUFA	Polyunsaturated fatty acid
SCAD	Short chain acyl CoA dehydrogenase
SCHAD	Short-chain L-3-hydroxyacyl-CoA dehydrogenase
SHYD	Short-chain enoyl-CoA hydratase
SKAT	Short-chain 3-ketoacyl-CoA thiolases
SNP	Single Nucleotide Polymorphism
SWPCR	Single worm PCR
RNAi	RNA interference
ROS	Reactive oxygen species
TAG	Triacyl glycerol
TBE	Tris/Borate/EDTA
TCA	Tricarboxylic acid
VDAC	Voltage dependent anion channel
vLCAD	Very long chain acyl CoA dehydrogenase
WT	Wildtype

Clarification of Contributions

I have been fortunate to have the help of many people in the course of my thesis work. All work except that described below and cited in the text was exclusively my own.

Backcrossing of the *ech-1.2, cpt-4* and *acs-3* lf mutants to 6x and confirmation of genotypes by PCR followed by restriction digestion and Sanger sequencing was performed by Brian Patchett.

Gina Blackwell performed the final round of backcrossing for acs-4, acdh-1 and T02G5.4 lf mutants from 4x to 6x and confirmation of genotypes by PCR.

Abstract

ROLE OF MITOCHONDRIAL BETA-OXIDATION IN ETHANOL RESPONSE: A CANDIDATE GENE STUDY USING *CAENORHABDITIS ELEGANS*

By Harini Pallikarana Tirumala
Master of Science in DNA Profiling from University of Central Lancashire, UK 2012

Directed by Jill C. Bettinger, Ph.D., Professor of Pharmacology and Toxicology

Virginia Commonwealth University, 2017

Alcohol use disorder (AUD) is the fourth leading cause of preventable death in the United States, and the fifth leading risk factor for premature death and disability, globally. There are currently very few treatment options for AUD and there is a need for effective preventive and treatment strategies for this condition. AUD risk has a significant hereditary component, with the contribution of genetic factors being estimated to be about 50%. The Davies-Bettinger laboratory uses *C. elegans* as a model organism to study the contribution of genetic factors in modulating neuronal responses to ethanol. In this project, we examined the role of mitochondrial beta-oxidation of fatty acids (FA) in altering ethanol responses using loss-of-function (lf) mutants and RNAi-mediated knockdown of specific genes in this pathway. We tested a total of 34 genes and found that lf in 13 genes significantly affected ethanol response phenotypes. We conclude that mitochondrial beta-oxidation of FA is essential for ethanol response behavior in *C. elegans.* Further experiments need to be conducted to dissect the specific contribution of various components of mitochondrial beta-oxidation in modifying the neuronal responses to ethanol.

1. INTRODUCTION

1.1. Alcoholism – National and Global Impact

"First you take a drink, then the drink takes a drink, then the drink takes you."

~ F. Scott Fitzgerald

Alcohol is ranked among the top ten most addictive substances in the world (Nutt et al., 2007). The National Institute on Alcohol Abuse and Alcoholism (NIAAA) defines AUD as 'problem drinking that becomes severe'. Medical diagnosis of AUD requires an individual to meet at least 2 out of the 11 criteria outlined in the Diagnostic and Statistical Manual of Mental Disorders (DSM), within the same 12-month period. AUD can be classified as mild, moderate or severe based on the number of criteria fulfilled.

According to the 2015 National Survey on Drug Use and Health (NSDUH), 15.1 million adults (18 years and older) in the United States had AUD and the financial burden due to alcohol misuse in the US in 2010 was $249 billion. While it is estimated that alcohol claims about 88,000 lives every year in the US, in 2014 alone, alcohol-impaired driving fatalities accounted for 31% of overall driving fatalities. With such a profound and significant impact on the mortality and economy of the country, alcohol is the fourth leading preventable cause of death in the United States. Statistics around the world reflect a similar scenario with alcohol misuse being ranked as the fifth leading risk factor for premature death and disability, globally (*Alcohol facts and*

statistics, 2017). Specifically, about 25% of total deaths in the 20-39 years age group are alcohol-attributable (*WHO alcohol fact sheet,* 2015).

Given the huge impact of alcohol abuse on individual and public health, global economy and productivity, there is a need for effective prognostic, preventive and therapeutic strategies to treat AUD. At present, the treatment for AUD is largely focused on therapeutic counseling and other forms of behavioral therapy. There are currently only three FDA approved drugs for treating individuals suffering from AUD: Disulfiram, Naltrexone and Acamprosate (Krishnan-Sarin et al., 2008). It is therefore important to invest in alcohol research to identify effective prevention, management and treatment options to curb the increasing rate of mortality associated with this debilitating condition.

1.2. Genetics of alcoholism

AUD is a multifactorial condition influenced by both environmental and genetic factors, like most psychiatric and behavioral disorders. The contribution of genetic factors to AUD risk has been estimated, by numerous family and twin studies, to be in the range of 40-60% (Palmer et al., 2012), with the most recent best-fit estimate being 49% (Verhulst et al., 2015). This is supported by a multitude of molecular genetic studies that have identified several genetic variants in candidate genes, which significantly influence the risk of developing AUD. However, all of these variants put together only account for a very small percentage of the genetic variance determined by the family studies. Thus it is clear that there are multiple genes and genetic interactions

that affect risk for AUD. This makes it a complex genetic condition to study, even without taking into consideration the role of social and environmental factors (Edenberg & Foroud, 2013).

Among the various negative effects of alcohol on human health, two of the major areas of AUD research are physiological effects of alcohol metabolism and the (direct) effects of alcohol on the brain and nervous system. Alcohol dehydrogenase subunit beta (ADH1B) and aldehyde dehydrogenase 2 (ALDH2) are two enzymes are involved in ethanol metabolism. ADH1B catalyzes the conversion of ethanol to acetaldehyde and the mitochondrial ALDH2 is involved in the second step of this metabolism converting acetaldehyde to acetate. Among genes that catalyze alcohol metabolism (primarily in the liver), variants in *ADH1B* and *ALDH2* are the most significantly associated with risk of AUD (Tawa et al., 2016). Reactions catalyzed by both these genes utilize NAD^+ to produce NADH, altering the $NADH/NAD^+$ ratio within the cell. This increased $NADH/NAD^+$ ratio inhibits mitochondrial beta-oxidation of FA, as it is an allosteric regulator of this pathway. Most of the acetate produced from the second reaction enters the circulation and is metabolized to CO_2 in heart, brain and skeletal muscle cells. Acetate is also metabolized to acetyl CoA, which then enters metabolic pathways such as ketone body production, amino acid and FA synthesis. Acetate produced from acetaldehyde also enters the brain. Though the brain primarily derives its energy from oxidation of glucose, the availability of acetate, which requires fewer steps for oxidation and energy production,

results in increased acetate uptake and decreased glucose utilization in the brain.

Alcohol also exerts a wide range of effects on the central nervous system (CNS) which can cause effects that include an increase in aggression, reduced inhibition and impaired memory as it affects multiple pathways and regions in the brain (M. Davies, 2003). The most prominent among these are neurotransmitter-signaling pathways that affect the inhibitory and excitatory systems in the brain (McIntosh & Chick, 2004). Genes in various neurotransmitter-signaling pathways (particularly receptors) have been implicated in AUD risk development. Some of the most widely researched ones in this group include the γ-Aminobutyric acid (GABA) receptors, genes in the serotonin, dopamine and glutamate pathways like the serotonin-transporter-linked polymorphic region (*5'-HTTLPR*), dopamine receptor D_2 (*DRD2*) (Banerjee, 2014) and glutamate metabotropic receptor 8 (*GRM8*) respectively (Morozova et al., 2014). Despite extensive research, little is known about the exact mechanisms of alcohol's action on the nervous system.

1.3. Neuronal response to alcohol

AUD is a heterogeneous condition with a spectrum of clinical manifestations, and several alcoholism typologies have been proposed to group together affected individuals with a similar clinical course, in order to better predict their response to treatment (Bogenschutz et al., 2009). Identifying genetic factors associated with the condition is complex, probably due to this heterogeneous

nature of AUD and the symptom-based diagnosis used (DSM criteria). Therefore, scientists identified certain endophenotypes that can be used as biomarkers and can be linked to specific genetic factors that could play a role in development of AUD (Gottesman & Shields, 1973). An endophenotype is any trait that is related to or part of a condition and might be influenced by a small number of genes. It can be used to bridge the gap between biology of the condition and its symptoms. In psychiatry research, a biomarker has to fulfill the following criteria to be considered an endophenotype: it must segregate with illness in the population and within families, must be heritable, must not be state-dependent, must be present at a higher rate within affected families than in the population, must be reliably measurable and specific to the illness.

There are several established endophenotypes of AUD (Eng et al., 2005; Salvatore et al., 2015). Level of response to alcohol is a reproducible and well-characterized endophenotype, and it is commonly used in animal models of alcohol research. Level of response can be defined as the ‘intensity of response to alcohol at a specific Blood Alcohol Concentration (BAC)’ (Schuckit et al., 2011). It has been consistently shown that low level of response (LR) to alcohol is a strong predictor of increased risk for AUD in the future and that it is to an extent genetically influenced (Schuckit, 1980; Schuckit, 1994). LR constitutes at least two components that are routinely used in the lab, namely initial sensitivity (which refers to the level of intoxication that appears soon after ethanol administration, when blood ethanol levels are rising) and acute functional tolerance (AFT, the

tolerance/adaptation of brain function developed within a single drinking session, recorded at an equivalent concentration of alcohol on the declining phase BAC relative to the rising phase BAC at initial sensitivity). These two components have been successfully used to study the impact of genetic factors on AUD in various invertebrate and vertebrate models (Engleman et al., 2016; Morozova et al., 2014; Ponomarev & Crabbe, 2002).

1.3.1. Using *C. elegans* to study the molecular basis of neuronal response to alcohol

Caenorhabditis elegans is a soil-dwelling, free-living nematode that has been used as a model for research since early 1960s. Being the first multicellular organism whose whole genome was sequenced, *C. elegans* is currently being extensively used in research areas such as neuronal development, molecular biology, genetics and developmental biology. Features like the ability to self-fertilize (hermaphrodites) and mate with males, large brood size, short life cycle, relatively small genome size (100.2Mb) and ease of genetic manipulation (mutagenesis, RNA interference) make it an ideal model organism for genetic studies. The primary reason for using *C. elegans* in neuronal research is that its nervous system is simple but one of the most extensively characterized among multicellular organisms, with a total of 302 neurons (in the adult hermaphrodite). Despite its small size, the *C. elegans* nervous system is complex and shares most of the mammalian neurotransmitters, receptors and their molecular components. Among them are serotonin, GABA, glutamate, dopamine and acetylcholine. Also, the basic structural organization of neuron subtypes into sensory neurons, interneurons,

and motor neurons is conserved between humans and *C. elegans*. The entire wiring of neural circuits or the connectome of *C. elegans* was mapped by John G. White in 1986, and this opened up the possibility of identifying the functions of each individual neuron and its contribution to the nervous system. *C. elegans* also exhibits complex behavioral traits (like chemo- and mechanosensation, thermotaxis and avoidance of noxious stimuli) and behavioral plasticity which makes it a useful model for neurobiology (Hobert, 2003).

Most behavioral studies in *C. elegans* utilize the change in locomotion pattern in response to stimuli, as a measurable phenotype. Worms move by undulatory propulsion; waves formed by the contraction and relaxation of dorsal and ventral longitudinal body muscles travel along the length of the body and allow forward propulsion (de Bono & Maricq, 2005). Motor behavior is a trait that is predominantly under the control of the nervous system. Therefore, effects on the nervous system are often displayed through changes in motor behavior.

Neuronal responses to alcohol appear to be conserved in some invertebrates including *C. elegans* (McIntire, 2005). Moreover, the intoxicating effects of ethanol in *C. elegans* occur at similar concentrations as in mammals, which make it an excellent model to study the effect of alcohol on the nervous system. Behavioral responses to ethanol in humans include loss of social inhibition and lack of coordination. Acute exogenous exposure to ethanol also results in behavioral changes in *C. elegans* and these effects were found to

be dose-dependent and reversible (A. Davies et al., 2003a). One such behavioral response to alcohol in *C. elegans* is the development of acute tolerance, a component of level of response. As is observed in vertebrate systems (Crabbe et al., 2013; Erwin et al., 2000; LeBlanc et al., 1975; Ritzmann & Tabakoff, 1976), including humans (Hiltunena et al., 2000; Kaplan et al., 1985), the level of response to ethanol in *C. elegans* involves development of AFT shortly after ethanol administration (A. Davies et al., 2004).

To dissect the genetic contribution to ethanol response behavior, which reflects risk for AUD, researchers have exploited this conserved behavioral effect in *C. elegans*. A. Davies et al., (2003b) conducted genetic screens to identify mutants with reduced sensitivity to ethanol and observed that exogenously applied ethanol modifies locomotion and egg-laying behavior in *C. elegans.* Exposing the worms to short continuous doses of ethanol, they saw that it produced reversible and dose-dependent decrease in speed of locomotion and amplitude of body bends during locomotion. Level of response to alcohol in *C. elegans* is typically measured by change in locomotion speed of the worms at different time points after acute exposure to ethanol. There is an initial depression in locomotion speed that is accompanied by fewer body bends (initial sensitivity) immediately after exposure. The speed of locomotion increases over the time course of the assay, despite constant (or in some instances, increased) internal concentration of ethanol, which supports previous findings that this increase in speed over time is due to a neuronal adaptation to the physiological effects of ethanol and not due to decrease in

the internal ethanol concentration (Davies et al., 2004). This increase in locomotion speed after the initial depression is termed AFT. It is important to note that these two components of LR, initial sensitivity and AFT have been found to be genetically separable (A. Davies et al., 2015).

1.4. Background research for current project

The Davies-Bettinger lab has identified several genes that modulate neuronal responses to ethanol in *C. elegans* including a calcium-activated potassium channel, Slowpoke protein 1 (*slo-1*) (A. Davies et al., 2003b), *eat-6* which encodes the alpha-subunit of the Na^+/K^+ ATPase (Hawkins et al., 2015), a neuropeptide Y (NPY) receptor-like protein (*npr-1*) (A. Davies et al., 2004) and a Ras-family GTPase (*rab-3*) (Kapfhamer et al., 2008). An area of interest to the lab is the role of the lipid environment in modulation of ethanol responses. Using an unbiased genetic screen, they determined that *lips-7* and *ctbp-1* (C-terminal binding protein 1), a transcriptional regulator of *lips-7* affect AFT to ethanol. In another study looking at the role of *ctbp-1* on lifespan in *C. elegans*, Chen et al., (2008) observed that *ctbp-1* mutants had altered triacylglycerol (TAG) levels. Since TAGs are components of the lipid membrane, Bettinger et al., (2012) tested the effect of lipid membrane environment on AFT by depleting cholesterol, another important component of the lipid membrane, in the media on which worms are grown. They observed that worms grown on cholesterol-depleted media displayed suppression of AFT development, which suggested that the composition and structure of the lipid membrane is important for normal development of AFT.

Additional studies in the lab, examining another component of the lipid environment, have shown that eicasapentanoic acid (EPA), an omega-3 long-chain polyunsaturated fatty acid (LC-PUFA), is required for development of AFT in *C. elegans* and dietary supplementation of EPA restored WT AFT in EPA-deficient mutants. Also, supplementation of EPA enhanced AFT significantly in N2 worms while the basal speeds remained unchanged implying that LC-PUFAs have an important role in regulating response to ethanol (Raabe et al., 2014).

In an effort to identify genes involved in the modulation of ethanol responses in *C. elegans*, Dr. Joseph Alaimo, a former student in the lab, performed a microarray analysis of ethanol responsive genes in two strains of *C. elegans*: N2 (wildtype, WT) and *npr-1(ky13)* which is a lf mutation (a C-to-T transition that introduces a stop codon) that shows significantly higher AFT compared to N2 (Alaimo, 2013). The *npr-1(ky13)* strain was chosen due to its marked increased tolerance to ethanol compared to the WT worms. Comparing the gene expression profiles between these two strains could potentially reveal genes that contribute to the increased AFT phenotype seen in *npr-1(ky13)*. These differentially expressed genes would make excellent candidates for further research for a role in ethanol responses. Dr. Alaimo compared gene expression differences between untreated (basal) and acute ethanol treated N2 (WT) worms and *npr-1(ky13)* mutant worms and generated three expression profiles: *npr-1(ky13)* basal (the set of genes differentially expressed between the untreated *npr-1(ky13)* and N2 worms), N2 ethanol (the set of genes differentially expressed between the ethanol-treated N2

worms and untreated N2 worms) and *npr-1(ky13)* ethanol (the set of genes differentially expressed between the untreated *npr-1(ky13)* and ethanol-treated *npr-1(ky13)* worms).

He looked at the intersection of these three expression profiles (i.e., genes common across the three groups) and found that 20 genes were differentially expressed in all three profiles, which suggested that these are top candidate genes in modulating the ethanol response phenotypes (as these are differentially expressed at the basal level in *npr-1(ky13)* and also are ethanol responsive). Out of these 20 genes, based on a ranking system that considered allele availability, known phenotypes reported on WormBase (http://www.wormbase.org), neuronal expression and presence of mammalian homologs, Dr. Alaimo selected *acs-2* (acyl-CoA synthase 2) for behavioral testing and he observed that *acs-2(lf)* mutants showed significantly reduced development of AFT compared to N2 (Figure 1A). He then performed an experiment to determine if the alteration in ethanol response in the *acs-2* mutants was due to increased ethanol entry or change in internal ethanol concentration. He showed that neither of these two phenomena was responsible for the reduced AFT observed (Figure 1B). This implied that the difference in behavioral responses to ethanol could be due to physiological differences in the effects of ethanol in these mutants.

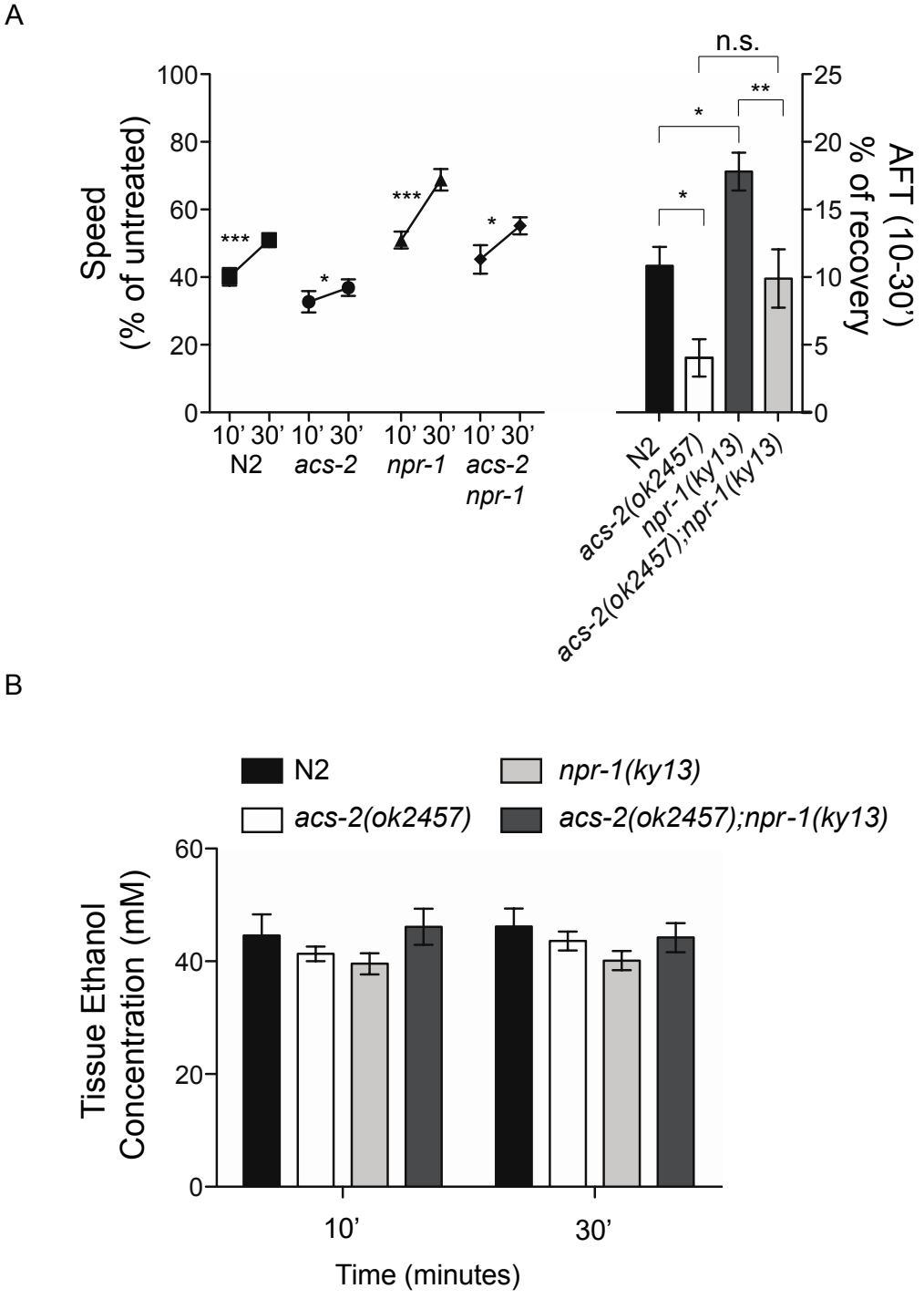

Figure 1. ***acs-2* modifies AFT and does not alter ethanol metabolism** (A) At 400mM exogenous ethanol, *acs-2(ok2457)* display a similar initial sensitivity to N2, but develop significantly less AFT. *acs-2(ok2457);npr-1(ky13)* animals also have a similar initial sensitivity relative to *npr-1(ky13)* and *acs-2(ok2457),* but have a reduced AFT that is significantly different than *npr-1(ky13),* but not *acs-2(ok23457) or* N2. (n = 9)(B). Internal ethanol concentrations are similar across all mutants suggesting the observed behavioral effects are not due to ethanol metabolism. (n = 4). Error bars are SEM. * $P < 0.5$, ** $P < 0.01$, *** $P < 0.001$. Reprinted with permission from "Identification and Characterization of Ethanol Responsive Genes in Acute Ethanol Behaviors in *Caenorhabditis elegans*", unpublished thesis, by J. Alaimo, 2013.

acs-2 is a gene involved in the first step of mitochondrial beta-oxidation, it codes for acyl-CoA synthase (ACS) which catalyzes the activation of FA to fatty acyl CoA (to facilitate entry into the mitochondria) (Van Gilst et al., 2005a). Lf mutants of *acs-2* exhibit accumulation of fat since there is a disruption of FA activation (Zhang et al., 2011). Dr. Alaimo conducted further behavioral assays by attempting to knockdown specific genes at different steps in mitochondrial beta-oxidation (*cpt-2, cpt-5, ech-1, ech-2, ech-4, ech-6, T08B2.7*) using RNA interference. These studies revealed that only knockdown of *ech-6* by RNAi altered AFT resulting in enhanced AFT compared to the control (L4440) (Figure 2), while none of the other RNAi experiments showed a significantly different ethanol response phenotype from the control, L4440. This could have been due to inefficient knockdown of genes by RNAi, so it does not rule out these genes as candidates. Therefore, these experiments suggested a role for mitochondrial beta-oxidation in regulating the ethanol response behavior in *C. elegans*. Treating this as preliminary evidence, we designed the current project to answer the following question: **Do genes involved in mitochondrial beta-oxidation of FA play a role in modulating ethanol response in *C. elegans*?**

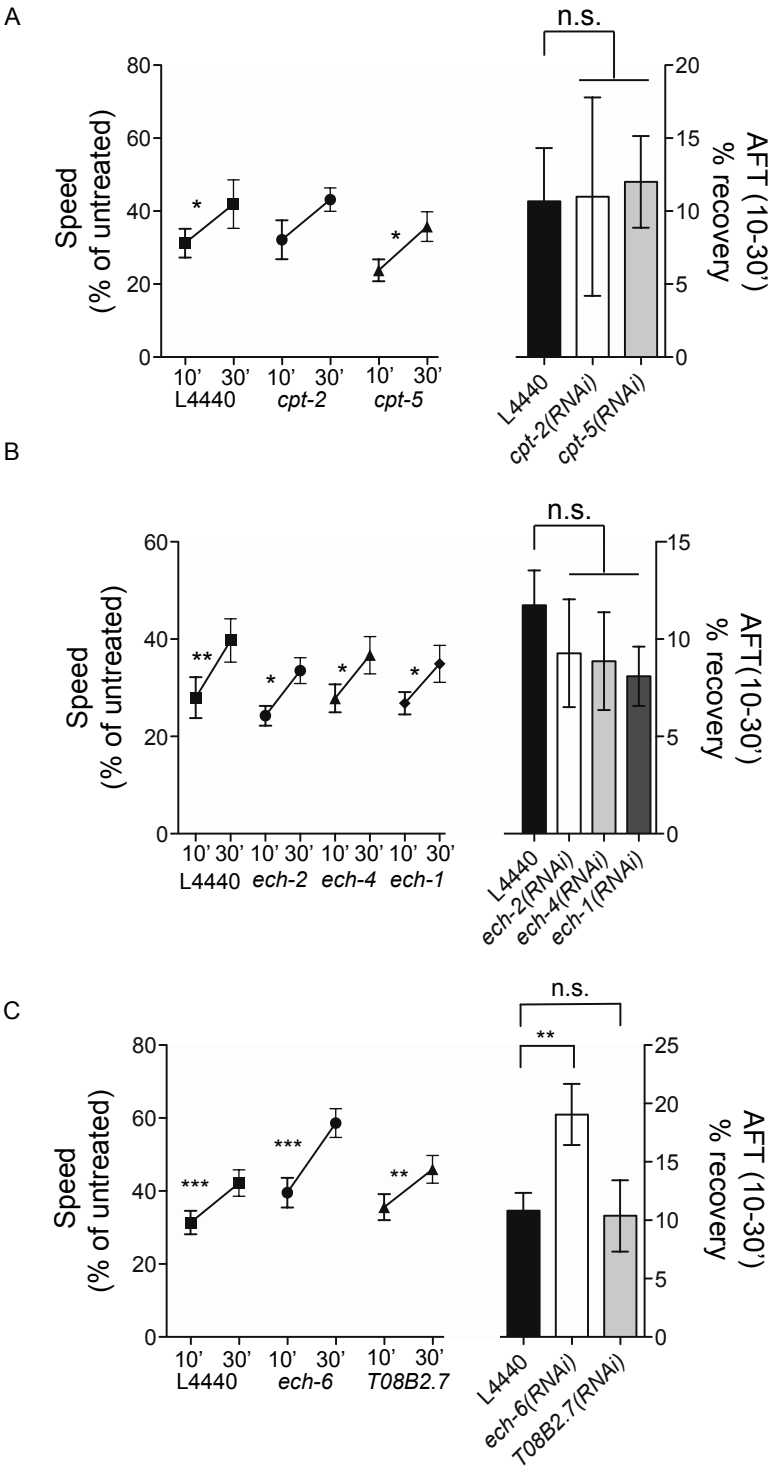

Figure 2. **Mitochondrial β-oxidation may influence acute ethanol behaviors.** (A) At 400mM exogenous ethanol *cpt-2(RNAi)* and *cpt-5(RNAi)* animals displayed similar initial sensitivity and development of AFT relative to control (n = 4). (B) *ech-2(RNAi), ech-4(RNAi),* and *ech-1(RNAi)* mutant animals also display similar initial sensitivity and AFT relative to control (n = 4). (C) *T08B2.7 (RNAi)* animals were not different than control for initial sensitivity or AFT. *ech-6(RNAi)* mutants displayed an enhanced AFT relative to WT, but initial sensitivity was not significantly different (n = 8). Error bars represent SEM * $P < 0.05$, ** $P < 0.01$, ***$P < 0.001$. Reprinted with permission from "Identification and Characterization of Ethanol Responsive Genes in Acute Ethanol Behaviors in *Caenorhabditis elegans*", unpublished thesis, by J. Alaimo, 2013.

1.5. Mitochondrial Beta-Oxidation

The first step in understanding the role of mitochondrial beta-oxidation genes in ethanol response was to characterize and annotate the mitochondrial beta-oxidation pathway. FA are a major energy source in multicellular organisms as they yield large quantities of ATP upon degradation and are also required for formation of various macromolecules. FA oxidation is an important metabolic process that maintains energy homeostasis, particularly under reduced glucose availability when FA act as the primary source of energy that can be directly used by most tissues, except the brain. FA are also converted to ketone bodies which serve as alternate energy sources for all tissues including the brain (Houten et al., 2010).

Mitochondrial beta-oxidation is the primary pathway of FA degradation and, as the name implies, it occurs in the mitochondria of eukaryotic cells (Kunau et al., 1995). Beta-oxidation also occurs in peroxisomes in some higher eukaryotic organisms, but a major difference between mitochondrial and peroxisomal beta-oxidation is that peroxisomes typically oxidizes very-long-chain FAs (> C22), pristanic acid, and the bile acid intermediates di- and trihydroxycholestanoic acid, while mitochondria are the site of oxidation for all other FA species. Also, FAs oxidized in the peroxisomes have to further undergo complete oxidation in the mitochondria (Wanders & Waterham, 2006). Beta-oxidation in the mitochondria occurs through the following steps (see Figure 3): (1) Activation: In the cytosol, FA are activated by the addition of CoA to form acyl CoA, and this is catalyzed by ACS in a two-step process.

FA reacts with ATP to give fatty acyl adenylate (an intermediate compound) and inorganic pyrophosphate in the first step, which then react with coenzyme A (CoA) to form acyl CoA and AMP (2) Transport: Long-chain acyl CoA esters are transported across the mitochondrial membrane into the matrix for oxidation by carnitine palmitoyl transferases (CPT) (short and medium chain acyl CoA esters are activated in the matrix and do not need carnitine shuttle for transport across the membrane). (3) Dehydrogenation (first): Acyl CoA dehydrogenases (ACAD/ACDH) catalyze the conversion of acyl CoA to trans-2-enoyl CoA. This creation of a trans double bond between C2 and C3 requires FAD^+ as electron acceptor that is reduced to $FADH_2$. (4) Hydration: Trans-2-enoyl CoA is converted to 3-hydroxy acyl CoA by enoyl CoA hydratase (ECH) enzymes. (5) Dehydrogenation (second): In the second dehydrogenation, 3-hydroxy acyl CoA is catalyzed by 3-hydroxy acyl CoA dehydrogenase (HADH/HACD) to form 3-keto acyl CoA, using NAD^+ as the electron acceptor which gets reduced to NADH. (6) Thiolytic cleavage: In the final step, 3-keto acyl CoA thiolase (KAT) cleaves keto acyl CoA to produce acetyl CoA and a fatty acyl CoA that is shortened by two carbons which goes through the same cycle again until it is completely oxidized (Wanders et al., 2010). Acetyl CoA enters the citric acid cycle to produce carbon dioxide (CO_2) and water (H_2O). The NADH and $FADH_2$ produced in beta-oxidation and citric acid cycle are utilized in the electron transport chain (ETC). The total energy yield from each cycle of oxidation is 14 ATP (acetyl CoA enters the citric acid cycle and yields 10 ATP, NADH and $FADH_2$ enter the ETC and produce 2.5 ATP and 1.5 ATP respectively).

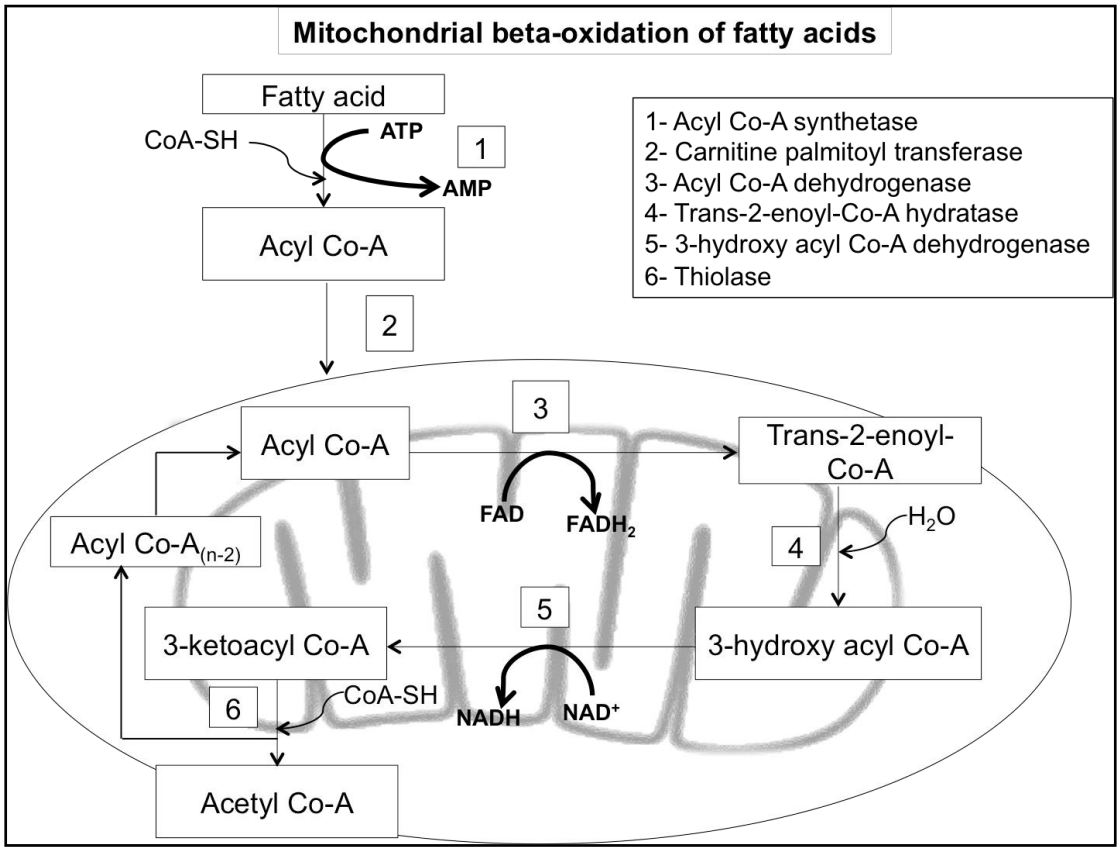

Figure 3. **Mitochondrial beta-oxidation of FA.** Reaction steps, enzymes and energy transfers involved in mitochondrial beta-oxidation of FA. Numbers within boxes at each step of the pathway correspond to enzymes listed in the top right corner of the figure.

1.5.1. Mitochondrial beta-oxidation in *C. elegans*

C. elegans is increasingly being utilized to model mammalian metabolic pathways and associated disorders as a majority of physiological processes appear to be conserved in these nematodes (Mullaney & Ashrafi, 2010). Looking specifically at mitochondrial beta-oxidation of FA, the general steps of the pathway appear to be conserved between mammals and *C. elegans* (Table 1). Though conserved in primary function, there is evolutionary divergence in terms of protein sequence between the mammalian and *C. elegans* beta-oxidation enzymes. Other aspects such as substrate specificity, expression pattern, subcellular localization and auxillary functions

have not yet been extensively studied in *C. elegans* to determine the extent of similarity to their human homologs/orthologs.

Mitochondrial beta-oxidation has not been very well characterized in *C. elegans* (Li et al., 2010). There are a significant number of studies exploring the role of mitochondrial dysfunction in the context of oxidative stress relating to various metabolic (Lowell & Shulman, 2005) and neurodegenerative diseases (Ray et al., 2014), lifespan and aging (Dai et al., 2014). However, only a small number of studies have looked at beta-oxidation of FA in particular, and these studies focused on subsets of genes mostly with relevance to transcriptional regulators mediating nutrient response and fat metabolism (Xu et al., 2015; Van Gilst et al., 2005a; Van Gilst et al., 2005) and none of these (published to date) have elucidated or comprehensively reviewed the mechanism of mitochondrial FA beta-oxidation in *C. elegans*.

A brief overview of each family of genes encoding the enzymes at each step of beta-oxidation in humans and *C. elegans* based on published literature is presented here to give the necessary background to appreciate the wide range of effects of these genes on ethanol response behavior in *C. elegans* which will be discussed in the Results and Discussion section.

Table 1. Step-by-step comparison of mitochondrial beta-oxidation in humans and *C. elegans*

Reaction	**Enzyme (Human)**	**Genes (Human)**	**Enzyme(*C. elegans*)**	**Genes (*C. elegans*)**
Activation: Fatty acid → Fatty acyl CoA	Acyl CoA Synthetase	(Long-chain) *ACSL1, ACSL3, ACSL4, ACSL5, ACSL6* (Bubblegum Family) *ACSBG1, ACSBG2*	Acyl CoA Synthase	*acs-1, acs-2, acs-3, acs-4, acs-5, acs-13, acs-15, acs-16, acs-17, acs-18* (long-chain)
Transport: Fatty acyl CoA → L-palmitoyl carnitine	Carnitine palmitoyl transferase	*CPT1A, CPT1B, CPT1C*	Carnitine palmitoyl transferase	*cpt-1*
Transport: L-palmitoyl carnitine → acyl CoA	Carnitine palmitoyl transferase	*CPT2*	Carnitine palmitoyl transferase	*cpt-2*
Dehydrogenation (first): Acyl CoA → Trans-2-enoyl CoA	Acyl Co-A dehydrogenase (ACAD)	*ACADS* (short chain) *ACADSB* (short/branched chain) *ACADM* (medium chain) *ACADL* (long chain) *ACADVL* (very long chain)	Acyl Co-A dehydrogenase (ACDH)	*acdh-1* (short-chain), *acdh-3* (short/branched chain), *acdh-4* (short/branched chain), *acdh-7* (medium chain), *acdh-8* (medium chain), *acdh-10* (medium chain), *acdh-12* (very long chain)
Hydration: Trans-2-enoyl CoA → 3-hydroxy acyl CoA	Enoyl CoA hydratase	*ECHS1* (short chain)	Enoyl-CoA hydratases	*ech-6* (short chain)
	Hydroxy acyl CoA dehydrogenase/3-ketoacyl CoA thiolase/enoyl CoA hydratase (trifunctional protein), alpha subunit	*HADHA*	Enoyl-CoA hydratases/long-chain 3-hydroxyacyl-CoA dehydrogenase	*ech-1.1, ech-1.2*
Dehydrogenation (Second): 3-hydroxy acyl CoA → 3-keto acyl CoA	Hydroxy acyl CoA dehydrogenase	*HADH*	Hydroxy acyl CoA dehydrogenase	*F54C8.1, hacd-1, B0272.3*
	Hydroxy acyl CoA dehydrogenase/3-ketoacyl CoA thiolase/enoyl CoA hydratase (trifunctional protein), alpha subunit	*HADHA*	Enoyl-CoA hydratases/long-chain 3-hydroxyacyl-CoA dehydrogenase	*ech-1.1, ech-1.2*
	Acetyl CoA transferase	*ACAA2*	Acetyl CoA transferase	*acaa-2*
Thiolytic cleavage: 3 keto acyl CoA → Acetyl CoA	Ketoacyl CoA thiolase beta-subunit of trifunctional protein	*HADHB*	Ketoacyl CoA thiolase beta-subunit of trifunctional protein	*B0303.3*
			3-keto acyl CoA thiolase	*kat-1*

1.5.1.1. Acyl CoA Synth(et)ases (ACS)

In humans, approximately 26 ACS enzymes have been identified and characterized or predicted to date (Watkins et al., 2007). These enzymes catalyze thioesterification of FA into fatty acyl CoA which can either enter the beta-oxidation pathway or other pathways that form membrane phospholipids, cholesterol esters and activation of certain transcriptional and signaling pathways as shown in Figure 4 (Cooper et al., 2015).

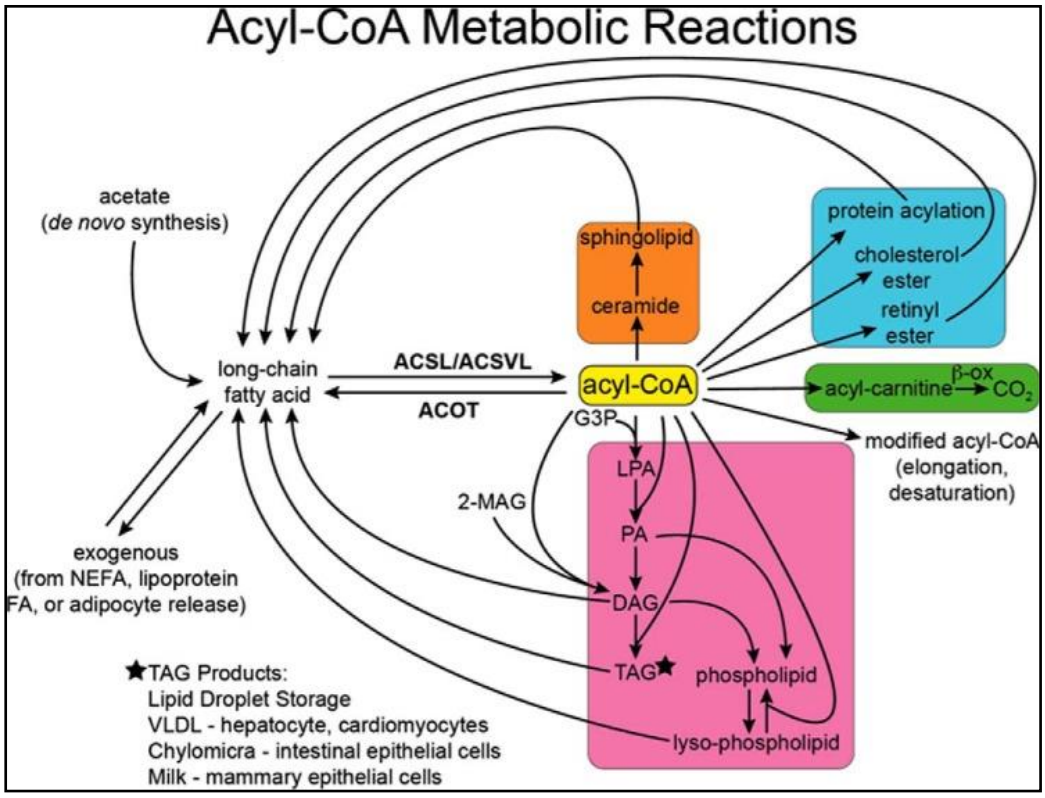

Figure 4. Metabolic reactions of acyl-CoAs. Long-chain FAs are synthesized *de novo* from acetate or enter cells from the plasma. They are converted to acyl-CoAs by ACSL and ACSVL. The reaction is reversed by acyl-CoA thioesterases (*ACOT*). Acyl-CoAs can be elongated and desaturated, converted to acylcarnitines, and metabolized to CO_2 via mitochondrial and peroxisomal enzymes, esterified to glycerol-3-phosphate to form lysophosphatidic acid (*LPA*), phosphatidic acid (*PA*), and TAG, and esterified to monoacylglycerol (*MAG*) to form diacylglycerol (*DAG*). Both phosphatidic acid and diacylglycerol are precursors for all the glycerophospholipids. Acyl-CoAs are also esterified to retinol and cholesterol, acylated to proteins, and incorporated into ceramide to form sphingolipids. Lipolysis of these products releases FA back into cellular pools. Triacylglycerol, cholesterol esters, and retinol esters are stored in lipid droplets within cells or secreted from specialized cells as lipoproteins or milk constituents. *NEFA*, non-esterified fatty acid. Reused with permission from "Physiological Consequences of Compartmentalized Acyl-CoA Metabolism", by Cooper et al., 2015, Copyright 2015, by the American Society for Biochemistry and Molecular Biology, Inc.

ACS enzymes have been broadly categorized into distinct groups based on their substrate-specificity, which is mostly defined by chain length of the FA substrate. There has been significant evidence from mice and cell line studies to show that members of the ACS family exhibit preference for specific chain lengths of FA. For example, Li et al. (2009) performed liver-specific knockout experiments in mice to show that ACSL1 is important for oxidation of long chain FA in the mitochondria. Another study (Marszalek et al., 2005) found that ACSL3, ACSL4 and ACSL6 preferentially activate PUFA for oxidation.

The *C. elegans* genome encodes at least 22 ACSs (WormBase) but there have been very few studies characterizing these enzymes and their roles in fat metabolism. One study looking at *acs-3,* which is predicted to encode a long chain ACS, showed that it has a role in regulating fat storage (Mullaney & Ashrafi, 2010) and *acs-4* and *acs-5* were shown to be involved in the serotonergic regulation of fat storage in *C. elegans* (Srinivasan et al., 2008). For most of these genes, there has been no recorded lf phenotype, and their functions (including their roles in beta-oxidation) and substrate-specificity have been predicted solely based on their orthology/homology to human or mouse ACS genes.

1.5.1.2. Carnitine Palmitoyl Transferases (CPT)

Carnitine palmitoyl transferases (CPTI and CPTII) transport long chain fatty acyl CoAs across the mitochondrial matrix for oxidation. CPTI is located on the outer mitochondrial membrane and, since it catalyzes the rate-limiting step of FA oxidation (transport of fatty acyl carnitine), it is regulated tightly by

malonyl CoA, which is the first intermediate product in FA synthesis. This allows for a physiological balance between FA synthesis and degradation. CPTII is located on the inner mitochondrial membrane as a membrane-associated enzyme that facilitates reconversion of long-chain fatty acyl carnitine into fatty acyl CoA once it enters the matrix. In humans, CPTI (gene: *CPT1*) and CPTII (gene: *CPT2*) have been studied extensively both with respect to structural and functional characterization (Woldegiorgis et al., 2000; Yamzaki, 2004) and their roles (particularly *CPT1*) in various neurological (Virmani et al., 2015; Xie et al., 2016) and metabolic diseases (Flanagan et al., 2010; Schreurs et al., 2010).

There are 6 members in the CPT family encoded in the *C. elegans* genome (WormBase), of which *cpt-1* and *cpt-2* are orthologous to the human *CPT1A* and *CPT2* genes respectively, while the other *CPT* genes (*cpt-3,4,5,6*) are predicted to also have acyl CoA transferase function. The literature available on this family of genes is mostly in the area of fat, adiposity and lipid metabolism regulation (Brock et al., 2007) by specific transcription factors such as *nhr-49* (Van Gilst et al., 2005b) and *mdt-15* (Taubert et al., 2006) through altering expression levels of these *CPT* genes.

1.5.1.3. Acyl CoA dehydrogenases (ACAD/ACDH)

ACAD/ACDH, as the name implies, catalyze the dehydrogenation of fatty acyl CoA once it enters the mitochondria. These are flavoprotein enzymes that require flavin adenine dinucleotide (FAD) as a co-factor to catalyze reactions. Nine major ACADs have been identified in eukaryotes, with five of these

involved in beta-oxidation of FA (SCAD, MCAD, LCAD, vLCAD, vLCAD2), and the other four involved in the catalysis of branched-chain amino acid synthesis (i2vD, i3vD, GD, iBD) (Ghisla & Thorpe, 2004). Based on their substrate specificity, the ACADs participating in beta-oxidation can be categorized into four groups but there is a certain degree of overlap in their substrate chain-lengths: (1) short-chain ACAD (SCAD) that preferentially act on C4-C6 fatty acyl-CoAs (2) medium-chain ACAD (MCAD) which catalyzes dehydrogenation of C6-C10 fatty acyl-CoAs (3) long-chain ACAD (LCAD) which acts on C10-C14 fatty acyl-CoAs and (4) very long-chain ACADs (vLCAD, vLCAD2) that is specific to C14-C20 fatty acyl-CoAs (Leslie et al., 2014). Since deficiencies of these enzymes in humans lead to serious metabolic consequences that can be detected in newborn screening, they have been well-studied and numerous groups have performed protein crystallization, functional analyses and gene knockout studies in animal and cell models.

However, in *C. elegans,* which has 13 ACDH genes (WormBase), a detailed crystal structure analysis has been performed only on *acdh-11.* Li et al., (2010) reported that while *acdh-11* shares 26% protein sequence identity with the human vLCAD, it is quite different from its human homolog in terms of structural properties. It shows affinity for C11/C12-FA but does not appear to have dehydrogenase activity, which suggested that *acdh-11* could be involved in sequestering long chain FA (specifically C11/C12), and thus may play a role in regulation of FA desaturation (Ma et al., 2015). This differential in function of *acdh-11* and its lack of dehydrogenase activity could explain the

low percentage of protein sequence similarity it shares with the human VLCAD. The other ACDH enzymes in *C. elegans* that have been found to be orthologous to the five different human ACADs are: *acdh-1, acdh-2* (short-chain), *acdh-3, acdh-4* (short/branched chain), *acdh-7, acdh-8, acdh-10* (medium chain), *acdh-5, acdh-6* (long chain) and *acdh-12* (very long chain). *acdh-13,* although predicted to possess ACDH activity, does not have a clear human ortholog.

1.5.1.4. Enoyl CoA hydratase (ECH), 3-hydroxy acyl CoA dehydrogenase (HACD/HADH) and 3-keto acyl CoA thiolase (KAT):

These three classes of enzymes together catalyze the final steps of mitochondrial beta-oxidation. ECH catalyzes the addition of one H_2O molecule to trans-2-enoyl CoA to form 3-hydroxy acyl CoA thioester (Agnihotri & Liu, 2003), which is subsequently acted upon by HACD/HADH to form 3-keto acyl CoA, it is then cleaved by KAT, resulting in acetyl CoA and an acyl CoA molecule that is shortened by two carbons.

Like the ACADs, these enzymes also exhibit substrate-specificity based on chain length of acyl CoA. The long chain fatty acyls CoAs are metabolized by long-chain 2,3-ECH (LYHD), long-chain hydroxy acyl coA dehydrogenase (LCHAD) and long-chain KAT (LKAT). As the chain length of the substrate shortens, short-chain 2,3-ECH (SHYD), a medium/short-chain L-3-hydroxyacyl-CoA dehydrogenase (M/SCHAD), and medium-chain, short-chain KAT (MKAT, SKAT) are activated to complete the oxidation (Bennett et al., 1996; Wanders et al., 1999).

In higher eukaryotes, the three enzymes catalyzing the final steps of mitochondrial beta-oxidation for long-chain fatty acyl CoA (LHYD, LCHAD and LKAT) exist as one trifunctional membrane-bound protein complex called the Mitochondrial Trifunctional Protein (MTP). This protein complex contains four alpha and four beta subunits; the alpha subunits are responsible for the ECH/HADH activity while the beta subunits carry out the thiolytic cleavage (Rakheja et al., 2002). The alpha subunit is encoded by the HADHA gene and the beta subunit is catalyzed by the HADHB gene. Mutations in these two genes cause LCHAD and MTP deficiencies in humans, the former being more common (Ushikubo et al., 1996).

C. elegans genes encoding the enzymes catalyzing these last three steps include the ECH family, *hacd-1* and *kat-1*. The ECH family in *C. elegans* has 10 members, and among these *ech-1.1* and *ech-1.2* are orthologs of the human MTP and have ECH/long-chain HADH activity. *ech-6* and *ech-7* are orthologous to the human short-chain ECH, ECSH1. *ech-8* and *ech-9* are predicted to function in the peroxisomes due to their similarity to the human bifunctional protein EHHADH which exhibits ECH and HADH enzyme activity and is involved in peroxisomal oxidation of FA. *ech-4,* containing an acyl CoA binding domain and ECH domain, has been shown to affect the beta-oxidation of unsaturated FA (Elle et al., 2011). There is not enough information on *ech-3* and *ech-5* to determine if they have a role in beta-oxidation.

1.6. Goal of Present Study

My goal in this project was to characterize the role of mitochondrial beta-oxidation in the behavioral response to ethanol using *C. elegans*. Using the results of Dr. Alaimo's microarray data (of ethanol responsive genes), and his observations of the effects of loss of function of *acs-2* and *ech-6* genes of mitochondrial beta-oxidation on ethanol response behaviors as preliminary data, we asked how mitochondrial beta-oxidation either through its substrates, products, intermediate compounds or enzymes plays a role in mediating ethanol responses in *C. elegans*. For this purpose, we selected candidate genes that catalyze each step of the pathway based on specific criteria and performed behavioral assays on the lf mutants of these genes to determine their ethanol response phenotype. We hypothesized that some of these mutants would exhibit altered ethanol response phenotypes compared to the WT, which would indicate that those genes have a role in the behavioral responses to ethanol.

1.7. Specific Aims

1. Selection of candidate genes in the mitochondrial beta-oxidation pathway for testing in ethanol response assays.
2. Behavioral testing of backcrossed lf mutant strains and RNAi-fed worms using locomotion assays, to determine the roles of candidate genes in altering ethanol response phenotypes

2. MATERIALS AND METHODS

2.1 Selection of candidate genes

The first aim of the project was to select candidate genes of interest in the mitochondrial beta-oxidation pathway, which could be tested for a role in ethanol response behavior. I performed a review of literature on mitochondrial beta-oxidation of FA and found that there were several versions of the mitochondrial beta-oxidation pathway (in humans and *C. elegans*) in various published articles. Though the steps of the pathway were consistent across publications, there was significant variation in the enzymes and genes catalyzing each step. Therefore, to obtain an exhaustive list of genes involved in this pathway, I decided to use the mitochondrial beta-oxidation pathways of human (http://www.genome.jp/kegg-bin/show_pathway?hsa00071) and *C. elegans* (http://www.kegg.jp/kegg-bin/show_pathway?cel00071) illustrated on the KEGG Pathway database, as these were the most comprehensive annotated versions available. We then formulated specific exclusion criteria based on which genes would be eliminated from this list. All genes that could not be eliminated based on the exclusion criteria were included in the list of candidate genes to be tested for their roles in responses to ethanol. The exclusion criteria were: strong (literature) evidence showing that the gene does not play a role in mitochondrial beta-oxidation, genes that were shown to have a role in biological processes unrelated to mitochondrial beta-oxidation and genes that were orthologous to human genes that were not involved in mitochondrial beta-oxidation of FA. For example, *acs-8* aka *mec-18*, is one of the genes in the ACS family. It is expressed only in touch cells and is involved

in sensory mechanotransduction and therefore is highly unlikely to play a role in beta-oxidation of FA.

For the second aim, prior to testing for ethanol response behaviors, I backcrossed the 23 lf mutants obtained from the *Caenorhabditis* Genetics Center (CGC) at least twice (2x) to N2 (WT) worms. Two of the 23 mutants, *kat-1* and *ech-7* were already backcrossed 6x and 10x respectively. So *kat-1* was not backcrossed further. However, the *ech-7* lf mutant carried a deletion in another gene, *paqr-2,* so this strain was backcrossed to N2 once more. Prior to testing, I ensured that the *paqr-2* variant allele was removed from the background using PCR with primers for the *paqr-2* allele to genotype the F1 and F2 offspring obtained from the backcross, and maintained the F2s that had the mutant *ech-7* allele and the WT *paqr-2* allele.

2.2 Maintaining strains

Worms were maintained on petri plates containing nematode growth media (NGM). After seeding the plates with OP50, which is a strain of *E. coli* used in the laboratory as food source for *C. elegans* (refer 'seeding plates with OP50'), five adult hermaphrodites (of N2, the WT strain used in lab) were plated on to seeded plates and stored at 20°C. For the mutant strains, six to eight adult hermaphrodites were maintained at 20°C. VC2240: Since the homozygous mutant of this strain is sterile, it is balanced by a GFP-carrying balancer, *hT2 [bli-4(e937) let-?(q782) qIs48] (I;III)*. For this strain, heterozygote adults with GFP were picked for maintaining the strain.

2.3 Chunking

This was done to maintain the mutant strains obtained from the CGC and also to salvage worms from starved plates. A small chunk of NGM agar (from the CGC/starved plates) was cut out using a spatula that was first sterilized using 70% ethanol and flamed, and the chunk was placed on the edge of the OP50 lawn on a seeded plate. The chunked plate was left on the bench for a few hours; this allows worms from the chunk to crawl onto the OP50 lawn. These worms are then transferred to another seeded plate and maintained.

2.4 Making OP50

OP50 is the strain of *E. coli* that worms are fed when being maintained in lab. A single colony of OP50 was picked using an inoculation loop from the OP50 stock culture plate and stirred into 50 mL of autoclaved LB. This was then allowed to grow overnight (~16 hours) at 37°C, with the lid of the container screwed on loosely, to allow for aeration. After ~16-20 hours the culture was removed from 37°C and shaken or swirled to check if the LB has turned cloudy, which indicates bacterial growth. It was then stored at 4°C for future use. OP50 was typically used within 30-45 days after preparation.

2.5 Seeding plates with OP50

Approximately two drops of OP50 were pipetted onto the NGM plates and spread into a square lawn on the center of the plates and allowed to typically grow overnight at room temperature before using the plates for maintaining worms.

2.6 *C. elegans* strains

Table 2. List of *C. elegans* strains used for the project. The genotype (Gene, allele, chromosome) is depicted for each strain and the gene of interest is highlighted. The strains generated by EMS mutagenesis for the Million Mutations Project (MMP) carry numerous mutations and are indicated by the acronym MMP next to the strain name. For these strains, only the genotype of interest is given.

Strain Name	**Genotype**	**Effect on protein**
N2 (var. Bristol)	WT	NA
VC40812 (MMP)	*acs-3(gk826522)V*	Y324Ochre
VC2240	***acs-4(ok2872)III****/hT2 [bli-4(e937) let-?(q782) qIs48] (I;III)*	Insertion/deletion (affects coding exon and intron)
RB2015	*Y76A2B.3(ok2668)III*	Deletion (not curated)
RB2147	*acs-13(ok2861)I*	Deletion (affects coding exon and intron)
RB1377	*acs-17(ok1562)X*	Deletion (not curated)
VC20634 (MMP)	*acs-22(gk364606)V*	R597Opal R470Opal R600Opal
VC20616 (MMP)	*cpt-3(gk356297)III*	Q636Amber
VC40798 (MMP)	*cpt-4(gk818803)V*	S519Opal
VC40360 (MMP)	*cpt-6(gk594576)V*	W39Opal
VC1087	*acdh-1(ok1514)I*	Deletion (not curated)
VC20502 (MMP)	*acdh-2(gk143151)II*	W19Opal G125E W185Opal
VC40973 (MMP)	*acdh-5(gk907299)I*	Q146Amber
VC40929 (MMP)	*acdh-6(gk886629)III*	W51Opal
VC40288 (MMP)	*acdh-7(gk556025)X*	Q361Ochre
VC40665 (MMP)	*acdh-11(gk753061)III*	L119Amber L110Amber
VC41029 (MMP)	*F54D5.7(gk936057)II*	W169Opal
VC40235 (MMP)	*ech-1.2(gk527451)I*	Q142Ochre Q142Ochre Q116Ochre
QC119	***ech-7(et6)I****; paqr-2(tm3410)III*	V175M
RB2101	*R09B5.6(ok2776)V*	Deletion (affects coding exon and intron)
RB1606	*ife-1&****F53A2.7(ok1978)****III*	Insertion (affects coding exon and intron)
VC2462	*T02G5.4(ok3160)II*	Insertion (not curated)
RB2566	*T02G5.7(ok3574)II*	Deletion (not curated)
VS24	*kat-1(tm1037)II*	Insertion (affects coding exon and intron)

2.7 DNA Isolation

DNA isolation was performed in order to obtain genomic DNA that was used as the template for PCR.

2.7.1 DNA Isolation for PCR

A full plate of worms (obtained by plating five adult hermaphrodites on a seeded plate and letting them grow and produce a population for three days) was used for DNA isolation. These worms were washed off the plate using ~1.7 mL ddH_2O into a 1.5 mL Eppendorf tube and centrifuged at 21,000 rcf (high speed) for 30 seconds. Most of the supernatant was removed, and one mL ddH_2O was added and centrifuged again for one min. The supernatant was removed until 0.1 mL of solution remained in the tube. The pellet was disturbed by shaking and the tube was placed at -80°C for 15 minutes to lyse the cells. Thirty three microlitres of a master mix made of lysis buffer and 10 mg/mL Proteinase K (35 µL lysis buffer + [(12/1000) x 35] µL Proteinase K) was added to the tube. The tube was incubated at 60°C for 90 minutes to digest the proteins, followed by a 20 minute incubation at 95°C to inactivate the Proteinase K. This lysate containing DNA was stored at -20°C (detailed protocol and recipes for solutions used are in Appendix I).

2.7.2 DNA Isolation for Single Worm PCR (SWPCR)

A master mix of 95 µL lysis buffer and five microlitres of 10 mg/mL Proteinase K was prepared and three microlitres of this solution was added to a 0.2 mL PCR tube. A single worm (on which PCR is to be performed) was placed in the solution and the tube was placed at -80°C for 20 minutes, followed by a 60 minutes incubation at 60°C and 15 minutes at 90°C. The DNA prepared was stored at -20°C (detailed protocol in Appendix I).

2.8 Polymerase Chain Reaction (PCR)

PCR was performed on all the mutant strains received from the CGC to confirm presence of mutant allele in the strains and for genotyping the F1 and F2 generations of backcrossed mutant strains.

2.8.1 Primers for PCR

Primer sequences were obtained from the website (https://cgc.umn.edu) for some mutant strains (Appendix II, Table 14), and for strains that did not have this information on the CGC or WormBase, I designed primers using the NCBI Primer-BLAST tool (www.ncbi.nlm.nih.gov/tools/primer-blast) using the DNA sequence of mutant strains obtained from WormBase (Appendix II, Table 15). The DNA sequence in the mutated region (that is either deleted or carries a complex substitution in the mutant strain) along with the flanking sequences (a few hundred base pairs on either side) was used to generate primers and the best primer pair was chosen based on primer length (optimal length of PCR primers is 18-22 base pairs, which is long enough for adequate specificity and short enough for primers to bind easily to the template at the annealing temperature), optimum melting temperature (temperature at which one half of the DNA duplex will dissociate to become single stranded and indicates the duplex stability. Primers with melting temperatures in the range of 52-58°C produce the best results) and self-complementarity (predictive of the tendency of primers to anneal to each other, which hinders amplification of template DNA).

2.8.2 PCR Setup

Unless mentioned otherwise, all polymerase chain reactions (PCR) were set up according to the following specifications (see Appendix I for detailed protocol):

Table 3. PCR Reaction components

Component	**Volume per sample (µL)**	**Final concentration**
ddH_2O	6.7	--
10X DreamTaq Green Buffer	1.0	1X
DreamTaq DNA polymerase (5U/µL)	0.1	0.5 U
dNTP (10mM)	0.2	2 mM
Forward Primer (10µM)	0.5	5 µM
Reverse Primer (10µM)	0.5	5 µM
DNA	1.0	--

Table 4. Standard PCR conditions

Condition	**Temperature**	**Time**
Initial Denaturation	94°C	2 minutes
Denaturation Annealing Extension	94°C 45-69°C* 72°C	15 seconds 45 seconds 1 minute/kb* (35 cycles)
Final Extension	72°C	5 minutes

*Annealing temperature and extension time vary depending on melting temperature of primers (T_m) and product size respectively.

2.8.3 Temperature gradient PCR

A trial PCR was set up for each of the primer pairs at 5-6 different annealing temperatures within a specific range that were picked based on the melting temperature of each primer pair using one microlitre of N2 DNA as template, to determine the optimal annealing temperature for each primer pair. The PCR reaction mix and the PCR program were set up as mentioned in section 2.8.2. Based on the band intensity (indicates robust amplification) and minimal non-specific bands (due to smaller non-specific amplification or primer-

dimers) when the PCR product is run on an Agarose gel, the best temperature was determined and used as annealing temperature for that primer pair for further PCR reactions.

2.8.4 Single worm PCR (SWPCR)

SWPCR was mainly performed to determine genotypes of progeny from crosses (see Appendix I for detailed protocol).

Table 5. PCR reaction components for SWPCR

Component	**Volume per sample (µL)**	**Final concentration**
ddH_2O	13.4	--
10X DreamTaq Green Buffer	2.0	1X
DreamTaq DNA polymerase	0.2	0.5 U
dNTP (10mM)	0.4	2 mM
Forward Primer (10µM)	1.0	5 µM
Reverse Primer (10µM)	1.0	5 µM
DNA	3.0	--

The three microliters DNA isolated from a single worm (refer to section 2.7.2) is used as template DNA to which 18 µL of the master mix is added. The PCR program is set up as detailed in 2.8.2.

2.9 Restriction digestion

For mutants that contain a single nucleotide polymorphism (SNP) within a restriction site, PCR was followed by restriction digestion to determine genotype of the SNP, using the appropriate restriction enzyme. The restriction digestion mix was set up as shown in Table 6, for a final volume of 10 µL. This type of genotyping using restriction digestion to detect Single Nucleotide

Polymorphisms (SNP) is called snipSNP. Restriction enzymes recognize and cleave (or 'snip') specific sequences of nucleotides. I chose particular enzymes that cut at nucleotide sequences, which contain the WT or variant allele at the target SNP, so that digestion using this enzyme resulted in cleaving of the amplicon at the SNP, in either the WT allele carriers or mutant allele carriers. Detection of genotype was based on the number of fragments and size of fragments observed when the digested PCR products were run on an Agarose gel. The list of restriction enzymes and digest conditions used are given in Table 16, Appendix II.

Table 6. Restriction digestion reaction mix components

Component	**Volume per sample (µL)**
ddH_2O	3.5
Buffer*	1.0
Restriction enzyme	0.5
PCR product	5.0

*Manufacturer guidelines were followed for buffer volume in case of buffer concentrations other than 10X and for setting up the digest conditions (temperature and time).

2.10 Agarose Gel Electrophoresis

We used Agarose gel electrophoresis for the following: to determine product sizes of amplified DNA fragments in WT and mutant worms to determine genotype based on the difference in product size (in case of mutants carrying deletions, the size of the amplified product in mutant worms would be smaller compared to that of WT worms); to determine the fragment size of restriction digested PCR products; for detecting genotype in snipSNP by running the

restriction digested fragments on a gel; to estimate the concentration of DNA in PCR samples sent for sequencing. The Agarose gels used for this project were 1% (if the predicted product size was greater than 600 bp), 1.5% (300-600 bp, if the predicted product sizes differed by at least 100 bp) and 2% (50-300 bp, if the predicted product sizes differed by at least 50bp). An Agarose gel was prepared using a specific amount of Agarose (depending on the percentage and size of the gel, for example, to prepare a 1% large gel of 100 mL, 1g of Agarose was used). The Agarose was dissolved in a specific volume of 0.5X TBE (Tris/Borate/EDTA) buffer and the solution was heated until the Agarose dissolved completely in the buffer. Three microliters Ethidium Bromide, a DNA-intercalating agent, was added to this and the gel was poured into a gel tray that has combs (to form lanes). This setup was allowed to cool down, the combs were removed and the gel was placed in a gel tank containing 0.5X TBE buffer. Five microlitres of sample (PCR product/digested sample) was loaded into each lane and an appropriate DNA ladder was used to serve as a guideline to determine the size of sample bands. The gel was run at a set voltage (80V-100V) for 45-120 minutes (depending on size of fragments) and then visualized in the UV transilluminator to determine band sizes of samples and estimate DNA concentration.

2.11 DNA sequencing

Sanger sequencing was performed for SNPs that were not detectable by restriction digestion or PCR. Sequencing was also used to confirm the results obtained by restriction digestion or PCR, in case of ambiguous results or

failed digests. PCR was performed using primers flanking the SNP to generate a reaction volume of 10 µL (in case of SWPCR, 21 µL). The concentration of DNA was estimated from running the samples on an Agarose gel and comparing the band intensity to a DNA ladder (of known band sizes and DNA concentrations). Two microlitres of ExoSAP^{TM} (a PCR product cleanup reagent) was added to five microliters of PCR product and incubated at 37°C for 15 minutes, to degrade excess primers and dNTPs, followed by 15 minutes incubation at 80°C to inactivate the ExoSAP reagent. The sequencing reaction was prepared according to the standard guidelines (for Sanger sequencing using Purified Template) provided by GENEWIZ (Appendix I). The purified PCR product was diluted for a final volume of 10 µL and an appropriate final concentration (ng/µl) based on the size of the PCR product (see Table 12 in Appendix I). Five microlitres of diluted forward primer (1 in 20 dilution: 95 µL ddH_2O and five microliters 100µM primer) was added to the diluted, purified PCR product to make up a 15 µL sequencing reaction. All sequencing reactions thus prepared were sent to the GENEWIZ facility for Sanger sequencing. 4Peaks software was used to interpret SNP genotype by visualizing the sequence trace files received from GENEWIZ.

2.12 RNA interference (RNAi)

All the RNAi experiments were performed based on the protocol published by (Kamath et al., 2003). I planned to perform RNAi for 14 candidate genes that did not have lf mutants available from CGC. Bacterial clones containing the sequences coding for double stranded RNA complementary to the genes of interest were obtained from the RNAi library generated by Ahringer. The RNAi

bacterial strain was not available in the library for one of the genes (*cpt-1*). For the other 13 genes, the corresponding bacterial colony was scraped using a micropipette tip and suspended in 2 mL of LB containing 50 µg/mL Ampicillin. This was also done for *dpy-17*, which we used as a positive control used for RNAi and L4440, which is the empty bacterial vector (used as 'WT' control for behavioral assays). These cultures were allowed to grow for 16 hours by incubating in the shaker at 37°C and 250 rpm (Appendix I: Making RNAi cultures from frozen stock). Five of the 13 RNAi cultures did not show any growth (*acs-15, acs-18, acdh-3, F54C8.1, B0272.2*) and hence the process was repeated for these, with no success. One and half milliliters of the other grown cultures were used for freezing by adding 300 µL of glycerol, in cryo-tube vials (Appendix I: Freezing RNAi Cultures). The grown bacterial cultures were also streaked on LB plates containing Ampicillin (50 mg/mL) and Tetracycline (15 mg/mL) using an inoculation loop, and incubated at 37°C for 16 hours (Appendix I: Preparing ampicillin + tetracycline plates for RNAi). These plates were then stored at 4°C and used for preparing liquid cultures of RNAi. Single colonies were picked from the plates and suspended in five milliliters of LB containing 50 µg/mL Ampicillin and grown for 16 hours in the shaker at 37°C and 250 rpm to obtain cultures that were ready to be used for feeding worms. Prior to performing behavioral assays, the bacterial clones in each of these cultures were confirmed by Sanger sequencing. For this, three milliliters of the culture was used for DNA extraction, which was performed using the Invitrogen PureLink HQ Mini Plasmid Purification Kit (Appendix I: Plasmid DNA extraction using Invitrogen PureLink HQ Mini Plasmid Purification Kit) and the plasmid DNA was quantified using a NanoDrop

machine (DNA concentrations are attached in Appendix II, Table 17). The samples were prepared for sequencing according to the requirements given on GENEWIZ for Purified Templates (Appendix I: Sanger sequencing sample preparation using Plasmid DNA template). DNA was diluted to a final concentration of 50 ng/µL in 10 µL and five microliters of diluted (1 in 20 dilution) UC19 primer was added to each diluted sample. Sanger sequencing was done by GENEWIZ and the sequences obtained were input in NCBI BLAST to confirm the gene sequence. All samples had the correct sequence except *acs-16,* for which sequencing was not successful due to lack of priming (this was repeated once, but with the same outcome). Therefore, RNAi bacterial cultures were successfully grown and confirmed for seven genes (*W03F9.4, acdh-4, acdh-8, acdh-10, acdh-12, ech-1.1, B0303.3*) for which behavioral assays on ethanol were performed.

For the confirmed gene sequences, 800 µL of each RNAi culture was seeded on NGM plates containing Carbenicillin (50 mg/mL) and IPTG (0.1 M) (Appendix I: Carbenicillin Plates for RNAi). N2 worms in the L4 stage were placed on each of these RNAi plates approximately 24 hours before the behavioral assay on ethanol was to be performed. The *dpy-17* RNAi was used as a positive control to confirm that RNAi setup was functional (the worms fed with *dpy-17* RNAi culture exhibited 'dumpy' phenotype, and at least three-fourths of the worms on this plate need to be 'dumpy' for the RNAi to be considered successful). This was done each time new RNAi cultures were made or new RNAi plates were prepared. The behavioral assays on ethanol were performed as described in section 2.14, using L4440 (N2 worms fed with *E. coli* carrying empty vector) as the WT strain.

2.13 Backcrossing mutant strains

All of the lf mutant strains received from the CGC that were not already backcrossed to N2 at least twice, were backcrossed twice to N2 (2x cross) to decrease the number of other mutations in the strain that could affect the behavioral response to ethanol. These 2x backcrossed mutants were used for behavioral assays on ethanol. The ones that showed a significantly different ethanol response phenotype compared to N2 were further backcrossed four additional times to N2 for a final number of 6x backcrosses. 6x generally will generate a mostly WT genetic background (~98.375%) and is the generally accepted standard in *C. elegans* genetics (Boulin & Hobert, 2012; Zuryn et al., 2010).

Refer to figures 5 and 6 for a graphic step-wise representation of the backcross with the genotypes and their ratios at each generation. Figure 5 represents the backcross for genes on autosomes (chromosomes I-V) and figure 6 represents the backcross for genes on the X-chromosome.

I set up Cross I using mutant hermaphrodites in the L4 stage with N2 males (in 5:10 ratio) and this is considered as ‘day 1’ of the cross. On the following day (day 2), each of the mated mutant hermaphrodite adults were transferred to separate freshly seeded plates and allowed to lay eggs. Three days later (day 5), five F1 hermaphrodite progeny (which are all heterozygous) were transferred to a separate seeded plate from each one of the day 2 plates. These plates are stored for backup if the second cross fails and needs to be

repeated. Also, on day 5, F1 males from these day 2 plates were used to set up a mating with N2 hermaphrodite L4s (in a ratio of 10:5) for Cross II. The next day (day 6), each one of the mated N2 hermaphrodite adults from Cross II were picked to individual plates and allowed to lay embryos. Four days later (day 10), ten or twelve F1 adult hermaphrodites from these plates were picked to individual plates and allowed to self-fertilize and lay eggs overnight. SWPCR was performed on these F1 hermaphrodites from cross II, on the following day (day 11), to determine the genotype. 8-10 F2 hermaphrodites (from the heterozygous F1 plate) were picked to individual plates four days after PCR, and this was repeated on the next day (day 16) and these are allowed to lay eggs overnight. SWPCR was performed on these F2 progeny to select the homozygous mutant worms. The embryos from the homozygous mutant F2 were used to maintain a population of 2x backcrossed mutant worms.

One of the mutant strains (VC2240, *acs-4(ok2872)*) was balanced by bli-4- and GFP-marked translocation (*acs-4(ok2872) III/hT2 [bli-4(e937) let-?(q782) qIs48] (I;III)*), since this is a homozygous sterile deletion. Therefore, for backcrossing this strain to WT background, it was first outcrossed to the balancer strain (*hT2 [bli-4(e937) let-?(q782) qIs48] (I;III),* obtained from Dr. Laura Mathies), followed by cross to N2. The steps in this cross are shown in Figure 7.

2x backcross for mutants of genes on Chr I-V

d1 Mutant hermaphrodite L4 $\frac{mut}{mut}$ X N2 Adult Male $\frac{+}{+}$ (Cross I)

d2 Singled mated mutant hermaphrodite adult

d5 F1 progeny (50% hermaphrodites; 50% males)

$\frac{mut}{+}$

F1 male $\frac{mut}{+}$ X N2 hermaphrodite L4 $\frac{+}{+}$ (Cross II)

d6 Singled mated N2 hermaphrodite adults

d10 F1 progeny of Cross II (50% hermaphrodites; 50% males)

$\frac{mut}{+}$ $\frac{+}{+}$ (1:1 ratio)

Singled F1 hermaphrodite adults (allowed to self-fertilize and lay embryos)

d11 SWPCR of F1 hermaphrodite adults that were allowed to lay eggs

d15 F2 progeny from heterozygous F1 hermaphrodite adults

$\frac{+}{+}$ $\frac{mut}{+}$ $\frac{mut}{mut}$ (1:2:1 ratio)

Singled 8-10 F2 hermaphrodite adults from the heterozygous mutant hermaphrodite adults from SWPCR of d11 (allowed to self-fertilize and lay embryos)

d16 SWPCR of singled F2 hermaphrodite adults from d15
Again singled 8-10 F2 hermaphrodite adults from the homozygous mutant hermaphrodite adults from SWPCR of d11 (allowed to self-fertilize and lay embryos)

d17 SWPCR of singled F2 hermaphrodite adults from d16
Selected worms from the homozygous mutant F2 hermaphrodite adult plates to maintain 2x backcrossed mutant strain

Figure 5. Genotypes and ratios of outcrossed progeny in the 2x outcross of mutants of genes on the autosomes (Chromosomes I-V)

2x backcross for mutants of genes on X-Chromosome

d1 Mutant hermaphrodite L4 $\frac{mut}{mut}$ X N2 Adult Male $\frac{+}{o}$ (Cross I)

d2 Singled mated mutant hermaphrodite adults

d5 F1 progeny (50% hermaphrodites; 50% males)

$\frac{mut}{+}$

F1 male X N2 hermaphrodite L4 $\frac{+}{+}$ (Cross II)

d6 Singled mated N2 hermaphrodite adults

d10 F1 progeny of Cross II (50% hermaphrodites; 50% males in 1:1 ratio)

$\frac{mut}{+}$

Singled F1 hermaphrodite adults (allowed to self-fertilize and lay embryos)

d15 F2 progeny from F1 hermaphrodite adults

$\frac{+}{+}$ $\frac{mut}{+}$ $\frac{mut}{mut}$ (1:2:1 ratio)

Singled 8-10 F2 hermaphrodite adults (allowed to self-fertilize and lay embryos)

d16 SWPCR of singled F2 hermaphrodite adults from d15
Again singled 8-10 F2 hermaphrodite adults (allowed to self-fertilize and lay embryos)

d17 SWPCR of singled F2 hermaphrodite adults from d16
Selected worms from the homozygous mutant F2 hermaphrodite adult plates to maintain 2x backcrossed mutant strain

Figure 6. Genotypes and ratios of outcrossed progeny in the 2x outcross of mutants of genes on the X-Chromosome

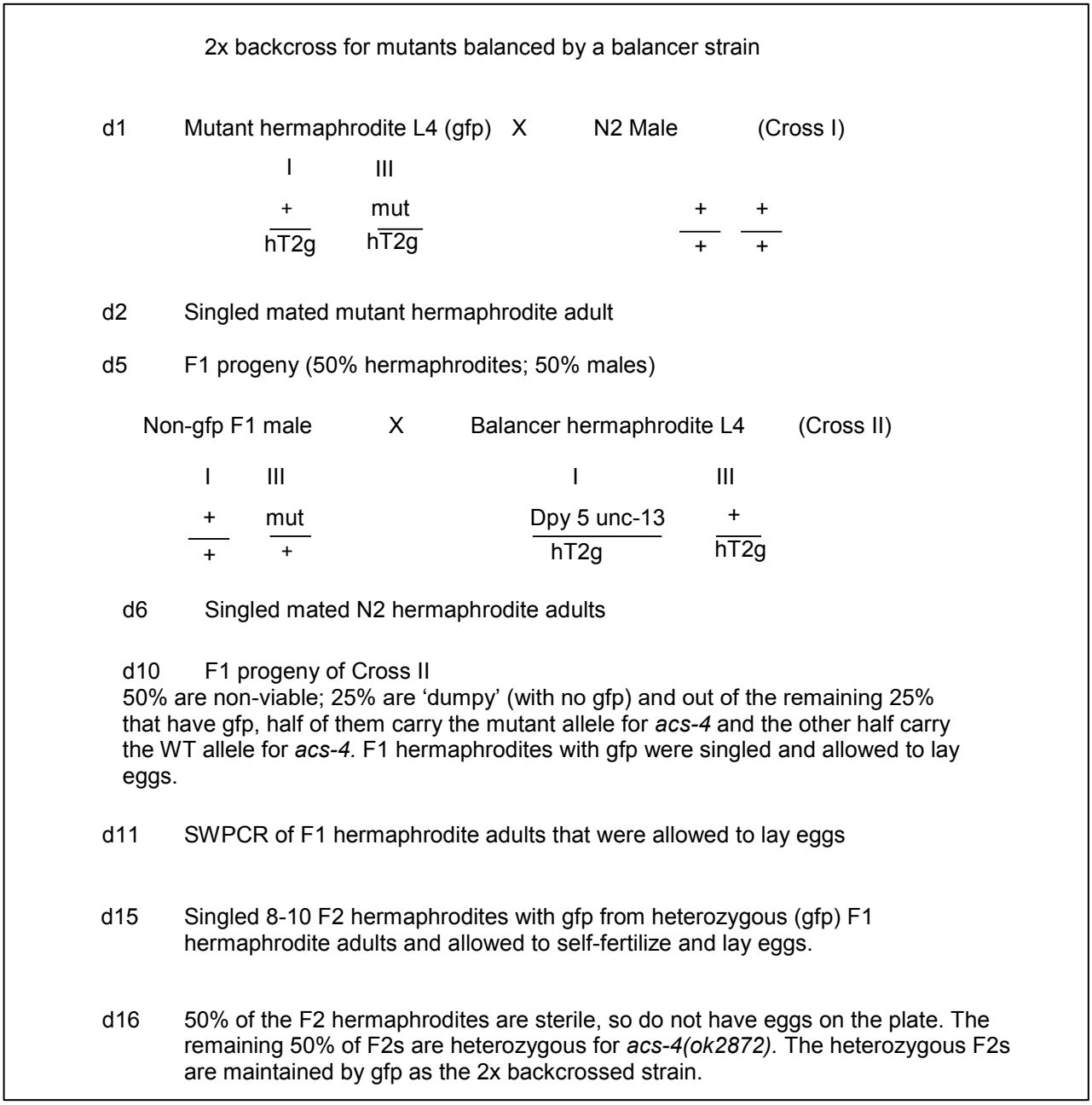

Figure 7. Genotypes of F1 and F2 progeny in the 2x backcross of mutants of balanced mutant strain: (acs-4(ok2872) III/hT2 [bli-4(e937) let-?(q782) qIs48] (I;III)

2.14 Behavioral assays on ethanol

Behavioral assays were performed to measure ethanol response of backcrossed If mutant strains and RNAi-fed worms.

The detailed protocol for performing behavioral assays on ethanol is given in Appendix I (Ethanol assay with copper rings). Approximately 24 hours before the assay, 20 L4s of each strain to be assayed were picked onto a separate seeded plate to get age-matched adults. NGM plates (unseeded) were dried for 2 hours at 37°C and weighed. Four copper rings were heated in a flame and were placed on the NGM agar in order to confine the worms to a small area, which allows us to assay four strains of worms on a plate. Copper is used for the rings because *C. elegans* are repelled by it. A volume of ice-cold (refrigerated at 4°C) 100% ethanol corresponding to the plate weight (to achieve a concentration of 400mM) was added (Appendix II, Table 18) to one of the plates (400mM assay plate). The plate was immediately sealed with Parafilm to prevent evaporation of ethanol and ethanol was allowed to equilibrate for two hours. Another plate of approximately the same weight was used as the 'control' 0mM assay plate. Two plates (for 0mM and 400mM) were used for acclimation to starve worms for 30 minutes prior to placing them on the assay plates. Each assay was performed with three strains of mutant worms and N2 as control, with 10 worms of each strain placed in each of the four copper rings. 2 minute time-lapse movies to track the locomotion of worms on the assay plates (0mM and 400mM) were captured using the ImagePro Plus software, at two different time points: 10 minutes and 30 minutes after worms were placed on the assay plates. The software captured 12-bit images of worms, one image per second, for 2 minutes (120 images), which tracked the movement of worms within each copper ring. Analysis of these assays was done using ImagePro Plus to obtain mean/average speeds of worms within each copper ring, at different time points, at the two

concentrations of ethanol (0mM and 400mM). In the analysis, the software was used to analyze speed of individual worms from one second to the next (over 120 seconds). The average velocity of each worm and the average velocity of all worms within the ring was calculated by the software. This data was exported into an excel file. The movies were recorded and analyzed as detailed in Appendix I (Computer Tracking and Analyzing Movies). Paired t-tests were performed on the mean/average speeds at the different time points and concentrations of ethanol (from the locomotion assays) using GraphPad Prism statistical software to determine initial sensitivity and acute tolerance of the mutant strains to ethanol, in comparison to N2/the WT strain.

Since acute exposure to ethanol is known to have a depressive effect on locomotion in *C. elegans*, we examined the following parameters using paired t-tests: a) if the speeds of mutant and WT worms were significantly different in terms of relative speeds at 10 minutes after exposure to ethanol (a measure of initial sensitivity) b) if the relative speeds of each strain (mutant and WT) were significantly different between 10 minutes and 30 minutes after exposure to ethanol (a measure of development of AFT) and c) if the recovery (difference between relative speeds at 10 minutes and 30 minutes of ethanol exposure) of mutant strain was significantly different compared to the recovery of WT strain.

These analyses helped us determine the ethanol responses in mutant strains; whether the mutant strain was more or less sensitive to ethanol compared to the WT strain and whether the recovery of mutant strain was more or less than that of the WT strain. This allowed us to draw inferences about the effects of target gene in ethanol response behavior.

For all the 2x backcrossed mutant strains, ethanol assays were performed at least four times (n=4) and among these, for the ones that did not show significant difference in ethanol responses compared to N2, n=6 was done. For the 6x backcrossed mutant strains, assays were done six times (n=6). All the RNAi fed worms were assayed at least eight times (n=8), since RNAi-mediated gene knockdown is usually more variable compared to a mutant.

3. RESULTS AND DISCUSSION

3.1 Candidate genes in mitochondrial beta-oxidation

As described in the Materials and Methods section, I began the candidate gene selection by identifying all the genes involved in the pathway by comparing the human and *C. elegans* mitochondrial beta-oxidation pathways. Based on this comparison, I derived three sets of genes (listed in Table 7): (1) genes from the *C. elegans* beta-oxidation pathway (2) *C. elegans* orthologs of the human beta-oxidation genes, obtained using an ortholog prediction tool, DIOPT v5.3 (DRSC Integrative Ortholog Prediction Tool) (Hu et al., 2011), (3) all other genes within each family of enzymes catalyzing the mitochondrial beta-oxidation pathway (for example, ACS family, ACDH family etc.,) that were not included in the human or *C. elegans* mitochondrial beta-oxidation pathways on KEGG.

Table 7. **List of all genes reviewed.** 'On KEGG & DIOPT' category includes the list of all genes that were common between the two sets of genes obtained from *C. elegans* KEGG mitochondrial beta-oxidation and the *C. elegans* genes that were found to be orthologs of human mitochondrial beta-oxidation pathway, using DIOPT. 'Only DIOPT' category includes the list of genes that were found to be orthologs of human mitochondrial beta-oxidation pathway but not included in the *C. elegans* mitochondrial beta-oxidation pathway. 'Only KEGG' category includes genes that were found in the *C. elegans* mitochondrial beta-oxidation pathway but not found to be orthologs of human mitochondrial beta-oxidation pathway, using DIOPT. 'Neither' category includes, genes that were members of the enzyme families catalyzing mitochondrial beta-oxidation but were not included in either of the above groups (KEGG or DIOPT).

On KEGG & DIOPT	**Only DIOPT**	**Only KEGG**	**Neither**
acs-3	*acs-23*	*acs-2*	*acs-1*
acs-4	*cpt-6*	*acs-16*	*acs-6*
acs-5	*W03F9.4*		*acs-7*
acs-13	*cpt-3*		*acs-8*
acs-15	*cpt-4*		*acs-9*
acs-17	*acdh-6*		*acs-10*
acs-18	*acdh-5*		*acs-11*
cpt-1	*acdh-2*		*acs-12*
cpt-2	*ech-7*		*acs-14*

acdh-7	*T02G5.4*		*acs-19*
acdh-8			*acs-20*
acdh-10			*acs-21*
acdh-12			*acs-22*
acdh-1			*cpt-5*
acdh-3			*acdh-9*
acdh-4			*acdh-11*
F54D5.7			*acdh-13*
ech-1.1			*ech-3*
ech-1.2			*ech-4*
ech-6			
ech-8			
ech-9			
B0272.3			
F54C8.1			
hacd-1			
acaa-2			
B0303.3			
T02G5.7			
kat-1			
TOTAL NUMBER OF GENES IN EACH CATEGORY			
29	10	2	19

We wanted to include the *C. elegans* orthologs of human mitochondrial beta-oxidation genes because this pathway has not been extensively studied in *C. elegans*, and hence it is possible that the roles of some *C. elegans* genes have not yet been identified in mitochondrial beta-oxidation and these would not be included in the pathway available on KEGG. There was some overlap between these two gene sets i.e., some genes that were found in the *C. elegans* mitochondrial beta-oxidation pathway were also orthologous to the human mitochondrial beta-oxidation genes (see Figure 8). The third set of 'all other genes in each enzyme family' was included to capture potential candidate genes that have not been characterized in mitochondrial-beta-oxidation and have also not been listed as orthologs to any of the human mitochondrial beta-oxidation genes in DIOPT, but possess enzymatic activity

in mitochondrial beta-oxidation (since they belong in the same family). These three sets of genes were reviewed based on the previously defined exclusion criteria, and the ones that could not be excluded were considered candidates. We did not use inclusion criteria to select candidate genes for this project because in order to have a strong basis for inclusion, these genes needed to be well characterized for their role in beta-oxidation. But for most of these genes there is little evidence implicating them in mitochondrial beta-oxidation. Therefore, using inclusion criteria would result in exclusion of majority of these genes due to lack of evidence. Lack of evidence does not mean that these genes do not have a role in mitochondrial beta-oxidation. So, we used exclusion criteria to make sure we did not miss any potential candidates due to lack of evidence. Excluded genes are listed in Table 8, along with the reason for exclusion for each gene. In retrospect, I am of the opinion that the C. elegans orthologs of human short-chain *ACS* genes (*ACSF, ACSS* and *ACSM*) should have been been included in the list of candidates. The reason for this is that the *C. elegans acs-2* gene is an ortholog of the human *ACSF2* and *acs-2* was found to have an effect on AFT in response to ethanol in *C. elegans*. This implies that the other *acs* genes that are orthologs of human short chain *ACS* genes could be potential candidates.

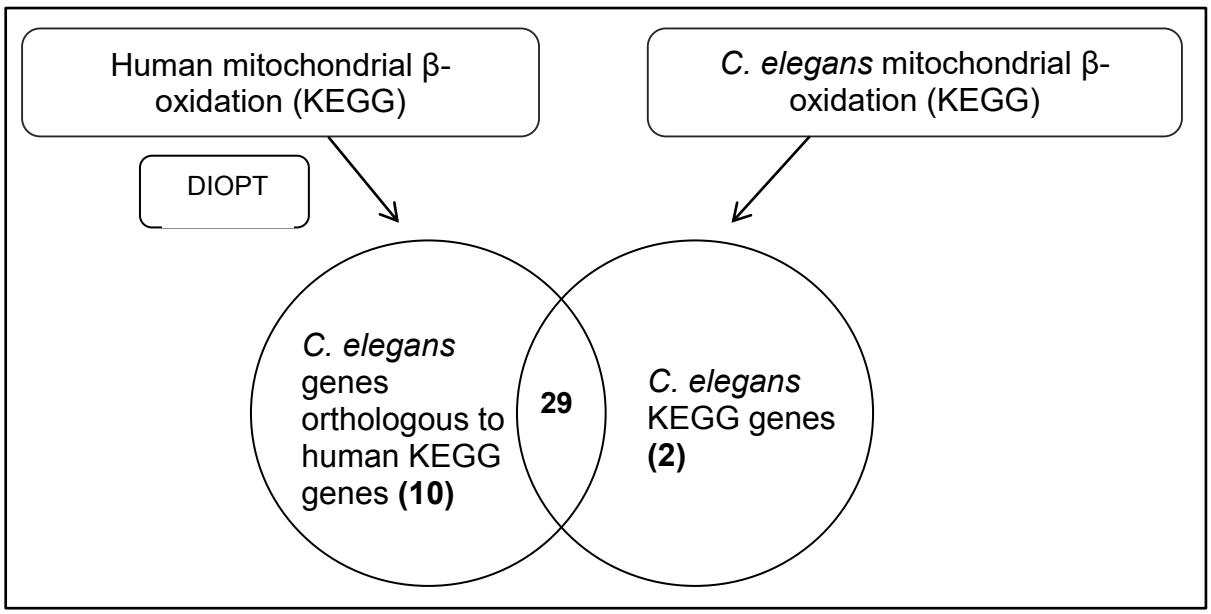

Figure 8. **Mitochondrial beta-oxidation genes in *C. elegans* and humans.** Two sets of genes were obtained by comparing the human and *C. elegans* mitochondrial beta-oxidation pathway on KEGG namely, *C. elegans* genes orthologous to human KEGG genes (that were determined using DIOPT, ortholog prediction tool) and genes from the *C. elegans* mitochondrial beta-oxidation pathway on KEGG.

Table 8. **Reasons for exclusion of genes.** This table contains a list of all genes that were excluded along with the reasons for exclusion.

Gene	Reason for exclusion
acs-1	Ortholog of ACSF2 which is not included in the human KEGG pathway of mitochondrial beta-oxidation
acs-6	Ortholog of ACSS1 which is not included in the human KEGG pathway of mitochondrial beta-oxidation
acs-7	Ortholog of ACSF2 which is not included in the human KEGG pathway of mitochondrial beta-oxidation
acs-8 (aka mec-18)	Irrelevant gene function – encodes protein similar to firefly luciferase. Also expressed exclusively in touch cells. Unlikely to be involved in mitochondrial beta-oxidation
acs-9	Ortholog of ACSS1, ACSS3 and ACSM1, ACSM5 - none of these genes are included in human KEGG pathway of mitochondrial beta-oxidation
acs-10	Ortholog of ACSS1 and ACSS2 – neither of these genes are included in human KEGG pathway of mitochondrial beta-oxidation
acs-11	Ortholog of ACSF3 which is not included in the human KEGG pathway of mitochondrial beta-oxidation
acs-12	Ortholog of ACSF2 and several ACSM genes which are not included in the human KEGG pathway of mitochondrial beta-oxidation
acs-14	Ortholog of ACSF2 which is not included in the human KEGG pathway of mitochondrial beta-oxidation
acs-19	Ortholog of ACSS2 which is not included in the human KEGG pathway of mitochondrial beta-oxidation
acs-20	Orthologs are FATP4 and several other solute carriers which are not included in the human KEGG pathway of mitochondrial beta-oxidation
acs-21	Ortholog ACSF3, ACSF2 which are not included in the human KEGG pathway of mitochondrial beta-oxidation
acs-23	Annotated as psuedogene on wormbase

acdh-9	Ortholog of ACAD8 and IVD - both of these are not included in the human KEGG pathway of mitochondrial beta-oxidation - ACAD8 catalyzes catabolism of valine amino acid in mitochondria, IVD catalyzes leucine catabolism; It is also annotated on KEGG as isobutyryl-CoA dehydrogenase to be involved in Valine, leucine and isoleucine degradation.
acdh-13 (aka gei-9)	Ortholog of human ACOX1 and ACOX2. Both these acyl CoA oxidases are involved in peroxisomal beta-oxidation of FA
ech-8	Ortholog of human EHHADH (ECH and HADH), a bifunctional enzyme that catalyzes peroxisomal beta-oxidation of FA
ech-9	Ortholog of human EHHADH (ECH and HADH), a bifunctional enzyme that catalyzes peroxisomal beta-oxidation of FA
ech-3	Ortholog of ECI1, which is not included in the human KEGG pathway of mitochondrial beta-oxidation. It is a peroxisomal auxillary enzyme that catalyzes an isomerization step in the oxidation of unsaturated fats.

Of the seven genes Dr. Alaimo tested, *acs-2* and *ech-6* lf exhibited significant ethanol responses, so these were not included in the candidate genes list. Among the remaining five genes he tested, I included *ech-1.1* and *ech-1.2* in the list of candidate genes and excluded the other three (*cpt-2, cpt-5* and *ech-4*) based on my exclusion criteria.

Therefore, for the first aim, I performed a review on 60 genes in total (see Table 7). I identified that 29 genes were common between the two gene sets (see Figure 8), 2 genes were exclusively present in the *C. elegans* KEGG pathway, 10 genes were obtained exclusively from DIOPT as orthologs of the human mitochondrial beta-oxidation genes and 19 genes were found in neither of the data sets, but reviewed because they were members of one of the gene families catalyzing beta-oxidation. Out of these 60 genes, based on the predetermined criteria, I excluded 18 genes (see Table 8). In total, I excluded 23 genes (18 genes that I reviewed and excluded + two genes (*acs-2, ech-6*) that Dr. Alaimo found to have a significant effect on ethanol responses + three genes (*cpt-2, cpt-5, ech-4*) that Dr. Alaimo already tested and I excluded). I considered the remaining 37 genes that could not be

excluded to be *bona fide* candidates and ensured that at least one gene in each step of the mitochondrial beta-oxidation pathway was included in these candidates. If mutant strains for 23 of the 37 candidate genes were available and we ordered these strains from the CGC. For the other 14 genes we decided to perform RNAi-mediated knockdown to test their role in ethanol response.

3.2 Ethanol response phenotypes of candidate genes in mitochondrial beta-oxidation

All the lf mutants and RNAi-mediated knockdown strains were assayed on ethanol for behavioral responses. Twenty-one of the 23 lf mutant strains were initially backcrossed twice (2x) and tested for their behavioral responses to ethanol (the results for these assays are summarized in Table 9 and the graphs are attached in Appendix III). Out of the 21 backcrossed mutants, 13 showed significantly different ethanol response phenotypes compared to WT (N2) and eight of them were not different from N2 in their ethanol responses. These eight strains were frozen and stored in the -80°C freezer. The 13 mutant strains that showed a significant difference were further backcrossed to 6x to achieve ~98.375% WT background and eliminate other, not closely linked, mutations, to ensure that the effect on ethanol response is likely to be due to lf of the candidate gene. These 6x-backcrossed mutants were assayed on ethanol to confirm the phenotypes observed in the 2x strains (the results for these assays are summarized in Table 10 and the graphs are attached in Appendix III). In five (*acs-4, acs-13, acs-22, cpt-3* and *T02G5.4*) of the 13 6x-backcrossed mutants tested, ethanol responses (initial sensitivity and/or AFT)

were no longer statistically significant in their difference from WT. A possible reason for this is that the ethanol response phenotypes observed in the 2x backcrossed strains could have been due to background mutations that were eliminated in the 6x backcross. The remaining 14 candidate genes did not have lf mutants available from the CGC, so we decided to perform RNAi to knockdown the function of these genes and test them on ethanol. One of the genes (*cpt-1*) was not available in the RNAi bacterial clones library (Ahringer, Geneservice, Cambridge, UK), five of the RNAi clones did not grow in culture and one RNAi clone did not carry the sequence of the target gene (*acs-16*). Therefore, seven genes were knocked down using RNAi clones and the effect of knockdown was tested on ethanol response (the results for these assays are summarized in Table 10 and the graphs are attached in Appendix III). Only two out of the seven RNAi genes (*acdh-10, acdh-12*) showed significantly different responses to ethanol compared to the L4440 (empty bacterial vector) treated worms. Since the effectiveness of RNAi across experimental trials and across different genes is not consistent, it is important to note that the lack of a significantly different ethanol response phenotype does not rule out the remaining five genes as potential candidates that could influence ethanol responses.

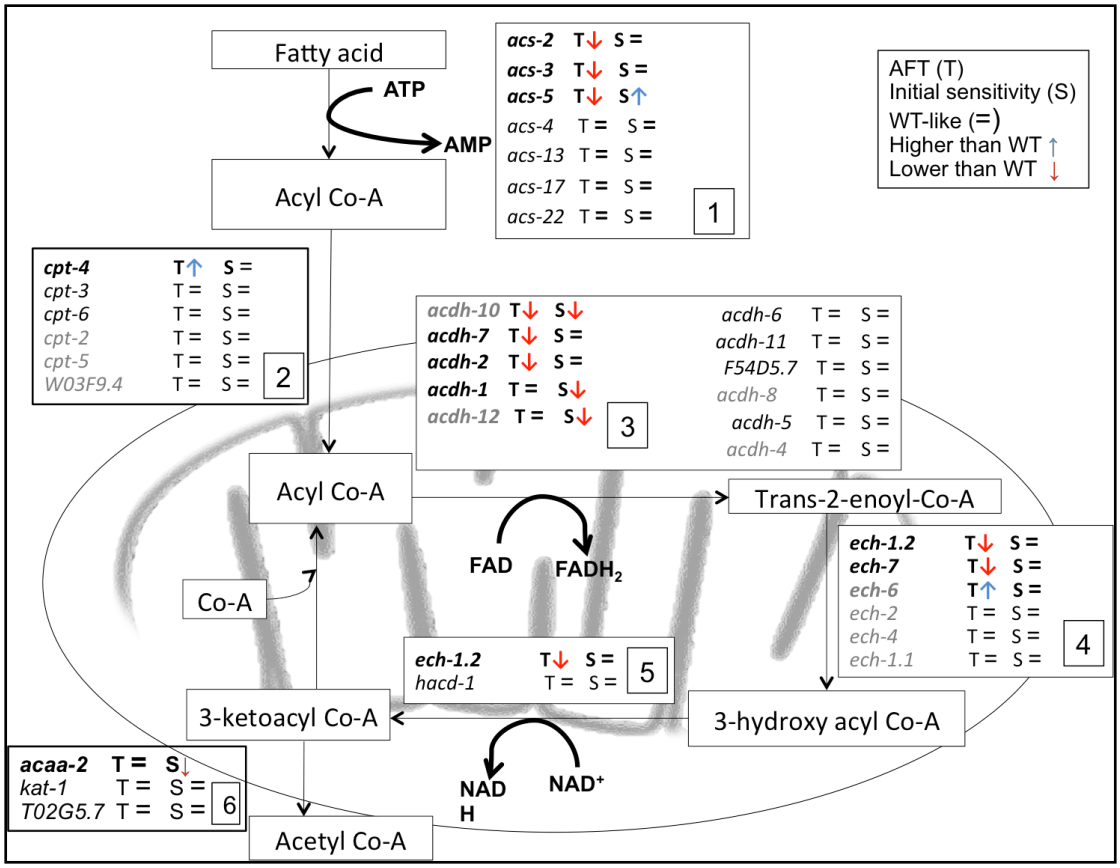

Figure 9. Mitochondrial beta-oxidation of FA showing genes tested at each step of the pathway and their ethanol response phenotypes: initial sensitivity (S) and AFT (T). The up (↑) arrow indicates more sensitive (S) or increased development of AFT (T) compared to WT worms (N2 or L4440) and down (↓) arrow indicates a less sensitive (S) or decreased AFT development (T) compared to WT worms. An 'equal to' (=) symbol indicates that the phenotype is not significantly different from that of WT worms. Genes that appear to modulate either one of the ethanol responses are highlighted in bold. RNAi knockdown genes are in gray font and lf mutants are in black font. Numbers in boxes
within each box of genes correspond to the following reaction steps, 1: Fatty acid → acyl CoA, catalyzed by acyl CoA synthetases (ACS) 2: Transport of acyl CoA from cytosol to mitochondria, catalyzed by carnitine palmitoyl transferases (CPT) 3: Acyl CoA → Trans-2-enoyl CoA, catalyzed by acyl CoA dehydrogenases 4: Trans-2-enoyl CoA → 3-hydroxy acyl CoA, catalyzed by enoyl CoA hydratases 5: 3-hydroxy acyl CoA → 3-keto acyl CoA, catalyzed by hydroxyl acyl CoA dehydrogenases 6: 3-keto acyl CoA → acyl $CoA_{(n-2)}$ + acetyl CoA, catalyzed by thiolases.

Table 9. Ethanol response phenotypes of 2x backcrossed loss of function (lf) mutants in the mitochondrial beta-oxidation pathway in *C. elegans*. The initial sensitivity and AFT values in this table are the relative speeds of the worms at the 10 minute and 30 minute time points respectively. The (10'-30') value for each strain represents the difference in relative speeds between the 10 minute and 30 minute time points, which is a measure of the degree of recovery.

Step catalyzed	**Genotype**	**Initial Sensitivity (IS)**			**Acute Functional Tolerance (AFT)**			**Ethanol response phenotypes**
		WT	**Mutant**	**Significance**	**WT**	**Mutant**	**Significance**	
Fatty acid → Fatty acyl CoA (ATP→AMP)	*acs-3(gk826522)*	N2 (10'): 35.48±2.78%	*acs-3* (10'): 26.89±2.046%	t_6= 3.36; P = 0.0437	N2 (30'): 51.19±1.84% N2 (10'-30'): 15.71±1.35%	*acs-3* (30'): 26.94±1.765% *acs-3* (10'-30'): 0.0400±0.52%	t_6= 11.88; P = 0.0013	More sensitive than N2; Reduced AFT than N2
	acs-4(ok2872)	N2 (10'): 42.90±3.97%	*acs-4* (10'): 25.90±2.87%	t_6= 5.596; P = 0.0025	N2 (30'): 59.30±4.71% N2 (10'-30'): 16.39±2.11%	*acs-4* (30'): 39.12±4.88% *acs-4* (10'-30'): 13.21±2.056	t_6= 2.513; P = 0.0536	More sensitive than N2; AFT not different from N2
	acs-5(ok2668)	N2 (10'): 40.61±2.75%	*acs-5* (10'): 12.11±1.97%	t_6= 7.161; P = 0.0008	N2 (30'): 53.07±1.99% N2 (10'-30'): 12.46±2.33%	*acs-5* (30'): 20.76±3.59% *acs-5* (10'-30'): 8.65±3.99%	t_6= 0.6185; P = 0.5633	More sensitive than N2; No (significant) development of AFT
	acs-13(ok2861)	N2 (10'): 35.48±2.78%	*acs-13* (10'): 49.68±2.67%	t_4 = 12.36; P = 0.0011	N2 (30'): 51.19±1.84% N2 (10'-30'): 15.71±1.35%	*acs-13* (30'): 64.31±3.05% *acs-13* (10'-30'): 14.63±2.76%	t_4 = 0.74; P = 0.5148	Less sensitive than N2; AFT not different from N2
	acs-17(ok1562)	N2 (10'): 40.61±2.75%	*acs-17* (10'): 42.04±2.29%	t_6= 0.3281; P = 0.7561	N2 (30'): 53.07±1.99% N2 (10'-30'): 12.46±2.33%	*acs-17* (30'): 51.51±1.50% *acs-17* (10'-30'): 9.47±2.58%	t_6= 0.6544; P = 0.5418	IS not different from N2; AFT not different from N2
	acs-22(gk364606)	N2 (10'): 37.52±3.28%	*acs-22* (10'): 38.35±2.16%	t_6= 0.1896; P = 0.8571	N2 (30'): 54.22±3.97% N2 (10'-30'): 16.71±2.33%	*acs-22* (30'): 44.59±3.00% *acs-22* (10'-30'): 6.23±1.61%	t_6= 6.565; P = 0.0012	IS not different from N2; Reduced AFT than N2
Cytosolic acyl CoA → Mitochondrial	*cpt-3(gk356297)**	N2 (10'): 39.64±2.43%	*cpt-3* (10'): 43.93±2.50%	t_8= 2.095; P = 0.0744	N2 (30'): 59.11±3.82% N2 (10'-30'):	*cpt-3* (30'): 56.10±2.15% *cpt-3* (10'-30'):	t_8= 1.751; P = 0.1234	IS not different from N2; AFT not different from N2

acyl CoA (Transport)					19.47±4.07%	12.17±2.30%		
	*cpt-4(gk818803)**	N2 (10'): 39.64±2.43%	*cpt-4* (10'): 37.97±2.96%	t_8= 0.5597; P = 0.5931	N2 (30'): 59.11±3.82% N2 (10'-30'): 19.47±4.07%	*cpt-4* (30'): 49.66±5.29% *cpt-4* (10'-30'): 11.70±3.16%	t_8= 1.348; P = 0.2211	IS not different from N2; AFT not different from N2
	cpt-6(gk594576)	N2 (10'): 33.71±0.92%	*cpt-6* (10'): 33.71±4.44%	t_4= 0.0010; P = 0.9992	N2 (30'): 50.85±1.42% N2 (10'-30'): 17.15±0.89%	*cpt-6* (30'): 48.94±2.45% *cpt-6* (10'-30'): 15.23±2.11%	t_4= 1.446; P = 0.2440	IS not different from N2; AFT not different from N2
Acyl CoA → Trans-2-enoyl CoA (FAD→$FADH_2$)	*acdh-1(ok1514)*	N2 (10'): 31.15%±1.38 %	*acdh-1* (10'): 42.17±3.03%	t_5= 2.857; P = 0.0461	N2 (30'): 48.12±1.40% N2 (10'-30'): 16.96±1.44%	*acdh-1* (30'): 55.29±1.14% *acdh-1* (10'-30'): 13.12±2.06%	t_5= 2.101; P = 0.1036	Less sensitive than N2; AFT not different from N2
	acdh-2(gk143151)	N2 (10'): 43.85±4.74%	*acdh-2* (10'): 43.80±3.85%	t_5= 0.008874; P = 0.9933	N2 (30'): 62.70±4.28% N2 (10'-30'): 18.86±1.41%	*acdh-2* (30'): 49.46±4.18% *acdh-2* (10'-30'): 5.66±0.54%	t_5= 8.252; P = 0.0012	IS not different from N2; Reduced AFT than N2
	acdh-5(gk907299)	N2 (10'): 35.31±1.23%	*acdh-5* (10'): 36.08±1.53%	t_6= 0.3125; P = 0.7673	N2 (30'): 52.20±1.58% N2 (10'-30'): 16.89±0.70%	*acdh-5* (30'): 51.88±2.35% *acdh-5* (10'-30'): 15.80±1.18%	t_6= 0.6510; P = 0.5438	IS not different from N2; AFT not different from N2
	acdh-6(gk886629)	N2 (10'): 35.31±1.23%	*acdh-6* (10'): 41.53±2.01%	t_6= 2.152; P = 0.0840	N2 (30'): 52.20±1.58% N2 (10'-30'): 16.89±0.70%	*acdh-6* (30'): 57.13±1.91% *acdh-6* (10'-30'): 15.60±0.42%	t_6= 2.132; P = 0.0862	IS not different from N2; AFT not different from N2
	acdh-7(gk556025)	N2 (10'): 31.15%±1.38 %	*acdh-7* (10'): 45.37±3.46%	t_5= 3.345; P = 0.0287	N2 (30'): 48.12±1.40% N2 (10'-30'): 16.96±1.44%	*acdh-7* (30'): 53.97±1.38% *acdh-7* (10'-30'): 8.59±2.47%	t_5= 3.090; P = 0.0366	Less sensitive than N2; Reduced AFT than N2
	acdh-11(gk753061)	N2 (10'): 35.31±1.23%	*acdh-11* (10'): 39.24±1.43%	t_6= 1.818; P = 0.1287	N2 (30'): 52.20±1.58% N2 (10'-30'): 16.89±0.70%	*acdh-11* (30'): 59.68±2.33% *acdh-11* (10'-30'): 20.44±1.71%	t_6= 1.593; P = 0.1720	IS not different from N2; AFT not different from N2
	F54D5.7(gk936057)	N2 (10'):	*F54D5.7* (10'):	t_4= 1.429; P	N2 (30'):	*F54D5.7* (30'):	t_4= 1.050; P	IS not different from N2; AFT

		33.71±0.92%	47.75±10.01%	= 0.2483	50.85±1.42% N2 (10'-30'): 17.15±0.89%	55.68±2.18% *F54D5.7* (10'-30'): 7.93±9.61%	= 0.3070	not different from N2
Trans-2-enoyl CoA → 3-hydroxy acyl CoA	*ech-1.2(gk527451)**	N2 (10'): 39.64±2.43%	*ech-1.2* (10'): 39.30±1.05%	t_8= 0.1110; P = 0.9147	N2 (30'): 59.11±3.82% N2 (10'-30'): 19.47±4.07%	*ech-1.2* (30'): 46.95±2.182% *ech-1.2* (10'-30'): 7.650±1.86%	t_8= 3.077; P = 0.0179	IS not different from N2; Reduced AFT than N2
3-hydroxy acyl CoA → 3-keto acyl CoA (NAD^+→NADH)	*hacd-1(ok2776)*	N2 (10'): 37.52±3.28%	*hacd-1* (10'): 36.23±2.15%	t_6= 0.3159; P = 0.7648	N2 (30'): 54.22±3.97% N2 (10'-30'): 16.71±2.33%	*hacd-1* (30'): 49.35±1.70% *hacd-1*(10'-30'): 13.12±1.46%	t_6= 2.007; P = 0.1010	IS not different from N2; AFT not different from N2
3 keto acyl CoA → Acetyl CoA (+ shortened fatty acyl CoA)	*T02G5.4(ok3160)*	N2 (10'): 31.15%±1.38 %	*T02G5.4* (10'): 40.26±1.86%	t_5= 3.472; P = 0.0255	N2 (30'): 48.12±1.40% N2 (10'-30'): 16.96±1.44%	*T02G5.4* (30'): 62.17±3.42% *T02G5.4* (10'-30'): 21.91±3.42%	t_5= 1.279; P = 0.2701	Less sensitive than N2; AFT not different from N2
	T02G5.7(ok3574)	N2 (10'): 33.71±0.92%	*T02G5.7* (10'): 37.39±2.24%	t_4= 1.926; P = 0.1498	N2 (30'): 50.85±1.42% N2 (10'-30'): 17.15±0.89%	*T02G5.7* (30'): 55.56±2.57% *T02G5.7* (10'-30'): 18.17±1.57%	t_4= 0.4682; P = 0.6715	IS not different from N2; AFT not different from N2
	acaa-2(ok1978)	N2 (10'): 40.61±2.75%	*acaa-2* (10'):46.73±2.21%	t_6= 2.010; P = 0.1006	N2 (30'): 53.07±1.99% N2 (10'-30'): 12.46±2.33%	*acaa-2* (30'): 54.37±1.29% *acaa-2* (10'-30'): 7.64±1.83%	t_6= 2.576; P = 0.0496	Less sensitive than N2; AFT not different from N2

Table 10. Ethanol response phenotypes of 6x backcrossed lf mutants and RNAi knockdown strains in mitochondrial beta-oxidation pathway in *C. elegans.* The initial sensitivity and AFT values in this table are the relative speeds of the worms at the 10 minute and 30 minute time points respectively. The (10'-30') value for each strain represents the difference in relative speeds between the 10 minute and 30 minute time points, which is a measure of the degree of recovery. (Note: For all the 6x backcrossed mutants, the N2s used as WT for the behavioral assays are different from the N2s used for the backcrossing. In the lab, it is standard practice to thaw out and use a new stock of N2 worms once a year or every few months since it is possible that the N2 strain being maintained in the lab accumulates genetic mutations over time and is no longer 'WT').

Step catalyzed	**Genotype**	**Initial Sensitivity (IS)**			**Acute Functional Tolerance (AFT)**			**Ethanol response phenotypes**
		WT	**Mutant**	**Significance**	**WT**	**Mutant**	**Significance**	
Fatty acid → Fatty acyl CoA (ATP→AMP)	*acs-3(gk826522)*	N2 (10'): 34.81±2.17%	*acs-3* (10'): 32.18±2.65%	t_6= 0.9188; P = 0.4003	N2 (30'): 47.03±1.96% N2 (10'-30'): 12.22±1.45%	*acs-3* (30'): 33.51±2.97% *acs-3* (10'-30'): 1.33±1.23%	t_6= 11.32; P < 0.0001	IS not different from N2; No development of AFT
	acs-4(ok2872)	N2 (10'): 35.04±2.03%	*acs-4* (10'): 35.60±5.49%	t_6= 0.1438; P = 0.8913	N2 (30'): 47.30±2.14% N2 (10'-30'): 12.27±1.06%	*acs-4* (30'): 50.81±5.27% *acs-4* (10'-30'): 15.21±3.76%	t_6= 0.8301; P = 0.4443	IS not different from N2; AFT not different from N2
	acs-5(ok2668)	N2 (10'): 30.75±2.61%	*acs-5* (10'): 16.03±1.99%	t_6= 5.336; P = 0.0031	N2 (30'): 45.27±2.24% N2 (10'-30'): 14.53±1.18%	*acs-5* (30'): 19.23±1.50% *acs-5* (10'-30'): 3.21±0.83%	t_6= 10.34; P = 0.0001	More sensitive than N2; Reduced development of AFT
	acs-13(ok2861)	N2 (10'): 30.75±2.61%	*acs-13* (10'): 37.88±4.24%	t_6 = 1.214; P = 0.2788	N2 (30'): 45.27±2.24% N2 (10'-30'): 14.53±1.18%	*acs-13* (30'): 66.50±23.73% *acs-13* (10'-30'): 28.62±19.93%	t_6 = 0.7020; P = 0.5140	IS not different from N2; AFT not different from N2
	acs-22(gk364606)	N2 (10'): 30.75±2.61%	*acs-22* (10'): 38.47±3.45%	t_6= 1.707; P = 0.1486	N2 (30'): 45.27±2.24% N2 (10'-30'): 14.53±1.18%	*acs-22* (30'): 47.11±3.12% *acs-22* (10'-30'): 8.64±2.62%	t_6= 1.937; P = 0.1104	IS not different from N2; AFT not different from N2
Cytosolic acyl CoA → Mitochondrial acyl CoA (Transport)	*cpt-3(gk356297)*	N2 (10'): 34.77±1.80%	*cpt-3* (10'): 38.50±3.44%	t_6= 1.369; P = 0.2293	N2 (30'): 45.15±3.15% N2 (10'-30'): 10.38±1.90	*cpt-3* (30'): 47.32±2.99% *cpt-3* (10'-30'): 8.817±1.698%	t_6= 1.074; P = 0.3319	IS not different from N2; AFT not different from N2
	cpt-4(gk818803)	N2 (10'):	*cpt-4* (10'):	t_6= 0.1537; P =	N2 (30'):	*cpt-4* (30'):	t_6= 3.777; P =	IS not different from N2;

		36.74±2.46%	37.14±0.50%	0.8838	47.65±2.08% N2 (10'-30'): 10.91±0.76%	54.32±0.87% *cpt-4* (10'-30'): 17.18±1.01%	0.0129	Higher development of AFT than N2
	W03F9.4 (RNAi)	L4440 (10'): 31.99±2.41%	*W03F9.4* (10'): 31.25±2.71%	t_8= 0.2630; P = 0.8002	L4440 (30'): 42.83±2.09% L4440 (10'- 30'): 10.84±2.09%	*W03F9.4* (30'): 45.18±3.42% *W03F9.4* (10'- 30'): 13.92±2.51%	t_8= 1.370; P = 0.2130	IS not different from L4440; AFT not different from L4440
Acyl CoA → Trans-2-enoyl CoA ($FAD \rightarrow FADH_2$)	*acdh-1(ok1514)*	N2 (10'): 32.31±2.22%	*acdh-1* (10'): 51.05±3.62%	t_6= 3.945; P = 0.0109	N2 (30'): 46.80±2.27% N2 (10'-30'): 14.10±0.87%	*acdh-1* (30'): 59.29±2.13% *acdh-1* (10'-30'): 8.24±3.65%	t_6= 2.222; P = 0.0770	Less sensitive than N2; AFT not different from N2
	acdh-2(gk143151)	N2 (10'): 32.31±2.22%	*acdh-2* (10'): 45.30±1.52%	t_6= 4.076; P = 0.0096	N2 (30'): 46.80±2.27% N2 (10'-30'): 14.10±0.87%	*acdh-2* (30'): 53.32±2.78% *acdh-2* (10'-30'): 8.02±2.89%	t_6= 2.525; P = 0.0529	IS not different from N2; Reduced AFT than N2
	acdh-4 (RNAi)	L4440 (10'): 28.54±1.69%	*acdh-4* (10'): 33.90±4.36%	t_8= 1.650; P = 0.1428	L4440 (30'): 44.09±2.11% L4440 (10'- 30'): 15.56±1.38%	*acdh-4* (30'): 48.66±4.91% *acdh-4* (10'-30'): 14.76±2.726%	t_8= 0.3117; P = 0.7644	IS not different from L4440; AFT not different from L4440
	acdh-7(gk556025)	N2 (10'): 32.31±2.22%	*acdh-7* (10'): 38.92±4.05%	t_6= 1.573; P = 0.1766	N2 (30'): 46.80±2.27% N2 (10'-30'): 14.10±0.87%	*acdh-7* (30'): 43.98±3.31% *acdh-7* (10'-30'): 5.065±2.83%	t_6= 3.510; P = 0.0171	IS not different from N2; Reduced AFT than N2
	acdh-8 (RNAi)	L4440 (10'): 28.46±1.93	*acdh-8* (10'): 30.03±2.46%	t_8= 1.357; P = 0.2169	L4440 (30'): 44.35±2.15% L4440 (10'- 30'): 15.89±1.34%	*acdh-8* (30'): 46.53±2.78% *acdh-8* (10'-30'): 16.50±1.46%	t_6= 0.3235; P = 0.7557	IS not different from L4440; AFT not different from L4440
	acdh-10 (RNAi)	L4440 (10'): 29.19±1.76%	*acdh-10* (10'): 38.72±1.89%	t_8= 6.182; P = 0.0005	L4440 (30'): 43.94±2.14% L4440 (10'- 30'): 14.75±1.22%	*acdh-10* (30'): 50.20±2.14% *acdh-10* (10'- 30'): 11.48±1.00%	t_8= 2.788; P = 0.027	Less sensitive than L4440; Reduced AFT than L4440

	acdh-12 (RNAi)	L4440 (10'): 31.05±2.69%	*acdh-12* (10'): 39.10±2.34%	t_8= 3.039; P = 0.0189	L4440 (30'): 44.07±2.47% L4440 Rec (10'-30'): 13.02±1.19%	*acdh-12* (30'): 54.16±2.94% *acdh-12* Rec (10'-30'): 15.07±2.41%	t_8= 0.7977; P = 0.4512	Less sensitive than L4440; AFT not different from L4440
Trans-2-enoyl CoA → 3-hydroxy acyl CoA	*ech-1.2(gk527451)*	N2 (10'): 36.74±2.46%	*ech-1.2* (10'): 43.60±3.69%	t_6= 1.457; P = 0.2048	N2 (30'): 47.65±2.08% N2 (10'-30'): 10.91±0.76%	*ech-1.2* (30'): 56.02±4.38% *ech-1.2* (10'-30'): 3.63±1.56%	t_6= 5.824; P = 0.0021	IS not different from N2; Reduced AFT than N2
	ech-1.1 (RNAi)	L4440 (10'): 31.05±2.69%	*ech-1.1* (10'): 36.90±4.23%	t_8= 1.133; P = 0.2946	L4440 (30'): 44.07±2.47% L4440 (10'-30'): 13.02±1.19%	*ech-1.1* (30'): 52.39±4.85% *ech-1.1* (10'-30'): 15.49±3.59%	t_8= 0.5919; P = 0.5726	IS not different from L4440; AFT not different from L4440
3 keto acyl CoA → Acetyl CoA (+ shortened fatty acyl CoA)	*T02G5.4(ok3160)*	N2 (10'): 34.77±1.80%	*T02G5.4* (10'): 43.60±2.44%	t_6= 2.427; P = 0.0596	N2 (30'): 45.15±3.15% N2 (10'-30'): 10.38±1.90%	*T02G5.4* (30'): 55.79±4.36% *T02G5.4* (10'-30'): 12.19±2.78%	t_6= 0.5017; P = 0.6372	IS not different from N2; AFT not different from N2
	acaa-2(ok1978)	N2 (10'): 34.77±1.80%	*acaa-2* (10'): 39.09±2.17%	t_6= 4.066; P = 0.0097	N2 (30'): 45.15±3.15% N2 (10'-30'): 10.38±1.90%	*acaa-2* (30'): 52.28±2.91% *acaa-2* (10'-30'): 13.19±1.89%	t_6= 0.9148; P = 0.4023	Less sensitive than N2; AFT not different from N2
	B0303.3 (RNAi)	L4440 (10'): 30.24±3.03%	*B0303.3* (10'): 29.75±2.86%	t_6= 0.2232; P = 0.8298	L4440 (30'): 44.74±2.50% L4440 (10'-30'): 14.51±1.51%	*B0303.3* (30'): 44.48±3.54% *B0303.3* (10'-30'): 14.74±1.82%	t_6= 0.1214; P = 0.9067	IS not different from L4440; AFT not different from L4440

3.3 Ethanol affects mitochondrial beta-oxidation

A search on NCBI (PubMed Central) for 'mitochondrial beta-oxidation AND ethanol' gives 13325 results, 8226 of them published in the last five years. A majority of studies examines the effects of alcohol/ethanol on mitochondrial function, particularly in hepatocytes, since the liver is the primary site for alcohol metabolism. Several research groups have also dissected the molecular mechanisms underlying mitochondrial dysfunction in neurodegenerative diseases like Alzheimer's disease, Parkinson's disease, Huntington's disease and alcoholic dementia (Akbar et al., 2016; Srivastava et al., 2010).

Ethanol has been found to cause mitochondrial dysfunction, damage to mitochondrial DNA and inhibition of mitochondrial beta-oxidation of FA. Ethanol also affects oxidative phosphorylation and electron transport chain processes in the mitochondria. The focus has been on the role of mitochondria in progression of alcoholic liver diseases (ALD) and its usefulness as a therapeutic target for ALD (Apostolova & Victor, 2015; King et al., 2016). Mitophagy has been found to prevent cell death in alcohol-induced liver injury by removing damaged mitochondria that are unable to perform beta-oxidation of FA (Ding et al., 2011).

Andringa et al., (2010) used Male Sprague-Dawley rats to analyze the effect of ethanol on the liver mitochondria proteome. They pair fed these rats a control diet and an ethanol-containing diet for at least 31 days and then

performed a series of experiments to look at how mitochondrial proteins respond to alcohol exposure. They extracted and separated mitochondrial proteins by isoelectric focusing followed by gel electrophoresis. The 2D gel image analysis of these mitochondrial proteins showed that 30 of the 76 proteins examined were altered in abundance in response to ethanol. Using mass-spectrometry analysis, they identified these proteins and grouped them into four functional classes, one of them being mitochondrial-beta-oxidation. They determined that several enzymes involved in mitochondrial beta-oxidation, long-chain ACDH, ECH and long-chain HADH, were significantly decreased in the alcohol-fed rats compared to controls.

To assess the effect of ethanol on mitochondrial outer membrane (MOM) permeability Holmuhamedov & Lemasters (2009) incubated isolated rat hepatocytes with ethanol and exposed the cells to a low concentration of digitonin, which selectively permeabilizes the plasma membrane to allow entry of adenine nucleotides and exogenous respiratory substrates like succinate. They measured oxygen consumption and adenylate kinase activity before and after digitonin treatment and found that ethanol pretreatment decreased succinate-supported respiration. Also, MOM permeabilization with high digitonin overcame the effects of ethanol and restored respiration and adenylate kinase activity. Moreover, high digitonin treatment of untreated hepatocytes did not change the rate of succinate-supported respiration or adenylate kinase activity. These results suggested that MOM permeability to hydrophilic metabolites decreases after ethanol treatment. Since voltage dependent anion channel (VDAC) is the only channel known to allow

hydrophilic metabolites to cross the outer membrane of the mitochondria in normal viable cells, they hypothesized that ethanol-induced decrease of mitochondrial outer membrane permeability could be through inhibition of VDAC.

In another study performed in cultured rat hepatocytes, Bailey et al., (1999) found that ethanol decreased mitochondrial FA oxidation and production of ATP. They hypothesized that this could be through the inhibition of the conductance of VDAC in the mitochondrial outer membrane since VDAC is essential for maintaining the permeability of outer mitochondrial membrane to molecules that are necessary for beta-oxidation such as ATP, ADP and fatty acyl CoA. Bailey and Cunningham (1998) found that ethanol also altered cellular energy balance, which plays a role in beta-oxidation. Specifically, they found that in isolated hepatocytes, acute ethanol exposure increased the cellular NADH/NAD^+ ratio, which would be predicted to inhibit mitochondrial beta-oxidation, as it is an allosteric regulator of the pathway. They hypothesized that this increase could be due to increase in production of mitochondrial reactive oxygen species (ROS) (Bailey et al., 1999). Thus, it is clear that ethanol affects various biological pathways occurring in the mitochondria, and that mitochondrial beta-oxidation of FA is one of them.

While the effects of ethanol on mitochondrial function and beta-oxidation of FA has been well studied, there has not been much research on how the various components of beta-oxidation in mitochondria affect ethanol metabolism and its effects on the organism. For the purpose of this project,

we were particularly interested in examining whether mitochondrial beta-oxidation has a role in neuronal responses to ethanol exposure. We tested genes at every step of mitochondrial beta-oxidation. Our results from behavioral assays of lf mutants and RNAi knockdown strains indicate that there is certainly more than one step or enzyme or reaction component of the pathway that is involved in mediating this effect.

It is important to keep in mind while interpreting this data that (1) a majority of the enzymes catalyzing this pathway exhibit chain-length specificity (2) there are several aspects of beta-oxidation that have diverse physiological functions, like free fatty acids (FFA, the first substrate of beta-oxidation), energy transfers that occur during beta-oxidation, and intermediate products like fatty acyl CoA. Long chain FFA increase mitochondrial permeability, uncouple oxidative phosphorylation and inhibit ATP synthesis while non-esterified FA are metabolized into diacyl glycerol (DAG) (Wojtczak & Schonfeld, 1993). Acyl CoA derivatives inhibit tricarboxylic acid (TCA) cycle and also competitively inhibit activation of pyruvate carboxylate, which is an enzyme involved in gluconeogenesis. Acyl CoA also plays a role in synthesis of polar and neutral lipids, and TAGs. The functions of these components of beta-oxidation are discussed in detail in subsequent paragraphs.

3.4 Acyl CoA Synthases (ACS)

Acyl CoA synthases (ACS) catalyze the first step of mitochondrial beta-oxidation, converting FA to fatty acyl CoA (Figure 9). We examined seven *acs*-family genes including *acs-2,* which was previously tested by Dr. Alaimo

(see Introduction) and three of the lf mutant strains showed a significantly different ethanol response phenotype. *acs-2* displayed reduced AFT compared to WT but did not differ significantly in initial sensitivity. *acs-3* mutants did not develop AFT in response to ethanol, but were not significantly different from WT in terms of initial sensitivity. *acs-5* showed reduced AFT development and increased sensitivity in response to ethanol compared to WT worms. *acs-4, acs-13, acs-17* and *acs-22* lf strains showed ethanol responses similar to WT. At the 2x backcrossed stage, *acs-4, acs-13* and *acs-22* also showed a significant ethanol response phenotypes, but the significance of this was lost when backcrossed to 6x. This may not be surprising, because by backcrossing we are eliminating possible background mutations. So, it is possible that the phenotypes are less robust in the 6x-backcrossed strain of certain mutants compared to their 2x-backcrossed strain which implies that the ethanol response phenotypes observed in the 2x-backcrossed mutants could have been due to the effect of background mutations in the mutant strains.

Disruption of the esterification or activation of FA to fatty acyl CoA would lead to an increase in the levels of FFA and decrease in acyl CoA. FFA, which are the first substrate in the beta-oxidation of FA, have diverse physiological functions. Among their functions is a role in the activation of protein kinase C (PKC) in different cells or organs (Boneh, 1996). PKC is a family of enzymes that activate or regulate other proteins by phosphorylation of hydroxyl groups on the serine and threonine residues of the target proteins. One member of this family is the PKCγ, which is solely expressed in the brain and spinal cord.

It is activated by Ca^{+2}, phosphatidylserine and DAGs. PKCγ is also activated by unsaturated FA, with the extent of activation being proportional to the degree of unsaturation (Nishizuka, 1992). Studies have shown that γ-aminobutyric acid A ($GABA_A$) receptors in the brain of PKCγ-deficient mice do not respond to ethanol, and the PKCγ-deficient mice show a reduced sensitivity to acute ethanol (measured using righting reflex and body temperature). Saito & Shirai (2002) suggested that PKCγ modulates the sensitivity of $GABA_A$ receptors to ethanol. GABA is an inhibitory neurotransmitter and $GABA_A$ is a class of GABA receptors. It has been shown in numerous research studies that ethanol potentiated $GABA_A$ mediated current, which increased the action of GABA at these receptors (Davies, 2003). Breaking down the hypothesis of Saito & Shirai, in the absence of PKCγ the $GABA_A$ receptors would not be potentiated by ethanol and therefore there would be decreased/no action of GABA at these receptors. This in turn, would result in decreased inhibitory action of GABA on the nervous system, which would explain the reduced sensitivity of PKCγ-deficient mice to acute ethanol. Applying these findings to the ethanol response phenotype we saw in some of the *acs* mutants (*acs-3, acs-4* and *acs-5* showed increased sensitivity to ethanol, and *acs-5* showed reduced development of AFT), I hypothesize that lack of ACS activity in these mutants would lead to the buildup of FFA. This could increase activation of PKCγ, which, in turn, could lead to increased sensitivity to ethanol compared to the WT worms in which there is comparatively less amount of FFA. To test this hypothesis, we could create and test a double mutant of *pkc-2;acs-5* (that has lf in *pkc-2,* which is the PKCγ in *C. elegans* and *acs-5*) for ethanol responses. We could then express

pkc-2 specifically in the neurons expressing $GABA_A$ receptors in the double mutants using the promoter of *unc-49*. The reason for creating a *pkc-2(lf)* specifically in these neurons is to make sure that the effect of *pkc-2(lf)* on ethanol response phenotypes we expect to see would not be confounded by potential action of PKC through other neurotransmitter receptors. If lack of *acs-5* activity is indeed modulating sensitivity to ethanol through PKC activation and GABA, we would expect the sensitivity of the *pkc-2;acs-5* lf double mutant to be lower than that of the *acs-5(lf)*, since there is no PKC for the FFA to activate and therefore, no potentiation of GABA.

FFA have also been found to affect neurotransmitter receptors; particularly neuronal nicotinic acetylcholine receptors (nAChRs) in various *in vitro* and *in vivo* models, but the results from these studies are conflicting (Albuquerque et al., 2009; Antollini & Barrantes, 2016) showed that FFAs had an inhibitory effect on nAChR. Ikeuchi et al., 1996 suggested that the effects of FA on nAChRs vary across species, possibly due to the differences in receptor subunit structure and composition in various organisms. They saw a potentiation effect of arachidonic acid (AA), a PUFA, on Torpedo nAChR expressed in Xenopus oocytes and treatment of chick α7 nAChR with AA caused a depression effect while treatment of rat α7 nAChR caused exclusively a potentiation effect by PKC activation.

α7 nAChRs have also been extensively studied in understanding the mechanism of ethanol's action on the brain. McDaid et al., 2016 tested effects of ethanol on α7 nAChRs using brain sections of male Sprague Dawley rats.

They performed electrophysiological studies to measure nAChR-mediated currents, on isolated sections containing laterodorsal tegmental nucleus (LDTg), where the α7 receptors are expressed abundantly. They found that pretreatment with 25mM ethanol for 10 minutes inhibited α7 nAChR currents significantly. Yu et al., (1996) using α7 nAChRs expressed in Xenopus oocytes, looked at the effect of ethanol on these receptors. Their electrophysiological recordings of nAChR currents using two-electrode voltage clamp, revealed that application of ethanol inhibited α7 nAChR currents in a concentration-dependent manner over a concentration range of 5-100 mM ethanol. Studies in cultured rat cortical neurons showed that ethanol potentiated non-α7 nAChR- but inhibited α7 nAChR-mediated currents. In Xenopus oocytes, ethanol at low concentrations inhibited α7 nAChR currents but potentiated α2β4, α4β4, α2β2, and α4β2 nAChRs at higher concentrations (Wu et al., 2014). Seeing that the α7 nAChR has been widely studied in the context of FFA and neuronal effect of ethanol, I consider it as an ideal candidate to pursue for future experiments.

Based on the evidence discussed above, I propose a model to test if the effect of *acs* lf on ethanol responses acts through regulation of α7 nAChR by FFA. In *C. elegans*, *acr-16* codes for a α7-like subunit of nAChR, which is orthologous to the human nAChR α7 (sharing 81.7% protein sequence identity). An *acr-16* mutant was tested by Patraic Lichtman (a student in the Davies-Bettinger lab) for effects on ethanol response phenotypes and he found that this mutant is resistant to ethanol (decreased sensitivity compared to N2), which supports previous findings that ethanol could be acting through

inhibition of α7 nAChR. Lf mutants of *acs-3, acs-4* and *acs-5* showed increased sensitivity to ethanol. If the effect of loss of *acs* function on sensitivity is due to action of FFA on ACR, I hypothesize that, a double mutant of *acs-5;acr-16* lf assayed on ethanol would display decreased initial sensitivity compared to *acs-5* lf mutants. *acs-5* lf would increase concentration of FFA, but due to lf in *acr-16*, the FFA would be unable to potentiate the α7-like receptor, due to which I predict that the initial sensitivity would be decreased compared to the *acs-5* mutant.

We can see that while *acs-5(lf)* results in increased initial sensitivity, *acs-2, acs-3* and *acs-5* appear to be important for AFT, since worms carrying deletions in these genes exhibit reduced AFT relative to N2. A possible reason for the varying effects of different *acs* genes on the two ethanol responses phenotypes could be that each of these enzymes catalyzes esterification of FA for different pathways, and some of these pathways might affect only one of the two ethanol response components we are studying. For example, loss of *acs-2* function affects tolerance but not sensitivity and loss of *acs-4* affects sensitivity, not AFT. On the other hand, *acs-22, acs-17* and *acs-13* lf do not have any effect on either sensitivity or AFT to ethanol. From studying human ACS genes, we know that each member of the ACS family preferentially catalyzes the esterification of specific chain lengths of FA and directs the FA-CoAs into different downstream processes (Figure 10). Therefore, it is possible that these *acs*-genes partition the acyl CoA into downstream pathways that vary in their effects on ethanol response behavior.

Since there has not been very extensive research conducted on worm ACS enzymes, we used evidence from human (cell culture studies) and mouse models looking at the orthologs of these worm genes to understand the various pathways into which acyl CoAs are partitioned by the different ACS genes (Table 11).

Table 11. Human and Mouse orthologs of *acs* genes tested for ethanol responses.

acs* genes in *C. elegans	**Human Ortholog**	**Mouse Ortholog**
acs-2	ACSF2	ACSF2
acs-4 & acs-17	ACSL3/ACS3 ACSL4/ACS4	ACSL3 ACSL4
acs-5, acs-3 & acs-13	ACSL1 ACSL5 ACSL6	ACSL5
acs-22	SLC27A1 (FATP1) SLC27A2 (FATP2) SLC27A3 (FATP3) SLC27A4 (FATP4) SLC27A5 (FATP5) SLC27A6 (FATP6)	SLC27A1 (FATP1) SLC27A2 (FATP2) SLC27A4 (FATP4) SLC27A5 (FATP5)

As briefly discussed in the Introduction, ACS enzymes catalyze the activation/esterification of FFA into fatty acyl CoA in an ATP-dependent reaction. The fatty acyl CoA produced can enter the mitochondrial matrix (long-chain FA-CoAs require carnitine for transport while short and medium-chain FA-CoAs can directly enter the matrix), or can become involved in a variety of other biological processes including synthesis of TAGs, sphingolipids, phospholipids, protein acetylation and transcriptional regulation of gene expression (Watkins & Ellis, 2012).

The Coleman group has been studying ACS enzymes for several years using a combination of *in vitro* overexpression in rat cell lines and *in vivo* knockout mouse models. They have characterized the structure, tissue localization (Mashek et al., 2007) and physiological functions various ACS family members (Cooper et al., 2015). Their experiments using broad and specific inhibitors of ACS enzymes revealed that both ACS1, which is expressed in heart, liver and adipose tissues, and ACS2, a brain-specific subtype, exhibit broad substrate specificity and show structural similarity. ACS3 is highly expressed in brain and uses laurate and myristate most efficiently among the C8–C22 saturated FA and arachidonate and eicosapentaenoate among the C16–C22 unsaturated FA. ACS4 shows a preference for arachidonate and eicosapentaenoate (PUFAs) and C14-C22 unsaturated FA, and exhibits a low affinity for palmitate (Kang et al., 1997). Also, the Coleman group showed that specific inhibition of ACS1 and ACS4 suggested that they are involved in triacylglycerol synthesis and *de novo* synthesis of phospholipids and phospholipid reacylation. This also suggested that oxidation must rely on acyl-CoA synthesized by other isoforms (Coleman et al., 2002).

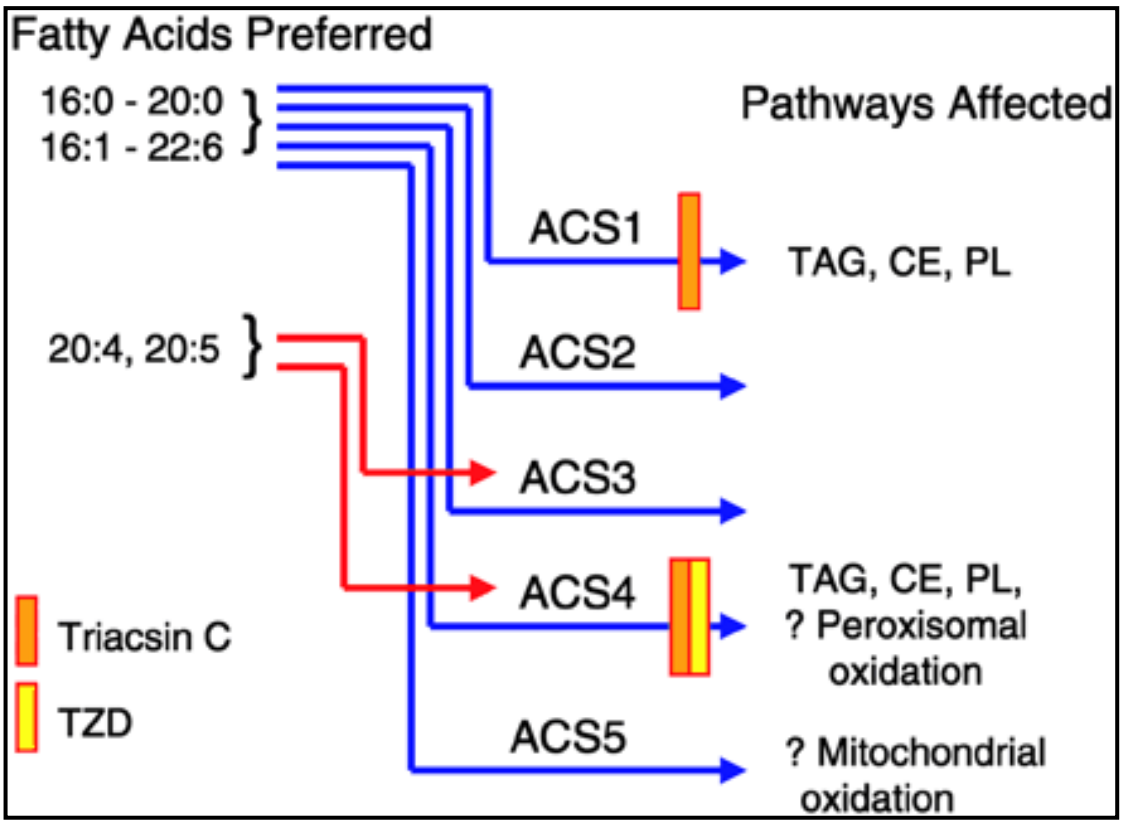

Figure 10. **Inhibitors suggest possible products of acyl-CoA produced by ACS isoforms.** Coleman et al., (2002) used two inhibitors, Triascin C (a fungal-derived competitive inhibitor of ACS) and Troglitazone, a thiazolidinedione (TZD), which selectively inhibits some pathways catalyzed by ACS enzymes. Triascin C was found to inhibit ACS1 and ACS4, but not ACS5, and TZD inhibited only ACS4. Using labeled FA of different chain lengths and recombinant expression of specific rat ACS isoforms in *E. coli* expression vectors, it was found that Triascin C inhibited the incorporation of [^{3}H]glycerol into phospholipid and triacylglycerol, in human fibroblasts and also blocked Incorporation of [^{14}C]oleate into triacylglycerol in rat hepatocytes. Abbreviations: ACS, acyl-CoA synthetase; CE, cholesteryl ester; PL, phospholipid; TAG, triacylglycerol; TZD, thiazolidinedione. Reused with permission from "Do Long-Chain Acyl-CoA Synthetases Regulate Fatty Acid Entry into Synthetic Versus Degradative Pathways?", by R.A. Coleman, et al., 2002, *The Journal of Nutrition, 132 (8),* p.2123. Copyright 2002, by The American Society for Nutritional Sciences.

Therefore, the ideal next step in identifying specific mechanisms through which these *acs* genes could be acting to modulate responses to ethanol, would be to characterize genes within each of these downstream pathways and test candidates that could give the most information about the role of that pathway in ethanol response (by choosing a gene that codes for an enzyme that is essential and exclusive for that particular pathway). For example, glycerol-3-phosphate acyl transferase (GPAT) is the enzyme catalyzing the

first step of phospholipids from glycerol-3-phosphate and a saturated acyl CoA, which forms lyophosphatidic acid. This is followed by addition of a second acyl CoA by acylglycerol-3-acyltransferase (AGPAT) to lyophosphatidic acid to form phosphatidic acid, which then is metabolized into DAG, TAG and other phospholipids like phosphatidyl inositol and phosphatidyl choline. GPAT acts in the outer mitochondrial membrane and AGPAT acts in the ER (Wendel et al., 2009). Using genetic mutants that block these two pathways that are essential for phospholipid, DAG and TAG synthesis could be a useful first step in narrowing down the possible mechanisms through which acyl CoA could be affecting ethanol response phenotypes. In *C. elegans*, *acl-6* codes for the mitochondrial GPAT and *acl-4* and *acl-5* code for the GPAT expressed in the ER. Testing the lf mutants of these genes for ethanol responses would help in determining if phospholipid synthesis and its downstream pathways affect ethanol response phenotypes. Also, testing the levels of FFA in these *acs* mutants would be a simple first step in determining if the effects of ACS lf on ethanol response phenotypes is due to an increase in levels of FFA. This would allow us to also examine the specific chain-length of FFA that is increased in these mutants, which could reveal the substrate-specificity of the different *acs* genes in *C. elegans*.

3.5 Carnitine Palmitoyl Transferases (CPT)

The carnitine shuttle transports long chain acyl CoA across the mitochondrial membrane, by reversibly converting it to acyl carnitine. *cpt-1* codes for CPTI which is localized in the outer mitochondrial membrane and conjugates activated long-chain FA with carnitine to form acyl carnitine, which is then

transported across the inner plasma membrane by Carnitine-acylcarnitine translocase (CACT). CPTII (gene, *cpt-2)* converts the acyl carnitine to fatty acyl CoA by the addition of coenzyme A. CPTI in mammals has three tissue-specific isoforms, CPT1A which is expressed in the liver, CPTIB, expressed in the muscle, and CPTIC, which is expressed in the brain (Sharma & Black, 2009). I tested *C. elegans* mutants of three (*cpt-3, cpt-4 and cpt*-6) of the six known *cpt* genes, and Dr. Alaimo, as part of his thesis project, performed RNAi for two of the other *cpt* genes (*cpt-2 and cpt-5*).

The 2x backcrossed *cpt-6* mutant strain, and the *cpt-2* and *cpt-5* RNAi-fed worms were not significantly different from the WT worms in their ethanol responses. Though behavioral assays of the 2x backcrossed *cpt-3* and *cpt-4* lf mutants did not show a statistically significant difference in initial sensitivity and AFT compared to WT, considering the high error on these assays and the trend towards reduced AFT seen in both mutants, we decided to backcross these to 6x and test them again. The 6x backcrossed mutant of *cpt-3* did not show a significant difference in its ethanol responses compared to WT worms and the 6x backcrossed mutant of *cpt-4* had higher AFT development compared to WT, but did not differ significantly from WT in terms of initial sensitivity.

Lack of CPT function would disrupt the entry of long-chain acyl CoA into the matrix thus halting mitochondrial beta-oxidation of these FA, and also leading to a buildup of cytosolic acyl CoA that cannot be transported into the mitochondria. Based on the behavioral assay results from the lf mutants and

Dr. Alaimo's data, it appears that only lf of *cpt-4* affects ethanol responses. This implies that either *cpt-4* function in mitochondrial beta-oxidation is unique, and not compensated for by other *cpt* genes or that *cpt-4* has some other function (apart from transport of fatty acyl CoA into the mitochondria) that has an effect on AFT in response to ethanol.

I also performed RNAi for *W03F9.*4, a *C. elegans* gene predicted to have carnitine O-octanoyltransferase function, which in humans has been shown to be involved in transport of long and medium-chain acyl CoA from the peroxisomes to mitochondria and cytosol. This gene was included for testing due to its orthology to CPT1A (from DIOPT), but the *W03F9.4* RNAi-fed worms did not show a significantly different ethanol responses compared to L4440. In case of RNAi, a positive result (significant phenotype) observed is considered as evidence for the importance of that gene in modulating the phenotype. However, failure to observe a phenotype (like in the case of RNAi–mediated knockdown of *W03F9.4, cpt-2* and *cpt-5*) does not mean that those genes do not have an effect on ethanol responses, and the results of this need to be confirmed with lf mutants. Also, it would be interesting to see if *cpt-1*, the *cpt* gene in *C. elegans* that we did not assay, could play a role in regulating ethanol responses.

3.6 Acyl CoA dehydrogenases (ACDH)

ACDHs catalyze the first dehydrogenation step in beta-oxidation within the mitochondria, converting acyl CoA to trans-2-enoyl CoA and require FAD as a co-factor to perform their function. As discussed in the Introduction, human

ACADs in the mitochondria are grouped into short, medium and long-chain enzymes based on their substrate chain-length specificity.

I tested 10 of the 12 *acdh* genes for a role in ethanol responses, using lf mutants for six *acdh* genes (*acdh-1, acdh-2, acdh-5, acdh-6, acdh-7* and *acdh-11*) and RNAi-mediated knockdown for the other four (*acdh-4, acdh-8, acdh-10* and *acdh-12*). Five of these ten genes showed significantly different ethanol responses phenotype compared to WT. Grouping these genes by their substrate-specificity, we see that, lf in the two short-chain *acdh* genes, *acdh-1* and *acdh-2* leads to ethanol resistance, but has no effect on AFT. Two of the three medium-chain *acdh* genes, *acdh-7* and *acdh-10,* have reduced AFT, and *acdh-10* also exhibits a decrease in sensitivity. The other medium-chain enzyme, *acdh-8,* did not appear to have an effect on ethanol responses based on RNAi knockdown. All three of the long-chain specific ACDH enzyme genes, *acdh-5, acdh-6* and *acdh-11* did not show difference in their ethanol responses, while RNAi of *acdh-12,* that catalyzes dehydrogenation of very long-chain acyl CoAs, showed decreased sensitivity but no effect on AFT.

Lf of ACDH would be predicted to prevent the formation of trans-2-enoyl CoA and result in accumulation of acyl CoA inside the mitochondria. This would also be predicted to alter the cellular ratio of $FAD/FADH_2$, and there would be decreased entry of $FADH_2$ into the ETC. This would disrupt the energy production from ETC in the form of ATP ($FADH_2$ provides energy required for the synthesis of 2 ATP molecules through the ETC), ultimately resulting in decreased ATP production. There is not much information available on this

class of enzymes apart from their role in mitochondrial beta-oxidation and associated metabolic diseases, hence it is difficult to hypothesize about which of the above events could most likely contribute to the ethanol response phenotypes being observed in these mutants. The $FAD/FADH_2$ ratio in these *acdh* mutants can be determined using fluorescence based assays. Comparing the ratio of $FAD/FADH_2$ between the *acdh* mutants displaying altered ethanol response phenotypes and the ones displaying WT-like ethanol responses could help us determine if this ratio is important in altering neuronal responses to ethanol in *C. elegans.* If the $FAD/FADH_2$ ratio correlates with the ethanol response phenotypes in the *acdh* mutants, the next step would be to examine the effect of the ETC on neuronal responses to ethanol since the $FADH_2$ molecules (released during this reaction) enter the ETC to produce energy.

3.7 Enoyl CoA Hydratases (ECH)

ECH catalyze the hydration of trans-2-enoyl CoA to form 3-hydroxy acyl CoA and in higher eukaryotes, the activity of ECH and the other two downstream enzymes HACD and KAT are carried out by a MTP for oxidation of long-chain FA. The *C. elegans ech* family of genes consists of seven members, of which I have tested three (*ech-1.1* using RNAi and *ech-1.2* and *ech-7* using lf mutants) and Dr. Alaimo tested the roles of four genes using RNAi (*ech-1.2, ech-2, ech-4* and *ech-6*). I tested a lf mutant of *ech-1.2,* though Dr. Alaimo had performed an RNAi knockdown of this gene and showed that it did not have a significant effect on ethanol response phenotypes, since the lack of phenotype seen by RNAi is not reliable. In *C. elegans*, to determine the

effectiveness of RNAi, (Kamath et al., 2003) compared the RNAi phenotypes to phenotypes of know lf mutants and found that while the false positive rate was <1%, the rate of false negatives was substantially higher, 30%. Possible reasons for this high false negative rate could be variation in RNAi feeding protocol, certain genes are more sensitive to RNAi feeding than others and that some phenotypes exhibit low penetrance, meaning that the phenotype is expressed in some worms in a population and not in others (Kamath et al., 2001). Therefore, such cases where we see no significant phenotype through RNAi feeding need to be confirmed with a lf mutant, when possible. Another way to confirm this would be to use overexpression of the enzyme to see if that exhibits a significant ethanol response behavior. The effectiveness of RNAi could be determined by qRT-PCR, before contemplating the use of lf or gf mutants.

RNAi knockdown of *ech-1.1* and *ech-1.2* (performed by Dr. Alaimo) did not show significantly different ethanol responses compared to WT, but the 2x backcrossed lf mutant of *ech-1.2* showed a significantly reduced AFT, so we backcrossed this mutant 6x and confirmed this phenotype. Also lf in *ech-7* caused reduced AFT. On the other hand, RNAi knockdown of *ech-6* showed an increase in AFT. The initial sensitivity in all these three cases was similar to WT.

Loss of ECH function would result in trans-2-enoyl CoA accumulation and a halt in the progression of mitochondrial beta-oxidation. In *C. elegans, ech-1.1* and *ech-1.2* are the two orthologs of HADHA, the alpha-subunit of the

mitochondrial trifunctional protein, which exhibits ECH/long-chain HADH activity. *ech-6* and *ech-7* are orthologous to the ECHS1, which catalyzes hydration of short-chain FA. This suggests that a disruption of ECH enzymes that act on both long-chain and short-chain FA has an effect on ethanol responses. All three of the *ech* genes appear to affect only the AFT component of ethanol response and not the initial sensitivity. Also, the change in AFT in *ech-6* and *ech-7* lf are in opposite directions, which is probably not due to chain-length specificity since both of these are orthologs of the short-chain ECH. While *ech-6* localizes to the mitochondria, the information on subcellular or tissue-specific expression of *ech-7* in *C. elegans* is not available. One possibility is that the expression pattern could explain the difference in direction of AFT between these two strains.

3.8 Hydroxy acyl CoA dehydrogenases (HACD/HADH)

These are oxidoreductases, which catalyze the oxidation of 3-hydroxy acyl CoA to 3-keto acyl CoA and this reaction is coupled with the reduction of NAD^+ to NADH. I examined a lf mutant of *hacd-1*, the only ortholog of the human *HADH* in *C. elegans*, and found that there was no effect on ethanol responses due to loss of *hacd-1* function. Since *ech-1.2* and *ech-1.1* are orthologs of the MTP, they are also predicted to be involved in this step of the pathway.

Among the consequences of disrupting of this step in beta-oxidation would be predicted to be an increase in the concentration of 3-hydroxy acyl CoA and alteration in the ratio of NADH/NAD^+. This ratio has shown to be involved in

the allosteric regulation of beta-oxidation, i.e., increase in the NADH/NAD^+ ratio has shown to inhibit beta-oxidation. Three independent studies (Grunnet & Kondrup, 1986; Lieber, 1994; Reitz, 1979) showed that ethanol metabolism (into acetate and acetaldehyde) alters the NADH/NAD^+ ratio, which inhibits HADH activity and thus decreases the level of mitochondrial beta-oxidation. Adachi & Ishii (2002) in their study of rat-cultured hepatocytes showed that acute ethanol exposure increased superoxide generation in the mitochondria, which they hypothesized was due to an increase in the NADH/NAD^+ ratio and thus an induction of mitochondrial dysfunction. However, there is not much literature that could clarify a role for this altered ratio in neuronal response to ethanol. Based on our analysis of these two genes, it is possible that disruption of this step in beta-oxidation could be significant in terms of FA and ethanol metabolism, but with this limited evidence, and *ech-1.2* potentially being involved in both steps of beta-oxidation, the reason for its effect on modulating behavioral responses to ethanol could be multifold. For example, ratio of NADH/NAD^+ is essential for metabolic pathways like glycolysis, gluconeogenesis, TCA cycle and FA synthesis. This ratio is also important for cell signaling and transcriptional regulation, since the enzymes involved in these processes require NAD^+ and NADH for their functions. Therefore, altered ethanol responses observed in the *ech-1.2* mutant could be due to disruption in any one or a combination of these pathways and enzymes. Measuring the NADH/NAD^+ ratio in the *ech-1.2* mutants could help us narrow down the possible mechanism of altered ethanol response. This ratio can be measured using commercially available fluorescence detection based NAD^+/NADH assay kits.

3.9 Keto-acyl CoA Thiolases

The two enzymes primarily involved in this pathway are KAT and ACAT. KAT catalyzes degradation of a broad range of 3-keto acyl CoA chain lengths to form an acyl CoA shortened by two carbons (acyl $CoA_{(n-2)}$) and acetyl CoA. ACAT specifically catalyzes the last round of degradation in beta-oxidation, i.e., degradation of acetoacetyl CoA. In *C. elegans*, I studied two genes to look at the importance of this step in ethanol response. *kat-1* is predicted to encode mitochondrial KAT and *acaa-2* is an ortholog of the human ACAT. While *kat-1* loss of function did not show difference in ethanol responses compared to WT, *acaa-2* lf mutants showed decreased sensitivity to ethanol and in both mutants, the AFT is similar to WT worms.

Loss of function of enzymes catalyzing the last step of mitochondrial beta-oxidation that generates an acetyl CoA and an acyl CoA shortened by two carbons would be predicted to prevent release of acetyl CoA into downstream pathways like ketone body synthesis, the glyoxylate cycle, the TCA cycle and de novo FA synthesis. It would also lead to increase in 3-keto acyl CoA levels in the mitochondria. Lack of *kat-1* functioning in beta-oxidation does not appear to affect neuronal response to ethanol and one possible reason for this is that *kat-1,* though predicted to be involved in mitochondrial beta-oxidation (KEGG), is orthologous to ACAT1, a thiolase that is involved in breakdown of isoleucine and ketone bodies, and has not been implicated in mitochondrial beta-oxidation. A likely explanation for the decreased sensitivity seen in *acaa-2* lf mutants is that acetyl CoA release into one or more of its downstream pathways is important for ethanol response. *acaa-2* specifically

catalyzes the last round of beta-oxidation, and there is no further reentry of shortened acyl CoA into another round of oxidation and the only end-product of this reaction is acetyl CoA. Since acetyl CoA has several roles in various pathways of energy metabolism, it is difficult to predict which one of these could be important for ethanol response.

Acetyl CoA is also utilized in cholinergic neurons for the synthesis of acetylcholine (Szutowicz et al., 2000). Several studies in humans and mouse models of alcohol-associated behavior have implicated neuronal nAChRs as potential targets of alcohol, though the exact mechanism and specific subunits of these receptors involved are not clear yet (Hendrickson et al., 2013; Tang & Liao, 2013). It would be interesting to see if the ethanol response phenotype seen in *acaa-2* mutants is due to decrease in availability of acetyl CoA for acetylcholine synthesis, which could be connected to potential changes in ethanol interaction with nAChRs. A preliminary experiment that could help explore this direction would be to express *acaa-2* in only the neurons expressing nAChRs (using *pacr-2,* promoter of *acr-2* that is expressed specifically in these neurons), in *acaa-2* deficient background. We could test ethanol responses of these worms to see if this rescues the phenotype. If *acaa-2* lf is modifying ethanol sensitivity solely through decrease in acetylcholine synthesis, the expression of *acaa-2* in the nAChR-expressing neurons should be able to restore WT initial sensitivity. But, if the initial sensitivity in these mutants is rescued to a certain extent (i.e., sensitivity is higher than *acaa-2* lf but also significantly lower than WT), it suggests that acetylcholine synthesis is one of the mechanisms through which *acaa-2* lf is

acting on sensitivity to ethanol and there are other mechanisms that contribute to this phenotype. Apart from acetylcholine synthesis, acetyl CoA is also involved in other metabolic pathways such as FA synthesis, which could be a mechanism through which the ethanol response phenotypes in the *acaa-2* mutants are being altered.

3.10 Conclusion

We tested various genes in the mitochondrial beta-oxidation pathway and saw that of the 34 genes we examined (including Dr. Alaimo's data), loss of function of 13 genes showed a significant effect on ethanol response phenotype in *C. elegans*. Looking at the ethanol response phenotypes of lf mutants of all genes across enzyme families, it is clear that initial sensitivity to ethanol is affected in a higher number of mutants (in either direction), compared to AFT. Based on our experiments, we conclude that mitochondrial beta-oxidation of FA is essential for ethanol response behavior in *C. elegans*. However, considering the various roles of the substrate, intermediate metabolites and end product of beta-oxidation within and outside the mitochondria, it is difficult to hypothesize a single mechanism of the effect of these genes on neuronal response to ethanol. There are certain aspects of this pathway that seem to be particularly important, like FFA, acyl CoA and its derivatives, ratio of $NADH/NAD^+$ and acetyl CoA. These components have been implicated in previous research on alcohol and its targets. It is likely that the effects of loss-of-function of the beta-oxidation enzymes are caused through more than one mechanism or compound that acts independently or

interacts with other pathways or compounds to influence ethanol response phenotypes.

As discussed in this chapter, there is abundant scope for dissecting the role of individual genes identified through this project in the various downstream pathways of beta-oxidation and its intermediate products. This project lays the groundwork for further research on these candidate genes to test the possible and most likely mechanisms of their action on ethanol responses.

4. LIST OF REFERENCES

Adachi, M., & Ishii, H. (2002). Role of mitochondria in alcoholic liver injury. *Free Radical Biology and Medicine, 32*(6), 487-491.

Agnihotri, G., & Liu, H. (2003). Enoyl-CoA hydratase: Reaction, mechanism, and inhibition. *Bioorganic & Medicinal Chemistry, 11*(1), 9-20.

Akbar, M., Essa, M., Daradkeh, G., Abdelmegeed, M., Choi, Y., Mahmood, L., et al. (2016). Mitochondrial dysfunction and cell death in neurodegenerative diseases through nitroxidative stress. *Brain Research, 1637*, 34-55.

Alaimo, J. (2013). *Identification and characterization of ethanol responsive genes in acute ethanol behaviors in caenorhabditis elegans.* Unpublished Doctor of Philosophy, Virginia Commonwealth University,

Albuquerque, E., Pereira, E., Alkondon, M., & Rogers, S. (2009). Mammalian nicotinic acetylcholine receptors: From structure to function. *Physiological Reviews, 89*(1), 73-120.

Alcohol facts and statistics. (2017). Retrieved March/1, 2017, from https://pubs.niaaa.nih.gov/publications/AlcoholFacts&Stats/AlcoholFacts&Stats.htm

Andringa, K., King, A., Eccleston, H., Mantena, S., Landar, A., Jhala, N., et al. (2010). Analysis of the liver mitochondrial proteome in response to ethanol and *S*-adenosylmethionine treatments: Novel molecular targets of disease and hepatoprotection. *American Journal of Physiology - Gastrointestinal and Liver Physiology, 298*(5), G732-G745.

Antollini, S., & Barrantes, F. (2016). Fatty acid regulation of voltage- and ligand-gated ion channel function. *Frontiers in Physiology, 7*(573)

Apostolova, N., & Victor, V. (2015). Molecular strategies for targeting antioxidants to mitochondria: Therapeutic Implications. *Antioxidants & Redox Signaling, 22*(8), 686-729.

Bailey, S., & Cunningham, C. (1998). Acute and chronic ethanol increases reactive oxygen species generation and decreases viability in fresh, isolated rat hepatocytes. *Hepatology, 28*, 1318-1326.

Bailey, S., Pietsch, C., & Cunningham, C. (1999). Ethanol stimulates the production of reactive oxygen species at mitochondrial complexes I and III. *Free Radical Biology and Medicine, 27*(7-8), 891-900.

Banerjee, N. (2014). Neurotransmitters in alcoholism: A review of neurobiological and genetic studies. *Indian Journal of Human Genetics, 20*(1), 20-31.

Bennett, M., Weinberger, M., Kobori, J., Rinaldo, P., & Burlina, A. (1996). Mitochondrial short-chain L-3-hydroxyacyl-coenzyme A dehydrogenase deficiency: A new defect of fatty acid oxidation. *Pediatric Research, 39*(1), 185-188.

Bettinger, J., Leung, K., Bolling, M., Goldsmith, A., & Davies, A. (2012). Lipid environment modulates the development of acute tolerance to ethanol in *caenorhabditis elegans*. *Plos One, 7*(5)

Bogenschutz, M., Tonigan, J., & Pettinati, H. (2009). Effects of alcoholism typology on response to naltrexone in the COMBINE study. *Alcoholism, Clinical and Experimental Research, 33*(1), 10-18.

Boneh, A. (1996). Protein kinase C activity, phosphate uptake and endogenous substrate phosphorylation are altered in zellweger syndrome. *Journal of Inherited Metabolic Disease, 19*(5), 661-666.

Boulin, T., & Hobert, O. (2012). From genes to function :The C. elegans genetic toolbox. *Wiley Interdisciplinary Reviews. Developmental Biology, 1*(1), 114-117.

Brock, T., Browse, J., & Watts, J. (2007). Fatty acid desaturation and the regulation of adiposity in caenorhabditis elegans. *Genetics, 176*(2), 865-875.

Chen, S., Whetstine, J., Ghosh, S., Hanover, J., Gali, R., Grosu, P., et al. (2008). The conserved NAD(H)-dependent corepressor CTBP-1 regulates caenorhabditis elegans life span. *Proceedings of the National Academy of Sciences of the United States of America, 106*(5), 1496-1501.

Coleman, R., Lewin, T., Van Horn, C., & Gonzalez-Baro, M. (2002). Do long-chain acyl-CoA synthetases regulate fatty acid entry into synthetic versus degradative pathways? *Recent Advances in Nutritional Sciences*

Cooper, D., Young, P., Klett, E., & Coleman, R. (2015). Physiological consequences of compartmentalized acyl-CoA metabolism. *The Journal of Biological Chemistry, 290*(33), 20023-20031.

Crabbe, J., Kendler, K., & Hitzemann, R. (2013). Modeling the diagnostic criteria for alcohol dependence with genetic animal Models. *Current Topics in Behavioral Neurosciences, 13*, 187-221.

Dai, D., Chiao, Y., Marcinek, D., Szeto, H., & Rabinovitch, P. (2014). Mitochondrial oxidative stress in aging and healthspan. *Longevity & Healthspan, 3*(6)

Davies, A., Bettinger, J., Thiele, T., Judy, M., & McIntire, S. (2004). Natural variation in the *npr-1* Gene modifies ethanol responses of wild strains of *C. elegans*. *Neuron, 42*(5), 731-743.

Davies, A., Blackwell, G., Raabe, R., & Bettinger, J. (2015). An assay for measuring the effects of ethanol on the locomotion speed of *caenorhabditis elegans*. *Journal of Visualised Experiments, 98*, 06/16/2017.

Davies, A., Pierce-Shimomura, J., Kim, H., VanHoven, M., Thiele, T., Bonci, A., et al. (2003). A central role of the BK potassium channel in behavioral responses to ethanol in *C. elegans*. *Cell, 115*, 655-666.

Davies, M. (2003). The role of GABAA receptors in mediating the effects of alcohol in the central nervous system. *Journal of Psychiatry and Neuroscience, 28*(4), 263-274.

de Bono, M., & Maricq, A. (2005). Neuronal substrates of complex behaviors in c. elegans. *Annual Review of Neuroscience, 28*, 451-501.

Ding, W., Li, M., & Yin, X. (2011). Selective taste of ethanol-induced autophagy for mitochondria and lipid droplets. *Autophagy, 7*(2), 248-249.
Edenberg, H. J., & Foroud, T. (2013). Genetics and alcoholism. *Nature Reviews. Gastroenterology & Hepatology, 10*(8), 487-494.

Elle, I., Simonsen, K., Olsen, L., Birck, P., Ehmsen, S., Tuck, S., et al. (2011). Tissue- and paralogue-specific functions of acyl-CoA-binding proteins in lipid metabolism in caenorhabditis elegans. *Biochemical Journal, 437*, 231-241.

Eng, M., Schuckit, M., & Smith, T. (2005). The level of response to alcohol in daughters of alcoholics and controls. *Drug and Alcohol Dependence, 79*(2005), 83-93.

Engleman, E., Katner, S., & Neal-Beliveau, B. (2016). *Caenorhabditis elegans* as a model to study the molecular and genetic mechanisms of drug addiction. *Progress in Molecular Biology and Translational Science, 137*, 229-252.

Erwin, V., Gehle, V., & Deitrich, R. (2000). Selectively bred lines of mice show response and drug specificity for genetic regulation of acute functional

tolerance to ethanol and pentobarbital. *Journal of Pharmacology and Experimental Therapeutics, 293*(1), 188-195.

Flanagan, J., Simmons, P., Vehige, J., Willcox, M., & Garrett, Q. (2010). Role of carnitine in disease. *Nutrition & Metabolism, 7*(30)

Fritz, B., Grahame, N., & Boehm, S. (2013). Selection for high alcohol preference drinking in mice results in heightened sensitivity and rapid development of acute functional tolerance to Alcohol's ataxic effects. *Genes, Brain, and Behavior, 12*(1), 78-86.

Ghisla, S., & Thorpe, C. (2004). Acyl-CoA dehydrogenases A mechanistic overview. *European Journal of Biochemistry, 271*, 494-508.

Gottesman, I., & Shields, J. (1973). Genetic theorizing and schizophrenia. *The British Journal of Psychiatry, 122*(566), 15-30.

Grunnet, N., & Kondrup, J. (1986). The effect of ethanol on the &oxidation of fatty acids. *Alcoholism, Clinical and Experimental Research, 10*, 64S-68S.

Hawkins, E. G., Martin, I., Kondo, L. M., Judy, M. E., Brings, V. E., Chan, C. L., et al. (2015). A novel cholinergic action of alcohol and the development of tolerance to that effect in *caenorhabditis elegans*. *Genetics, 199*(1), 135-149.

Hendrickson, L., Guildford, M., & Tapper, A. (2013). Neuronal nicotinic acetylcholine receptors: Common molecular substrates of nicotine and alcohol dependence. *Frontiers in Psychiatry, 4*(29)

Hiltunena, A., Saxona, L., Skagerbergb, S., & Borga, S. (2000). Acute tolerance during intravenous infusion of alcohol: Comparison of performance during ascending and steady state concentrations — a pilot study. *Alcohol, 22*(2), 69-74.

Hines, M., Ray, L., Hutchison, K., & Tabakoff, B. (2005). Alcoholism: The dissection for endophenotypes. *Dialogues in Clinical Neuroscience, 7*(2), 153-163.

Hobert, O. (2003). Behavioral plasticity in C. elegans: Paradigms, circuits, genes. . *Journal of Nerobiology, 54*(1), 203-223.

Holmuhamedov, E., & Lemasters, J. (2009). Ethanol exposure decreases mitochondrial outer membrane permeability in cultured rat hepatocytes. *Archives of Biochemistry and Biophysics, 481*(2), 226-233.

Houten, S., & Wanders, R. (2010). A general introduction to the biochemistry of mitochondrial fatty acid β-oxidation. *Journal of Inherited Metabolic Disease, 33*(5), 469-477.

Hu, Y., Flockhart, I., Vinayagam, A., Bergwitz, C., Berger, B., Perrimon, N., et al. (2011). An integrative approach to ortholog prediction for disease-focused and other functional studies. *BMC Bioinformatics, 12*(357)

Ikeuchi, Y., Nishizaki, T., Matsuoka, T., & Sumikawa, K. (1996). Arachidonic acid potentiates ACh receptor currents by protein kinase C activation but not by receptor phosphorylation. *Biochemical and Biophysical Research Communications, 221*(3), 716-721.

Kamath, R., Fraser, A., Yan Dong, Y., Poulin, G., Durbin, R., Gotta, M., et al. (2003). Systematic functional analysis of the caenorhabditis elegans genome using RNAi. *Nature, 421*, 231-237.

Kamath, R., Martinez-Campos, M., Zipperlen, P., Fraser, A., & Ahringer, J. (2001). Effectiveness of specific RNA-mediated interference through ingested double-stranded RNA in *caenorhabditis elegans*. *Genome Biology, 2*(1), research0002.1-research0002.10.

Kang, M., Fujino, T., Sasano, H., Minekura, H., Yabuki, N., Nagura, H., et al. (1997). A novel arachidonate-preferring acyl-CoA synthetase is present in steroidogenic cells of the rat adrenal, ovary, and testis. *Proceedings of the National Academy of Sciences of the United States of America, 94*(7), 2880-2884.

Kapfhamer, D., Bettinger, J. C., Davies, A. G., Eastman, C. L., Smail, E. A., Heberlein, U., et al. (2008). Loss of RAB-3/A in *C. elegans* and the mouse affects behavioral response to ethanol. *Genes, Brain, and Behavior, 7*(6), 669-676.

Kaplan, R., Cooney, N., Baker, L., Gillespie, R., Meyer, R., & Pomerleau, O. (1985). Reactivity to alcohol-related cues: Physiological and subjective responses in alcoholics and nonproblem drinkers. *Journal of Studies on Alcohol, 46*(4), 267-272.

King, A., Mantena, S., Andringa, K., Millender-Swain, T., Dunham-Snary, K., Oliva, C., et al. (2016). The methyl donor *S*-adenosylmethionine prevents liver hypoxia and dysregulation of mitochondrial bioenergetic function in a rat model of alcohol-induced fatty liver disease. *Redox Biology, 9*, 188-197.

Krishnan-Sarin, S., O'Malley, S., & Krystal, J. (2008). Treatment implications using neuroscience to guide the development of new pharmacotherapies for alcoholism. *Alcohol Research : Current Reviews, 31*(4), 400.

Kunau, W., Dommes, V., & Schulz, H. (1995). β-Oxidation of fatty acids in mitochondria, peroxisomes, and bacteria: A century of continued progress. *Progress in Lipid Research, 34*(4), 267-342.

LeBlanc, A., Kalant, H., & Gibbins, R. (1975). Acute tolerance to ethanol in the rat. *Psychopharmacologia, 41*(1), 43-46.

Leslie, N., Valencia, C., Strauss, A., Connor, J., & Zhang, K. (2014). Very long-chain acyl-coenzyme A dehydrogenase deficiency. In R. Pagon, M. Adam & H. Ardinger (Eds.), *Gene reviews [internet]* (). Seattle, WA: University of Washington, Seattle.

Li, L., Ellis, J., Paich, H., Wang, S., Gong, N., Altshuller, G., et al. (2009). Liver-specific loss of long chain acyl-CoA synthetase-1 decreases triacylglycerol synthesis and β-oxidation and alters phospholipid fatty acid composition. *The Journal of Biological Chemistry, 284*(41), 27816-27826.

Li, Z., Zhai, Y., Fang, J., Zhou, Q., Geng, Y., & Sun, F. (2010). Purification, crystallization and preliminary crystallographic analysis of very-long-chain acyl-CoA dehydrogenase from caenorhabditis elegans . *Acta Crystallographica Section F: Structural Biology and Crystallization Communications, 66*, 426-430.

Lieber, C. (1994). Alcohol and the liver: 1994 update. *Gastroenterology, 106*, 1085-1105.

Lowell, B., & Shulman, G. (2005). Mitochondrial dysfunction and type 2 diabetes. *Science, 307*(5708), 384-387.

Ma, D., Li, Z., Lu, A., Sun, F., Chen, S., Rothe, M., et al. (2015). Acyl-CoA dehydrogenase drives heat adaptation by sequestering fatty Acids. *Cell, 161*(5), 1152-1163.

Marszalek, J., Kitidis, C., DiRusso, C., & Lodish, H. (2005). Long-chain acyl-CoA synthetase 6 preferentially promotes DHA metabolism. *The Journal of Biological Chemistry, 280*, 10817-10826.

Mashek, D., Li, L., & Coleman, R. (2007). Long-chain acyl-CoA synthetases and fatty acid channeling. *Future Lipidology, 2*(4), 465-476.

McDaid, J., Abburi, C., Wolfman, S., Gallagher, K., & McGehee, D. (2016). Ethanol-induced motor impairment mediated by inhibition of α7 nicotinic Receptors. *The Journal of Neuroscience, 36*(29), 7768-7778.

McIntire, S. (2005). *Ethanol. in: WormBook: The online review of C. elegans biology.* Retrieved 07/13, 2017, from https://www.ncbi.nlm.nih.gov/books/NBK116077/

McIntosh, C., & Chick, J. (2004). Alcohol and the nervous system. *Journal of Neurology, Neurosurgery and Psychiatry, 75*(Suppl III), iii 16-iii 21.

Morozova, T., Ayroles, J., Jordan, K., Duncan, L., Carbone, M., Lyman, R., et al. (2009). Alcohol sensitivity in drosophila: Translational potential of systems genetics. *Genetics, 182*(2), 733-745.

Morozova, T., Mackay, T., & Anholt, R. (2014). Genetics and genomics of alcohol sensitivity. *Molecular Genetics and Genomics, 289*(3), 253-269.

Mullaney, B., & Ashrafi, K. (2010). Regulation of *C. elegans* fat uptake and storage by acyl-CoA synthase-3 is dependent on NR5A family nuclear hormone receptor *nhr-25*. *Cell Metabolism, 12*(4), 398-410.

Nishizuka, Y. (1992). Intracellular signaling by hydrolysis of phospholipids and activation of protein kinase C. *Science, 258*(5082), 607-614.

Nutt, D., King, L. A., Saulsbury, W., & Blakemore, C. (2007). Development of a rational scale to assess the harm of drugs of potential misuse. *The Lancet, 369*(9566), 1047-1053. doi:http://dx.doi.org/10.1016/S0140-6736(07)60464-4

Palmer, R., McGeary, J., Francazio, S., Raphael, B., Lander, A., Heath, A., et al. (2012). The genetics of alcohol dependence: Advancing towards systems-based approaches. *Drug and Alcohol Dependence, 125*(3), 179-191.

Ponomarev, I., & Crabbe, J. (2002). Ethanol-induced activation and rapid development of tolerance may have some underlying genes in common. *Genes, Brain, and Behavior, 1*, 82-87.

Raabe, R., Mathies, L., Davies, A., & Bettinger, J. (2014). The Omega-3 fatty acid eicosapentaenoic acid is required for normal alcohol response behaviors in *C. elegans*. *Plos One, 9*(8)

Rakheja, D., Bennett, M., & Rogers, B. (2002). Long-chain L-3-hydroxyacyl-coenzyme A dehydrogenase deficiency: A molecular and biochemical review. *Laboratory Investigation, 82*, 815-824.

Ray, A., Martinez, B., Berkowitz, L., Caldwell, G., & Caldwell, K. (2014). Mitochondrial dysfunction, oxidative stress, and neurodegeneration elicited by a bacterial metabolite in a *C. elegans* Parkinson's model. *Cell Death & Disease, 5*(1), e984.

Reitz, R. (1979). The effects of ethanol ingestion on lipid metabolism. *Progress in Lipid Research, 18*, 87-115.

Ritzmann, R., & Tabakoff, B. (1976). Dissociation of alcohol tolerance and dependence. *Nature, 263*, 418-420.

Saito, N., & Shirai, Y. (2002). Protein kinase Cγ (PKCγ): Function of neuron specific isotype. *Journal of Biochemistry, 132*(5), 683-687.

Salvatore, J., Gottesman, I., & Dick, D. (2015). Endophenotypes for alcohol use disorder: An update on the field. *Current Addiction Reports, 2*(1), 76-90.

Schreurs, M., Kuipers, F., & van der Leij, F. (2010). Regulatory enzymes of mitochondrial beta-oxidation as targets for treatment of the metabolic syndrome. *Obesity Reviews, 11*(5), 380-388.

Schuckit, M. (1980). Self-rating of alcohol intoxication by young men with and without family histories of alcoholism. *Journal of Studies on Alcohol, 41*(3), 242-249.

Schuckit, M. (1994). Low level of response to alcohol as a predictor of future alcoholism. *American Journal of Psychiatry, 151*(2), 184-189.

Schuckit, M., Smith, T., Heron, J., Hickman, M., Macleod, J., Lewis, G., et al. (2011). Testing a level of response to alcohol-based model of heavy drinking and alcohol problems in 1,905 17-year-olds. *Alcoholism, Clinical and Experimental Research, 35*(10), 1897-1904.

Sharma, S., & Black, S. (2009). Carnitine homeostasis, mitochondrial function, and cardiovascular disease. *Drug Discovery Today. Disease Mechanisms, 6*(1-4), e31-e39.

Srinivasan, S., Sadegh, L., Elle, I., Christensen, A., Faergeman, N., & Ashrafi, K. (2008). Serotonin Regulates *C. elegans* Fat and feeding through independent molecular mechanisms. *Cell Metabolism, 7*(6), 533-544.

Srivastava, V., Buzas, B., Momenan, R., Oroszi, G., Pulay, A., Enoch, M., et al. (2010). Association of *SOD2*, a mitochondrial antioxidant enzyme, with gray matter volume shrinkage in alcoholics. *Neuropsychopharmacology, 35*(5), 1120-1128.

Szutowicz, A., Tomaszewicz, M., Jankowska, A., & Madziar, B. (2000). Acetyl-CoA metabolism in cholinergic neurons and their susceptibility to neurotoxic inputs. *Metabolic Brain Disease, 15*, 29-44.

Tang, J., & Liao, Y. (2013). Alcohol and nicotinic acetylcholine receptors. *QScience Connect, 15*

Taubert, S., Van Gilst, M., Hansen, M., & Yamamoto, K. (2006). A mediator subunit, MDT-15, integrates regulation of fatty acid metabolism by NHR-49-

dependent and -independent pathways in C. elegans. *Genes & Development, 20*, 1137-1149.

Tawa, E. A., Hall, S. D., & Lohoff, F. W. (2016). Overview of the genetics of alcohol use disorder. *Alcohol and Alcoholism, 51*(5), 507-514.

Ushikubo, S., Aoyama, T., Kamijo, T., Wanders, R., Rinaldo, P., Vockley, J., et al. (1996). Molecular characterization of mitochondrial trifunctional protein deficiency: Formation of the enzyme complex is important for stabilization of both alpha- and beta-subunits. *American Journal of Human Genetics, 58*(5), 979-988.

Van Gilst, M., Hadjivassiliou, H., Jolly, A., & Yamamoto, K. (2005). Nuclear hormone receptor NHR-49 controls fat consumption and fatty acid composition in C. elegans. *PLoS Biology, 3*(2), 0301-0312.

Van Gilst, M., Hadjivassiliou, H., Jolly, A., & Yamamoto, K. (2005). Nuclear hormone receptor NHR-49 controls fat consumption and fatty acid composition in C. elegans. *PLoS Biology, 3*(2), e53.

Van Gilst, M., Hadjivassiliou, H., & Yamamoto, K. (2005). A *caenorhabditis elegans* nutrient response system partially dependent on nuclear receptor NHR-49. *Proceedings of the National Academy of Sciences of the United States of America, 102*(38), 13496-13501.

Verhulst, B., Neale, M. C., & Kendler, K. S. (2015). The heritability of alcohol use disorders: A meta-analysis of twin and adoption studies. *Psychological Medicine, 45*(5), 1061-1072.

Virmani, A., Pinto, L., Bauermann, O., Zerelli, S., Diedenhofen, A., Binienda, Z., et al. (2015). The carnitine palmitoyl transferase (CPT) system and possible relevance for neuropsychiatric and neurological conditions. *Molecular Neurobiology, 52*(2), 826-836.

Wanders, R., Ruiter, J., IJlst, L., Waterham, H., & Houten, S. (2010). The enzymology of mitochondrial fatty acid beta-oxidation and its application to follow-up analysis of positive neonatal screening results. *Journal of Inherited Metabolic Disease, 33*(5), 479-494.

Wanders, R., Vreken, P., den Boer, M., Wijburg, F., van Gennip, A., & IJlst, L. (1999). Disorders of mitochondrial fatty acyl-CoA beta-oxidation. *Journal of Inherited Metabolic Disease, 22*(4), 442-487.

Wanders, R., & Waterham, H. (2006). Biochemistry of mammalian peroxisomes revisited. *Annual Review of Biochemistry, 75*, 295-332.
Watkins, P., & Ellis, J. (2012). Peroxisomal acyl-CoA synthetases. *Biochimica Et Biophysica Acta (BBA) - Molecular Basis of Disease, 1822*(9), 1411-1420.

Watkins, P., Maiguel, D., Jia, Z., & Pevsner, J. (2007). Evidence for 26 distinct acyl-coenzyme A synthetase genes in the human genome. *Journal of Lipid Research, 48*(12), 2736-2750.

Wendel, A., Lewin, T., & Coleman, R. (2009). Glycerol-3-phosphate acyltransferases: Rate limiting enzymes of triacylglycerol biosynthesis. *Biochimica Et Biophysica Acta, 1791*(6), 501-506.

WHO alcohol fact sheet. (2015). Retrieved March 01, 2017, from http://www.who.int/mediacentre/factsheets/fs349/en/

Wojtczak, L., & Schonfeld, P. (1993). Effect of fatty acids on energy coupling processes in mitochondria. *Biochimica Et Biophysica Acta (BBA) - Bioenergetics, 1183*(1), 41-57.

Woldegiorgis, G., Shi, J., Zhu, H., & Arvidson, D. (2000). Functional characterization of mammalian mitochondrial carnitine palmitoyltransferases I and II expressed in the yeast pichia pastoris. *Journal of Nutrition, 130*(2S Suppl), 310S-314S.

Wu, J., Gao, M., & Taylor, D. (2014). Neuronal nicotinic acetylcholine receptors are important targets for alcohol reward and dependence. *Acta Pharmacologica Sinicia, 35*(3), 311-315.

Xie, Z., Jones, A., Deeney, J., Hur, S., & Bankaitis, V. (2016). Inborn errors of long chain fatty acid β-oxidation link neural stem cell self-renewal to autism. *Cell Reports, 14*(5), 991-999.

Xu, X., Hu, J., Wu, M., Li-Shun Wang, L., & Fang, N. (2015). CCAAT/enhancer-binding protein CEBP-2 controls fat consumption and fatty acid desaturation in caenorhabditis elegans. *Biochemical and Biophysical Research Communications, 468*(1-2, 4-11), 312-318.

Yamzaki, N. (2004). Identification of muscle-type carnitine palmitoyltransferase I and characterization of its gene structure. *Journal of the Pharmaceutical Society of Japan, 124*(12), 893-908.

Yu, D., Zhang, L., Eiselé, J., Bertrand, D., Changeux, J., & Weigh, F. (1996). Ethanol inhibition of nicotinic acetylcholine type alpha 7 receptors involves the amino-terminal domain of the receptor. *Molecular Pharmacology, 50*(4), 1010-1016.

Zhang, J., Bakheet, R., Parhar, R. S., Huang, C., Hussain, M., Pan, X., et al. (2011). Regulation of fat storage and reproduction by krüppel-like transcription factor KLF3 and fat-associated genes in *caenorhabditis elegans*. *Journal of Molecular Biology, 411*(3), 537-553.

Zuryn, S., Le Gras, S., Jamet, K., & Jarriault, S. (2010). A strategy for direct mapping and identification of mutations by whole-genome sequencing. *Genetics, 186*(1), 427-430.

APPENDICES

APPENDIX I

1. DNA Isolation for PCR

- Obtain a plate with full of adults, on the verge of starvation (more cells = more DNA)
- Label a 1.5 mL eppendorf tube with strain name and “DNA” and date/initials
- Use pure ddH_2O (2 pumps of 850 mL = 1,700 mL) to wash plate
- Decant and place in 1.5 mL Epp. tube
- Centrifuge at highest speed for 30 seconds
- Set pipetter to 1,000 μL
- Decant all of the supernatant and discard
- Add one mL of ddH_2O
- Spin in centrifuge again for one min
- Remove all of the waste until there is only 0.1 mL left. Disturb pellet with a shake
- Freeze in a -80°C freezer for 15 min (lysing step) (At this point the DNA can potentially stay in the freezer for a while, so this is an appropriate stopping point if you are too busy to finish.)
- Set up the 95°C heat block and the 60°C water bath
- Make a master mix of lysis buffer (refer to pg.121 for components of lysis buffer) and Proteinase K (12 μL Proteinase K/1,000 μL lysis buffer)
- Add 1/3 of the solution in tubes (100 μL in tube = 33 X # of tubes + some for the PCR fairies)

- Example: 35µL Lysis Buffer X 5 DNA samples = 175, so 175 µL is the total volume of Lysis Buffer
- Add 180 µL of Lysis Buffer to the master mix tube
- 175 Lysis Buffer X 12/1,000 = 2.1 µL Proteinase K (10 mg/mL)
- Add the Pro K to the master mix tube and vortex to mix well.
- Add 33 µL of master mix to each of your DNA samples.

- Incubate at 60°C (the functional temperature of Proteinase K) Stick all tubes in a "floatie", swirl, and let sit for about 90 min.
- Incubate at 95°C to inactivate Proteinase K for 20 min. (use heat block)
- When saving excel data, enter name of strain, conc., and time point
- Store DNA tubes in -20°C incubator

2. DNA Isolation for SWPCR

- Add 5µL of 10 mg/mL Proteinase K to 95µL of lysis buffer in a 1.5mL eppendorf tube
- Add 3µL of mix to 0.2mL PCR tubes
- Pick 1-5 worms and place them into the solution
- Place the tubes in the -80°C incubator for at least 20 minutes
- Heat the tubes at 60°C for 60 minutes
- Heat the tubes at 95°C for 15 minutes
- Tap or spin the tubes to get the condensation to the bottom of the tube
- The lysate can be used for PCR or can be stored in the -20°C incubator

3. Standard PCR protocol

Note: All PCR is to be done on ice or in a cold storage box. Never leave out primers, enzymes, or DNA, as this will ruin it!

- Dilute all primers to be used. Stock powdered primers are diluted in TE buffer unless they are to be used by the sequencing center. The sequencing center prefers all primers to be diluted in ddH_20. The primers come with an information sheet detailing how much water or buffer is required to bring the primer up to 100 uM. Then make a personal dilution with 90 uL of ddH_20 and 10 uL of the stock primer in a labeled 1.5 mL eppendorf tube.
- The next step is to create the PCR master mix. Label a 1.5 mL eppendorf tube with the pair of primers to be used, one tube per pair of primers. Always set up extra reaction mixtures because there is always loss via pipetting. Add the following per reaction:
  - ddH_2O 6.7 uL
  - Reaction Buffer 1.0 uL
  - dNTP 0.2 uL
  - DreamTaq 0.1 uL
  - Forward Primer 0.5 uL
  - Reverse Primer 0.5 uL
- Vortex the master mix to ensure contents are thoroughly mixed. Aliquot 9.0 uL of master mix to each of the PCR tubes. Then add 1.0 uL of DNA to each of the reaction tubes. If you desire to increase or decrease the amount of DNA used, be sure to alter the volume of water accordingly in the master mix. The total volume should always be 10 uL.

- If using the strips of tubes place all the caps on. If using a plate then affix the adhesive film securely on. Use the speedball to help securely fasten the film.
- Put the strips or plate into the thermal cycler.
- Select the “mapping program”:
  - 94° pause
  - 94° 2 minutes
  - 94° 15 seconds
  - 58° 45 seconds
  - 72° 1 minute

  (35 cycles)
  - 72° 5 minutes
- Store PCR products at -20°C.

4. Single Worm PCR (SWPCR) protocol

- Prepare a master mix in a 1.5 mL eppendorf tube (must be used immediately)
  - Add the following per reaction (taking into account the PCR fairies):

ddH_2O	13.4 µL
Reaction Buffer	2.00 µL
dNTP	0.40 µL
DreamTaq	0.20 µL
Forward Primer	1.00 µL
Reverse Primer	1.00 µL

- Aliquot 18µL of master mix to each PCR tube
- Place in a thermocycler (times, temperatures and cycles between dotted lines may vary):
  - Select the “mapping program”:

94° pause

94° 2 minutes

94° 15 seconds

58° 45 seconds — 35 cycles

72° 1 minute

72° 5 minutes

- Store PCR products at -20°C.

5. GENEWIZ Guidelines for sample preparation for Sanger Sequencing (using Purified PCR Template)

- Label your tubes on the side with your initials and sample number.
- Dilute your sequencing primer (forward/reverse) to 5 µM (pmol/µl) using water. You will need 5 µl for each sequencing reaction.
- For the amount of template needed for PreMixed sample, please refer to the table below. Prepare template in 10 µl for each sequencing reaction. Please make dilutions in water or Tris. For best results, do not use Tris-EDTA (TE) because EDTA will inhibit the sequencing reaction.
- In the same tube, mix template (10 µl) and your primer (5 µl) according to the table below.

Table 12. Concentration of DNA template and primer used for Purified PCR products in Sanger sequencing sample preparation

DNA Type	DNA/Product Length	Template Concentration in 10 µl	Template Total Mass	Your Primer Total Picomoles	Premixed Volume* (Template + Your Primer)
Purified PCR Products	<500 bp	~1 ng / µl	~10 ng	25 pmol	15 µl
	500 - 1000 bp	~2 ng / µl	~20 ng		
	1000 - 2000 bp	~4 ng / µl	~40 ng		
	2000 - 4000 bp	~6 ng / µl	~60 ng		
	> 4000 bp	Treat as plasmid	Treat as plasmid		

6. RNAi Protocols

a. Making RNAi Cultures from Frozen Stock

1.) Turn on shaker and set at 37°C

2.) Make LB/AMP solution

- Take a bottle of LB (50 mL)
- Add 50 ug/mL of ampicillin
- 50 mL x 50 ug/mL = 2500 ug = 0.0025g
- Vortex bottle for 30 seconds

3.) Aliquot 5 mL of LB/AMP solution into 15 mL falcon tubes and label with gene name and date

4.) Go to the -80 and take out frozen stock culture

5.) Using the P2.5 with tip attached scrape frozen culture a few times to cover tip

6.) Eject tip into falcon tube

7.) Place tubes in the shaker at 37°C for 8-12 hours

b. Freezing RNAi Cultures

- Properly label (Formal name of gene, Gene name – if available, Library it came from, Date, Initals) **1.8 mL** cryo tube vials
- Note: you should have 1 tube for the -80°C freezer and 1 tube to be placed in the nitrogen tank
- Pipette **300 uL** of glycerol into the cryo tubes (Glycerol is very viscous so be sure to wait and make sure the correct amount is pipetted into your tip and expelled into the cyro tube)
- Add **1.5 mL** of inoculated RNAi culture into the cyro tube with glycerol, pipette up and down until mixed evenly

OR

- Add **1.5 mL** of inoculated RNAi culture into the cyro tube with glycerol.
- Using an inoculation loop, flame loop
- Immerse loop into inoculated RNAi culture
- Then transfer loop, inoculating the culture in the cryo tube
- Pipette inoculated culture and glycerol mixture up and down until evenly mixed
- Place tubes into the -80°C freezer

c. Preparing Ampicillin (+tetracycline) Plates for RNAi

- 250 mL LB
- 4.0g bacto-agar
- - Autoclave -
- Place in 60C water for ~20minutes then add:
- 250uL 50mg/mL Ampicillin
- (167uL 15mg/mL tetracycline)
- Pours ~25 medium plates

d. **Carbinacillin Plates for RNAi**

The following will make about 60 plates, which is equivalent to 0.75L.

1. 0.722 L dH20
2. 2.25 g NaCl
3. 12.0 g Bacto-Agar
4. 1.875 g Bacto-Peptone
5. Swirl flask

6. Autoclave for 90 minutes under liquid cycle (usually takes 2 hours)
7. Let cool for 30 minutes at room temperature
8. 0.75 mL of MgSO4 (1M)
9. 0.75 mL CaCl2 (1M)
10. 0.75 mL Cholesterol (5 mg/mL)
11. 18.75 mL KP04 (1M)
12. 0.1875 mL Carbenicillin (100 mg/mL)
13. 7.50 mL IPTG (0.1 M)

Why we use these numbers

For steps 8 – 11:

We want a final concentration of 1 mM (0.001M) for each of these components.

C1 = 1M

V1 = X

C2 = 0.001M

V1 = 750 mL

We have solutions that are at a 1 M concentration and we want to know how much of that solution do we need to add to give use a 0.001 M concentration of this solution in the total volume (750 mL) of our sample. X = 0.75 mL

For step 10:

We want a final concentration of 25 ug/mL (0.025 mg/mL).

C1 = 100 mg/mL

V1 = X

C2 = 0.025 mg/mL

V2 = 750 mL

We have the antibiotic that is at a concentration of 100 mg/mL. This is a standard concentration the lab makes. However, if you are ever using a different antibiotic, it is important to check the bottle or the manufactures website on how to suspend the chemical. I obtained 0.025 mg/mL final concentration of the antibiotic solution in the total volume (750 mL) of our sample.

For Step 13:

IPTG is our inducer for the vector/plasmid that is carrying the clone of our gene. The inducer allows for the initiation of the expression of the gene in the bacteria. The bacteria will produce a dsRNA and the worms eat the colonies on the plate allowing the dsRNA to be introduced to their system. dsRNA is obtained by allowing transcription in both directions of the plasmid rather than in one direction, which would just generate one strand that would not produce a knockdown of the gene. Once the dsRNA is in the system, the Dicer enzyme will breakdown the structure into smaller interfering RNA fragments called siRNAs (22 n.t.). The fragments are incorporated into a multicomponent nuclease, called RNA-induced silencing complex (RISC) and becomes activated with ATP. RISC then unwinds the siRNAs and uses them as a guide for substrate selection for the endogenous mRNA of the gene. Activated RISC

complexes can regulate gene expression at many levels. Such complexes act by promoting RNA degradation and translation inhibition.

We want a final concentration of 1 mM (.001 M) for IPTG. In this case IPTG is recommended to be stored in a 0.1 M concentration. We have 0.1 M solution of IPTG but need to add X amount of this solution to end up with a final IPTG concentration of 0.001 M in 750 mL. X = 7.50 mL

Making solutions:

Carbenicillin:

1.) Weigh out 100 mg

2.) Add to tube

3.) Bring the volume up to 1 mL

4.) Vortex

IPTG

M.W. = 238.3 g

1 Molar solution = 238.3 g / 1L

0.1 Molar solution = 1.20 g / 50 mL

1.) Weigh out 1.20 g

2.) Add to tube

3.) Bring volume up to 50 mL

4.) Vortex

5.) Aliquot out into smaller volumes

It is important to note, that if you are changing the amount of plates you need, you have to redo the calculations. For example, Steps 8-12 need to be subtracted from the total volume you what to give you the amount of water to add. Usually we will add some chemical and bring it up to volume to make some concentrated solution. This is the only case where we don't account for dry contents such as steps 2-4, but it is important to get the concentrations right of the chemicals that matter.

e. Plasmid DNA extraction using Invitrogen PureLink HQ Mini Plasmid Purification Kit

Preparing Lysate

- Prepare the Resuspension Solution with RNase A. Resuspend the lyophilized RNase A (12 mg) in 200 µl of Resuspension Solution, and then add the resuspended mixture to the remaining Resuspension Solution for a final concentration of 0.1 mg/ml RNase A. After mixing, Resuspension Solution should be stored at 4°C.
- Prepare the Wash Buffer with ethanol. Add 64 ml of 96–100% ethanol to the entire volume of Wash Buffer (16 ml).
- Check the Neutralization Buffer and Lysis Buffer before use for salt precipitate. If present, place each buffer in a 37°C water bath for 5 minutes until the salts redissolve and the solution clears. Do not shake the Lysis Buffer, as this can lead to foaming.

Preparing Cell Lysate

- In a microcentrifuge tube, pellet 1–3 ml (1–2 × 109) of E. coli cells from overnight cultures by centrifugation in a tabletop centrifuge at 1,500 × g for 15 minutes.
- Completely resuspend the pellet in 240 µl of Resuspension Solution, prepared with RNase A as described above.
- Add 240 µl of Lysis Buffer to the above solution. Mix gently by inverting the tube 4–8 times.
- Incubate for 3–5 minutes at room temperature. Do not exceed 5 minutes.
- Add 340 µl of Neutralization/Binding Buffer, and mix gently by inverting the tube 4–8 times.
- Centrifuge for 10 minutes at maximum speed in a tabletop centrifuge to clarify the cell lysate.
- Proceed to Binding DNA.

Binding DNA

- Place a PureLinkTM spin column inside a 2 ml collection tube.
- Pipette or decant the supernatant from step 6, previous page, into the spin column.
- Centrifuge the column at room temperature at 10,000–14,000 × g for
- 1 minute. Discard the flowthrough, and place the column back in the tube.
- If loading multiple samples on the same column (up to 1.5 × 1010 cells), repeat Steps 2–3 for each lysate.
- Add 650 µl of Wash Buffer, prepared with ethanol as described on the previous page, to the column.
- Centrifuge the column at room temperature at 10,000–14,000 × g for

- 1 minute. Discard the flowthrough from the collection tube, and place the column back in the tube.
- Centrifuge the column at maximum speed for 1–3 minutes to remove the residual wash buffer.
- Proceed to Eluting DNA.

Eluting DNA

- Place the spin column in a clean 1.7 ml elution tube. Add Elution Buffer or sterile, distilled water as specified below
- · Add 50 µl of Elution Buffer or water to the center of the column if the expected DNA yield is <30 µg.
- · Add 100 µl of Elution Buffer or water to the center of the column if the expected DNA yield is >30 µg.
- Incubate the column at room temperature for 1 minute, then centrifuge at maximum speed for 1 minute.
- The elution tube contains your purified DNA. Remove and discard the column.

f. GENEWIZ– Guidelines for sample preparation for Sanger Sequencing (using Plasmid DNA Template)

- Label your tubes on the side with your initials and sample number.
- Dilute your sequencing primer (forward/reverse) to 5 µM (pmol/µl) using water. You will need 5 µl for each sequencing reaction.
- For the amount of template needed for PreMixed sample, please refer to the table below. Prepare template in 10 µl for each sequencing reaction. Please

make dilutions in water or Tris. For best results, do not use Tris-EDTA (TE) because EDTA will inhibit the sequencing reaction.

- In the same tube, mix template (10 µl) and your primer (5 µl) according to the table below.

Table 13. Concentration of DNA template and primer used for Plasmid DNA template in Sanger sequencing sample preparation

DNA Type	DNA Length (include vector)	Template Concentration in 10 µl	Template Total Mass	Your Primer Total Picomoles	Premixed Volume* (Template + Your Primer)
Plasmids	<6 kb	~50 ng / µl	~500 ng	25 pmol	15 µl
	6 - 10 kb	~80 ng / µl	~800 ng		
	> 10 kb	~100 ng / µl	~1000 ng		

7. Ethanol Assay with Copper Rings

- Dry NGM plates with the lids removed in the 37°C incubator for two hours.
- Remove the plates and allow them to equilibrate to room temperature for about 15 minutes, evaporation will continue to occur.
- Weigh each plate and record the weight on the side of the plate.
- Heat the copper rings and melt them into the surface of the agar, be careful to not touch the hot forceps to the agar. Tap the rings with the forceps to make sure the ring is melted completely into the agar. If the ring is not completely in the agar then the worms will be able to crawl out. Four rings maximum per plate.
- Using the available ethanol table select the correct concentration and the weight of your plate and add that much ethanol to your assay plate. Be sure to save an equal number of plates with rings and no ethanol for starvation plates.

- Record the weights of your plates and the amount of ethanol added in your laboratory notebook.
- Allow the ethanol to equilibrate for approximately 2 hours
- After the ethanol has equilibrated move your animals into their rings and remove all food by gently scraping it off with your pick. Be sure to flame in between rings to avoid transferring worms of one strain into a ring of worms of a different strain.
- Allow the worms to starve for 30 minutes. This minimizes the food left on their bodies.
- Transfer the worms from the starvation plates onto the assay plates. This transfer must be as speedy as possible to ensure accurate data, aim for less than 2 minutes per plate. Parafilm the plates after the worms have all been transferred and start a timer.
- Depending on the type of assay you may need to observe your assay plates or you may need to track your worms using the computer and camera rig.

8. Computer Tracking and Analyzing Movies

a. Taking movies:

- Open Image-Pro Plus 6.0
- Turn on the camera and the light source
- Click on “Acquire” at the tope of the Image Pro window
- Select “Video/Digital Capture”
- The window that pops up on the right half of the screen (labeled “QImaging Digital Camera”) will have information regarding different camera settings.

The settings already in place should be the ones most commonly used unless Jill or Andrew says otherwise.

- Click on “Preview” at the top left corner of the QImaging Digital Camera window.
- Place ringed plate on the light source at the base of the microscope using the “Live Preview” window to put all rings in the camera’s field of view. Also use the preview window to adjust the lab light source to the proper brightness to take a clear image.
- Click on “Snap” at the top left corner of the QImaging Digital Camera window, and save the image (as a .seq file) to designated folder.

b. Analyzing movies:

- Open Image-Pro Plus 6.0
- Click on “File” and select “Open” to load video saved in a designated file
- Click on “Macro” heading at the top of the Image-Pro window and select
- “flatten_magnify_add_ring”
- Drag the white ring that appears over to the ring of worms to analyze, and adjust the white ring to fit the shape of the copper ring
- Click on “Measure” heading at the top of the Image-Pro window and select “Track Objects”
- Click on the track objects automatically icon (yellow lightning bolt icon on top right side of the “Tracking Data Table” window
- Three smaller windows will pop up. On “Count/Size” window click on “Select Ranges” and adjust vertical line to adjust brightness in order to outline each

worm, but without making the background appear too bright. Close window when properly adjusted.

- Use “Sequencer Toolbar” to select the movie frame that captures the most number of worms in the selected ring.
- Click on “Count” in the Count/Size window, and then click on “Continue” in the Tracking window.
- Two sets of boxes with questions will pop up. For the first box that pops up click on “Yes,” and for the second window that pops up click on “No.”
- A list of tracks with speeds will appear in the Tracking Data Table window. Click on tracks making sure they accurately records paths of worms, deleting tracks that are recording miscellaneous objects (using blue X to delete selected track).
- Once true worm tracks are remaining, open up an Excel file, and click on the green Excel icon at the top right of the Tracking Data Table window to import list of tracks and speeds to Excel. Because mean speed is the information of interest, on a separate worksheet on the Excel file, make a table for the mean speeds for each strain of worms for each time point recorded.
- ****Make sure to make a new worksheet before importing the tables for each ring. Otherwise, the table will import over the previously imported table.

9. Recipes

S Basal (400 mL)

- 8 mL 5 M NaCl
- 20 mL 1 M KPO4 (pH 6)
- 372 mL dH2O

- Post Autoclave -

- 400 µL 5 mg/mL cholesterol

M9 (1 Liter)

- 6 g Na2HPO4
- 3 g KH2PO4
- 5 g NaCl
- 1 mL of 1M MgSO4

- Autoclave -

Freezing Solution (1 Liter)

- 18 mL 5 M NaCl (Must be heated and swirled vigorously)
- 50 mL 1 M KPO4 (pH 6)
- 300 mL DMSO
- 632 mL dH2O S Buffer (1L)
- 129 mL 0.05 M K2HPO4
- 871 mL 0.05 M KH2PO4
- 5.85 g NaCl

- Autoclave -

4X Lysis Buffer (100 mL)

- 1.491 g KCl
- 0.4856 g Tris
- 0.2033 g MgCl2
- 0.04 g Gelatin

- 1.8 mL NP4O
- 1.8 mL Tween-20

- Autoclave (Filter)-

1L KPO4 (pH 6.0) in H2O

- 110.26g KH2PO4
- 33.064g K2HPO4

2.5 mM dNTP

- 2.5 µL of each of the 4 dNTPs
- 90 µL ddH20

LB

- 1 Tablet per 50 mL H2O

- Autoclave (same day) -

Cholesterol

- 5 mg/mL in 95% EtOH

- Filter Sterilize -

Proteinase K

- 10 mg/mL in H2O

APPENDIX II

Table 14. Primers for PCR of mutant *C. elegans* strains obtained from *Caenorhabditis* Genetics Center website.

Strain	Genotype	Forward Primer(s)	Reverse Primer(s)	Annealing temperature (°C)
VC2240	*acs-4 (ok2872)*	CTGTTTCAGGCAAATTGGGT (out)	TTCCTGTGCTCAAGTCGTTG (out)	69.6
		ATGTTTGGGAACTCGACAGC (in)	ATCCTTGAACAACAGGGCAG (in)	69.6
RB2015	*acs-5 (ok2668)*	AACAACACGTTGCTGGAGTG (out)	CCACCCATGGCCTAACTCTA (out)	Not used
		TCTAATCGAGTTGGATTCACG (in)	TGCAATTACAGGGTCAACCA (in)	64
RB1377	*acs-17 (ok1562)*	GGTCGATTCTTCGATTTCCA (out)	TGGGGAGCATAGGTTTTTCA (out)	Not used
		CCTAAAACATATGGCCACCG (in)	TGAACGCACGGTATGTTTGT (in)	64
VC1087	*acdh-1 (ok1514)*	GTCACCTCAAACCAAGGGAA (out)	GGTGGGATGTACGGTAGGAG (out)	62
		CTTCAGCAATATTCCAGCCC (in)	AACGGAAGGCGAATCAATTA (in)	64
RB2101	*hacd-1 (ok2776)*	AAGCTCAATGGCTTTTTCCA (out)	CGTTTTTCTGCCAAGCTTTC (out)	64
		CAGAAATTTTCCCCCACAAA (in)	CAGCGACCAATTTGTCCATAA (in)	64
RB1606	*acaa-2 (ok1978)*	TTCGTGAAGCATATTGCGAG (out)	GCCCCTTGATAGTGATTCCA (out)	Not used
		CCATTTCCTATTTTCCCCGT (in)	GTATTGTGCGCCCAACTTCT (in)	64
RB2566	*T02G5.7 (ok3574)*	CAGTCTATCGCAATGTCGGA (out)	GGAGTTGACGATTCGGAGAC (out)	63.5
		CCGAGGATCTTTCGCTAACTT (in)	TTTCCGAAAACGCTCACTG (in)	Not used

Table 15. Primers for PCR of mutant C. elegans strains designed on NCBI Primer-BLAST

Strain	Genotype	Forward Primer(s)	Reverse Primer(s)	Annealing temperature (°C)
VC40812	*acs-3 (gk826522)*	TCCTTAGCTCACATCTATGAGC	GTTAAAAAACGTCTGCAGTTTCC	63.5
RB2015	*acs-5 (ok2668)*	CCCAGATAGTGTCACGACCG (within deletion)	GAGCAGCTCACTCACTGGAC (within deletion)	67.2
RB2147	*acs-13 (ok2861)*	TGAACAAATGATTGAGCGACA (out)	ACCGATGAGCTCAAAACGAC (out)	63.5
		CGACACATTCCGTTTGACCG (in)	GGCTCACATGCTCGAGAGAG (in)	Not used
VC20634	*acs-22 (gk364606)*	TGTCGTCAAGGATGGAACGG	AAGTGAAATGAGCCGAGAGGG	69.6
VC20616	*cpt-3 (gk356297)*	GAAACAAACCCGAAGACAACTG	AGAATGATAAGAGGTGATGTGA ACC	63.5
VC40798	*cpt-4 (gk818803)*	TACTCTTCCAGGAACGGGCT	TCGACATTAGGCAATTTTGGCA	66
VC40360	*cpt-6 (gk594576*)	ACATGGCTTCTTTGGGTTGTC	CACCACAACATCACTCACGTTC	63.5
VC20502	*acdh-2 (gk143151)*	TCCTGCACGCATTCCAAGAT (out)	CCTACAAGGCGACCTACACC (out)	69.6
		CCTGAAAGTTTTACAC (in)	TTCTCAACGGATCAAAACGG (in_WT nucleotide at SNP) TTCTCAACGGATCAAAACGA (in_mutant nucleotide at SNP)	60
VC40973	*acdh-5 (gk907299)*	GAACTTGGAAGAATAACTTCCAGG	GTGTGTGTGCACAGCTGATA	63.5
VC40929	*acdh-6 (gk886629)*	TCAGGCACAACACAAAAGTCG	CTCACCAAATTGTGCAAGAGCA	63.5
VC40288	*acdh-7 (gk556025)*	CGGGAAAGCATATTTAACCTGC	TCACTCTTCCAGGTTGACG	63.5
VC40665	*acdh-11 (gk753061)*	CGTTGAGACCAGGTACCGTAT	GTCATAGCCATCGGACAGGA	66
VC41029	*F54D5.7 (gk936057)*	GTGGAACGAGTCGATTCGGGA	ACTTTTCCCTCATCTTTCAGGCG	63.5
VC40235	*ech-1.2 (gk527451)*	TTTGGGTACCTCCAGCTCCT	AGATGTTGCCGTGGTGAAGA	63.5
QC119	*ech-7 (et6)*	TGTGCTTACATCGGCCCTAC	CATCTAGGCAGACAGGCAGG	66
VC2462	*T02G5.4 (ok3160)*	GCATTCCAATTTTTCCAGGTCTGT	GCTCCTCCATGTGGGTTCAC	63.5
VS24	*kat-1 (tm1037)*	GTCTCTCATTCATCTCGATCCG (out)	AACTGCTTCCTGTGAGGCAA (out)	63.5
		AGGAGGCGAGTGTGTTCTTT (within deletion)	ATAAGCATCGGTCAGTCCGTC (within deletion)	63.5

Table 16. Restriction enzymes and digest conditions used for snipSNP genotype detection

Strain	Genotype	SNP (WT/Variant)	Restriction site sequence	Restriction enzyme	Restriction Digest Conditions	
					Incubation	Inactivation
VC20634	*acs-22 (gk364606)*	C/T	5′…T▼CGA…3′ 3′…AGC▲T…5′	TaqI	65 °C (4hr)	80 °C (20 minutes)
VC40812	*acs-3 (gk826522)*	T/A	5′…C▼TNAG…3′ 3′…GANT▲C…5′	DdeI	37 °C (4hr)	65 °C (20 minutes)
VC20616	*cpt-3 (gk356297)*	C/T	5′…ACN▼GT…3′ 3′…TG▲NCA…5′	Hpy188I	37 °C (4hr)	65 °C (20 minutes)
VC40360	*cpt-6 (gk594576*)	C/T	5′…GG▼CC…3′ 3′…CC▲GG…5′	HaeIII	37 °C (4hr)	80 °C (20 minutes)
VC41029	*F54D5.7 (gk936057)*	G/A	5′…C▼CCAGC…3′ 3′…GGGTC▲G…5′	BseYI	37 °C (4hr)	80 °C (20 minutes)
VC40798	*cpt-4 (gk818803)*	G/C	5′…C▼AATTG…3′ 3′…GTTAA▲C…5′	MfeI	37 °C (4hr)	No inactivation

Table 17. RNAi plasmid DNA concentrations quantified using NanoDrop

Gene name	**Gene name (in RNAi library)**	**DNA Concentration (ng/µL)**
acs-16	F47G6.2	74.8
W03F9.4	W03F9.4	28.9
acdh-4	T10E9.9	91
acdh-8	K05F1.3	24.4
acdh-10	T08G2.3	22.5
acdh-12	E04F6.5	49.9
ech-1.1	C29F3.1	34.9
B0303.3	B0303.3	32.3

Table 18. 100% Ethanol volumes for various plate weights for specific final concentrations of ethanol (in mM).

Plate weight (g)	Agar Vol (ml)	50	100	150	200	250	300	350	400	450	500
17.9	10.0	30.1	60.2	90.3	120.4	145.5	180.7	206.8	232.9	262.0	291.1
17.8	9.9	29.8	59.6	89.4	119.3	144.1	178.9	204.7	230.6	259.4	288.2
17.7	9.8	29.5	59.0	88.6	118.1	142.7	177.1	202.7	228.3	256.8	285.4
17.6	9.7	29.2	58.4	87.7	116.9	141.3	175.3	200.7	226.0	254.3	282.5
17.5	9.6	28.9	57.9	86.8	115.7	139.8	173.6	198.6	223.7	251.7	279.7
17.4	9.5	28.6	57.3	85.9	114.5	138.4	171.8	196.6	221.4	249.1	276.8
17.3	9.4	28.3	56.7	85.0	113.4	137.0	170.0	194.6	219.2	246.5	273.9
17.2	9.3	28.0	56.1	84.1	112.2	135.5	168.3	192.6	216.9	244.0	271.1
17.1	9.2	27.7	55.5	83.2	111.0	134.1	166.5	190.5	214.6	241.4	268.2
17.0	9.2	27.5	54.9	82.4	109.8	132.7	164.7	188.5	212.3	238.8	265.4
16.9	9.1	27.2	54.3	81.5	108.6	131.3	162.9	186.5	210.0	236.3	262.5
16.8	9.0	26.9	53.7	80.6	107.4	129.8	161.2	184.5	207.7	233.7	259.7
16.7	8.9	26.6	53.1	79.7	106.3	128.4	159.4	182.4	205.4	231.1	256.8
16.6	8.8	26.3	52.5	78.8	105.1	127.0	157.6	180.4	203.2	228.6	254.0
16.5	8.7	26.0	52.0	77.9	103.9	125.5	155.9	178.4	200.9	226.0	251.1
16.4	8.6	25.7	51.4	77.0	102.7	124.1	154.1	176.3	198.6	223.4	248.2
16.3	8.5	25.4	50.8	76.2	101.5	122.7	152.3	174.3	196.3	220.8	245.4
16.2	8.4	25.1	50.2	75.3	100.4	121.3	150.5	172.3	194.0	218.3	242.5
16.1	8.3	24.8	49.6	74.4	99.2	119.8	148.8	170.3	191.7	215.7	239.7
16.0	8.2	24.5	49.0	73.5	98.0	118.4	147.0	168.2	189.5	213.1	236.8
15.9	8.1	24.2	48.4	72.6	96.8	117.0	145.2	166.2	187.2	210.6	234.0
15.8	8.0	23.9	47.8	71.7	95.6	115.6	143.4	164.2	184.9	208.0	231.1
15.7	7.9	23.6	47.2	70.8	94.5	114.1	141.7	162.1	182.6	205.4	228.3
15.6	7.8	23.3	46.6	70.0	93.3	112.7	139.9	160.1	180.3	202.9	225.4
15.5	7.7	23.0	46.0	69.1	92.1	111.3	138.1	158.1	178.0	200.3	222.5
15.4	7.6	22.7	45.5	68.2	90.9	109.8	136.4	156.1	175.8	197.7	219.7
15.3	7.5	22.4	44.9	67.3	89.7	108.4	134.6	154.0	173.5	195.2	216.8
15.2	7.4	22.1	44.3	66.4	88.5	107.0	132.8	152.0	171.2	192.6	214.0
15.1	7.3	21.8	43.7	65.5	87.4	105.6	131.0	150.0	168.9	190.0	211.1
15.0	7.2	21.5	43.1	64.6	86.2	104.1	129.3	147.9	166.6	187.4	208.3

Table 19. Average basal speeds of 2x backcrossed mutant strains at 0mM ethanol concentration at two different time points (10 minutes and 30 minutes after being transferred to the assay plate)

Genotype	Number of assays	Average speed (μm/s) at 0mM (10 minutes)	Average speed (μm/s) at 0mM (30 minutes)
acs-3(gk826522)	6	177.14	161.03
acs-4(ok2872)	5	178.28	171.06
acs-5(ok2668)	6	138.99	119.65
acs-13(ok2861)	6	183.71	173.99
acs-17(ok1562)	6	222.56	213.14
acs-22(gk364606)	6	163.51	166.90
cpt-3(gk356297)	8	164.42	173.25
cpt-4(gk818803)	8	197.20	190.09
cpt-6(gk594576)	6	177.41	187.07
acdh-1(ok1514)	5	144.56	155.14
acdh-2(gk143151)	6	168.21	161.27
acdh-5(gk907299)	6	203.16	198.63
acdh-6(gk886629)	6	192.58	195.61
acdh-7(gk556025)	5	165.92	173.96
acdh-11(gk753061)	6	196.31	192.36
F54D5.7(gk936057)	6	156.83	177.66
ech-1.2(gk527451)	8	189.90	188.60
hacd-1(ok2776)	6	189.65	187.49
T02G5.4(ok3160)	5	169.56	165.47
T02G5.7(ok3574)	6	170.32	173.06
acaa-2(ok1978)	6	211.28	214.60

Table 20. Average basal speeds of 6x backcrossed mutant strains at 0mM ethanol concentration at two different time points (10 minutes and 30 minutes after being transferred to the assay plate)

Genotype	Number of assays	Average speed (μm/s) at 0mM (10 minutes)	Average speed (μm/s) at 0mM (30 minutes)
acs-3(gk826522)	6	108.53	110.71
acs-4(ok2872)	6	130.99	140.57
acs-5(ok2668)	6	124.63	117.14
acs-13(ok2861)	6	200.30	187.15
acs-22(gk364606)	6	178.62	165.34
cpt-3(gk356297)	6	203.25	210.77
cpt-4(gk818803)	6	188.81	183.07
acdh-1(ok1514)	6	139.50	142.72
acdh-2(gk143151)	6	173.58	179.21
acdh-7(gk556025)	6	169.38	177.73
ech-1.2(gk527451)	6	67.90	58.06
T02G5.4(ok3160)	6	198.62	194.25
acaa-2(ok1978)	6	220.67	219.10
ech-7(et6)	6	188.48	195.41
kat-1(tm1037)	6	173.86	171.21

Table 21. Average basal speeds of RNAi-mediated knockdown worms at 0mM ethanol concentration at two different time points (10 minutes and 30 minutes after being transferred to the assay plate)

Genotype	**Number of assays**	**Average speed (μm/s) at 0mM (10 minutes)**	**Average speed (μm/s) at 0mM (30 minutes)**
W03F9.4 (RNAi)	8	215.73	209.00
acdh-4 (RNAi)	8	212.82	200.93
acdh-8 (RNAi)	8	208.47	193.41
acdh-10 (RNAi)	8	205.54	196.66
acdh-12 (RNAi)	8	209.97	195.93
ech-1.1 (RNAi)	8	220.20	209.62
B0303.3 (RNAi)	8	216.41	198.93

APPENDIX III

1. Graphs of ethanol response phenotypes of 2x backcrossed mutants of candidate genes in the mitochondrial beta-oxidation pathway

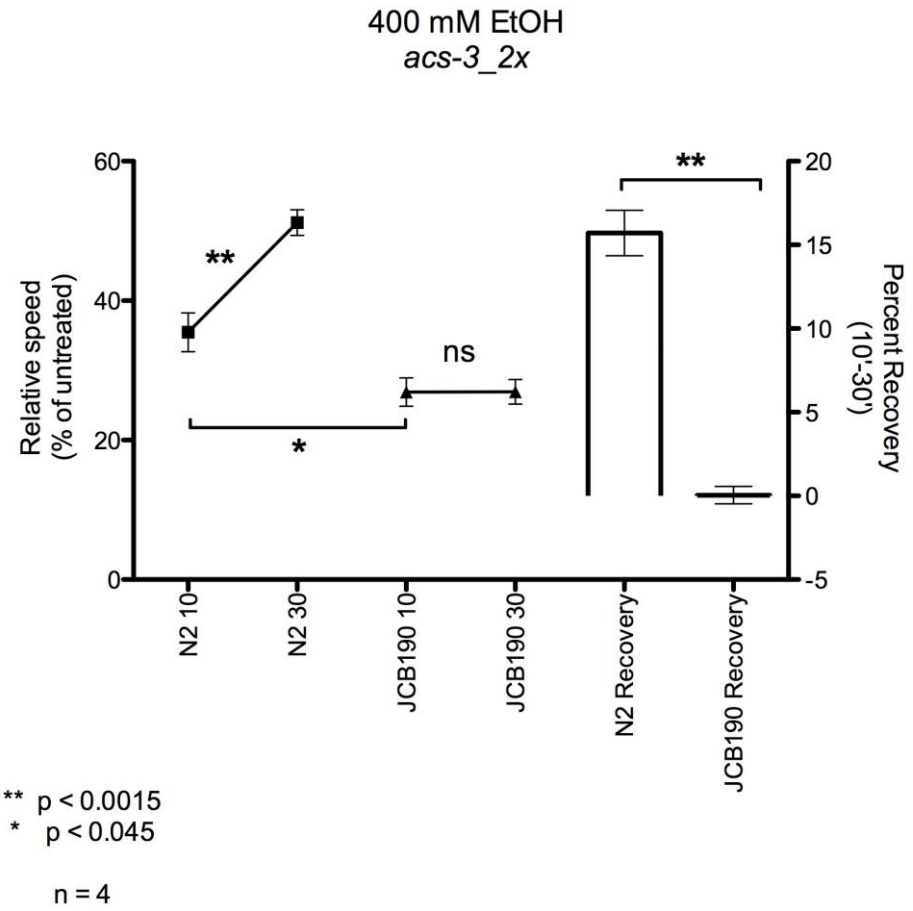

Figure 11. Ethanol sensitivity and acute functional tolerance (AFT) of 2x backcrossed *acs-3* lf mutant. At 400mM exogenous ethanol these mutants displayed increased initial sensitivity and reduced development of AFT relative to N2 (n = 4)

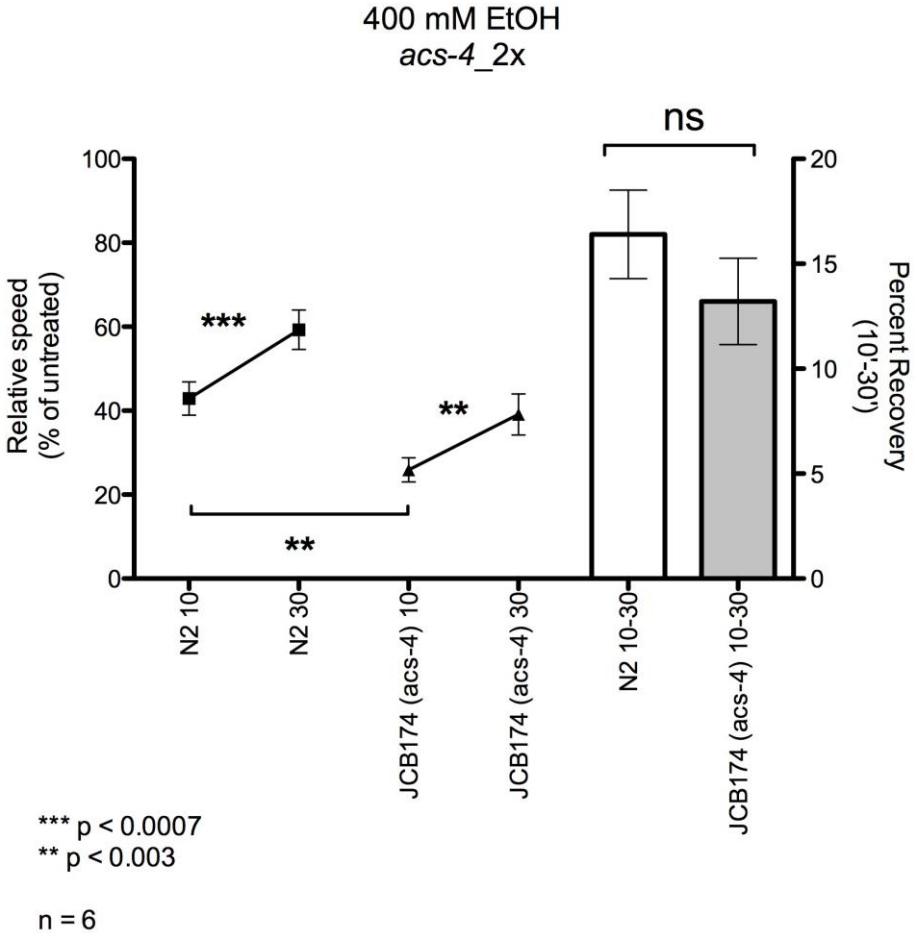

Figure 12. Ethanol sensitivity and acute functional tolerance (AFT) of 2x backcrossed *acs-4* lf mutant. At 400mM exogenous ethanol these mutants displayed increased initial sensitivity but no significant difference in development of AFT relative to N2 (n = 6)

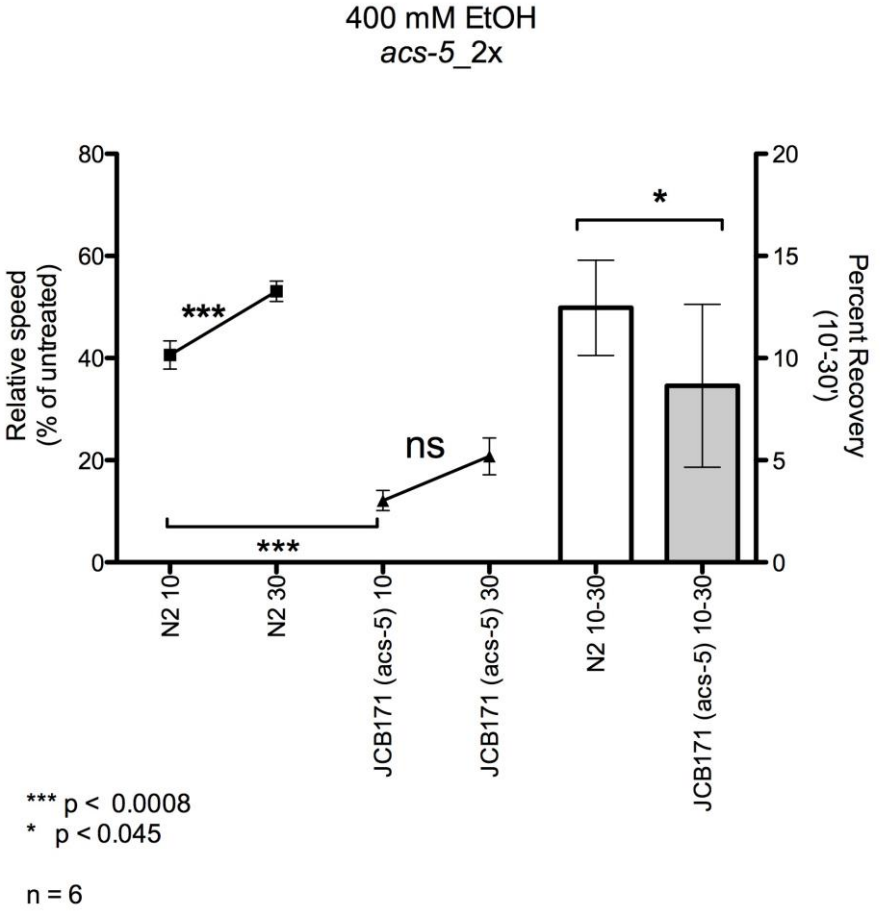

Figure 13. Ethanol sensitivity and acute functional tolerance (AFT) of 2x backcrossed *acs-5* lf mutant. At 400mM exogenous ethanol these mutants displayed increased initial sensitivity and no significant development of AFT relative to N2 (n = 6).

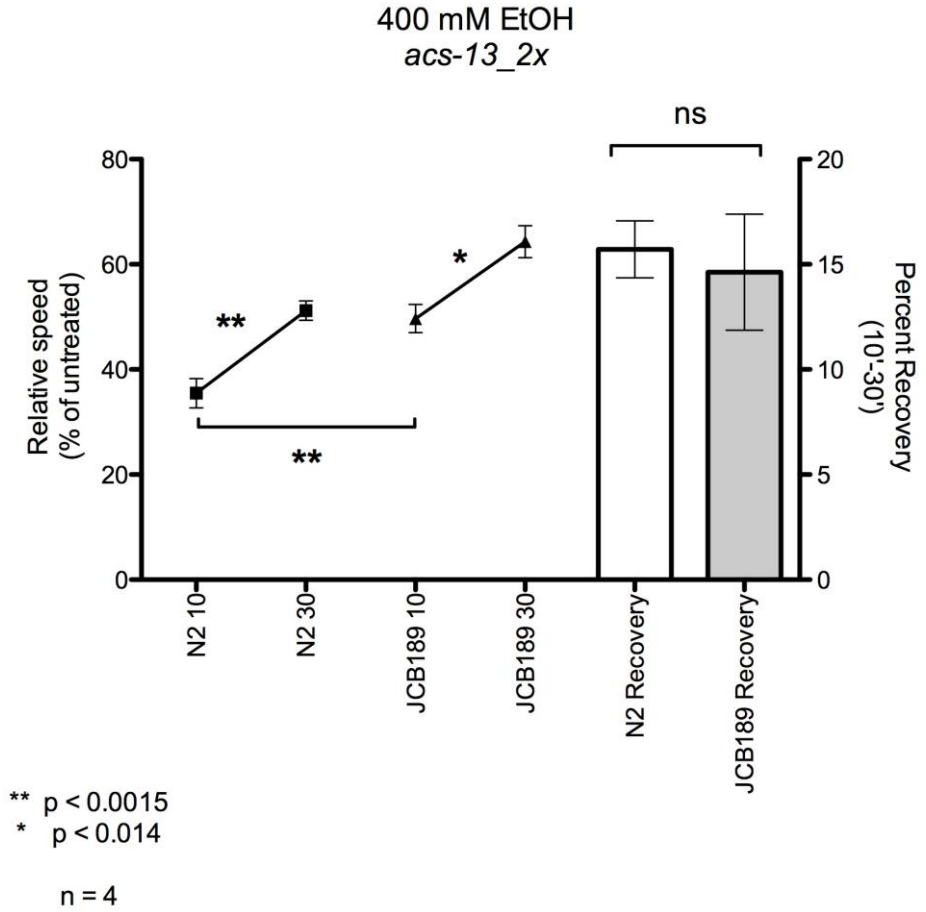

Figure 14. Ethanol sensitivity and acute functional tolerance (AFT) of 2x backcrossed *acs-13* lf mutant. At 400mM exogenous ethanol these mutants displayed decreased initial sensitivity and no significant difference in the development of AFT relative to N2 (n = 4)

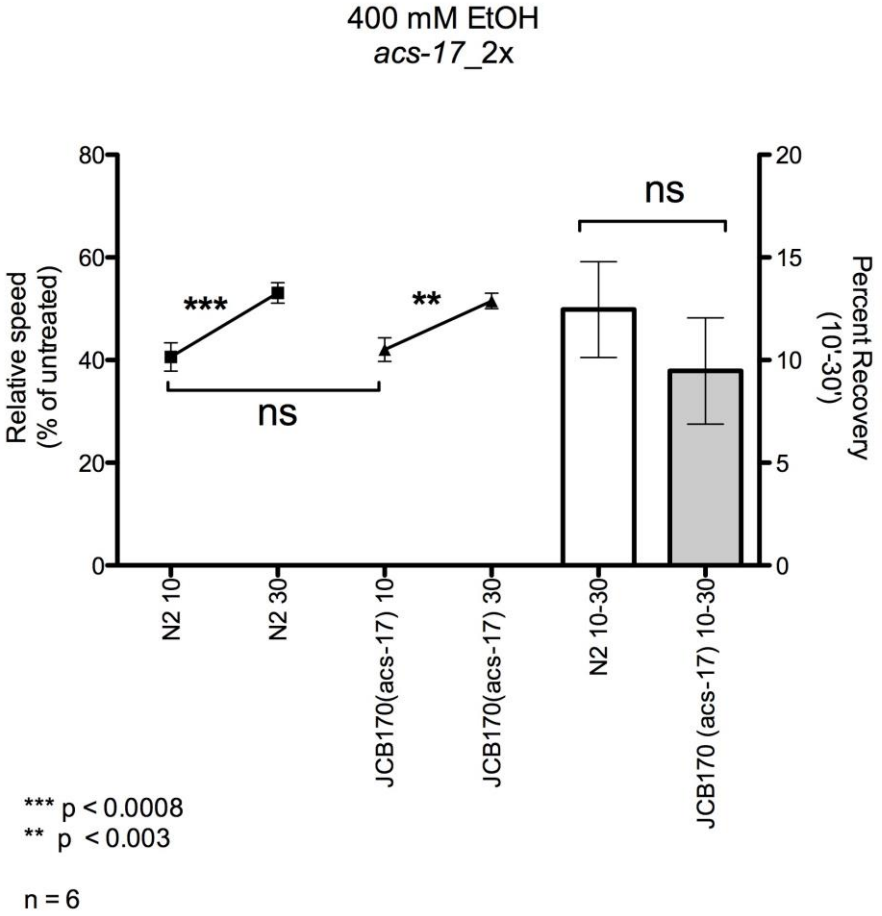

Figure 15. Ethanol sensitivity and acute functional tolerance (AFT) of 2x backcrossed *acs-17* lf mutant. At 400mM exogenous ethanol these mutants did not differ significantly from N2 in terms of initial sensitivity and AFT development (n = 6)

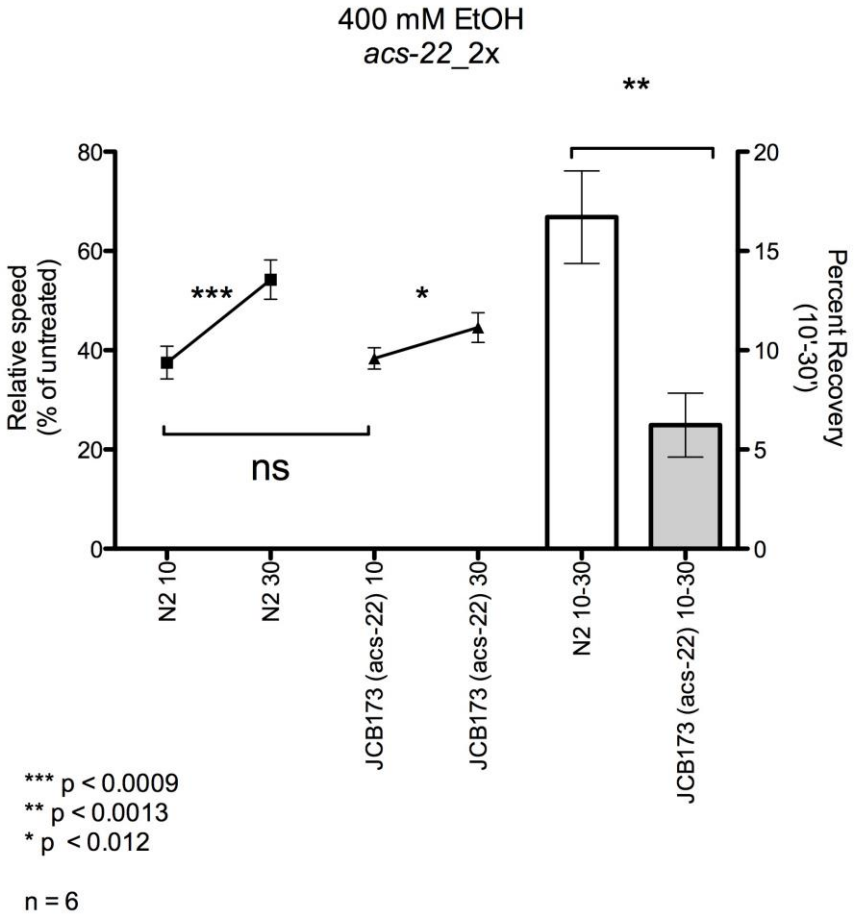

Figure 16. Ethanol sensitivity and acute functional tolerance (AFT) of 2x backcrossed *acs-22* lf mutant. At 400mM exogenous ethanol these mutants displayed reduced development of AFT, but not significantly different initial sensitivity relative to N2 (n = 6)

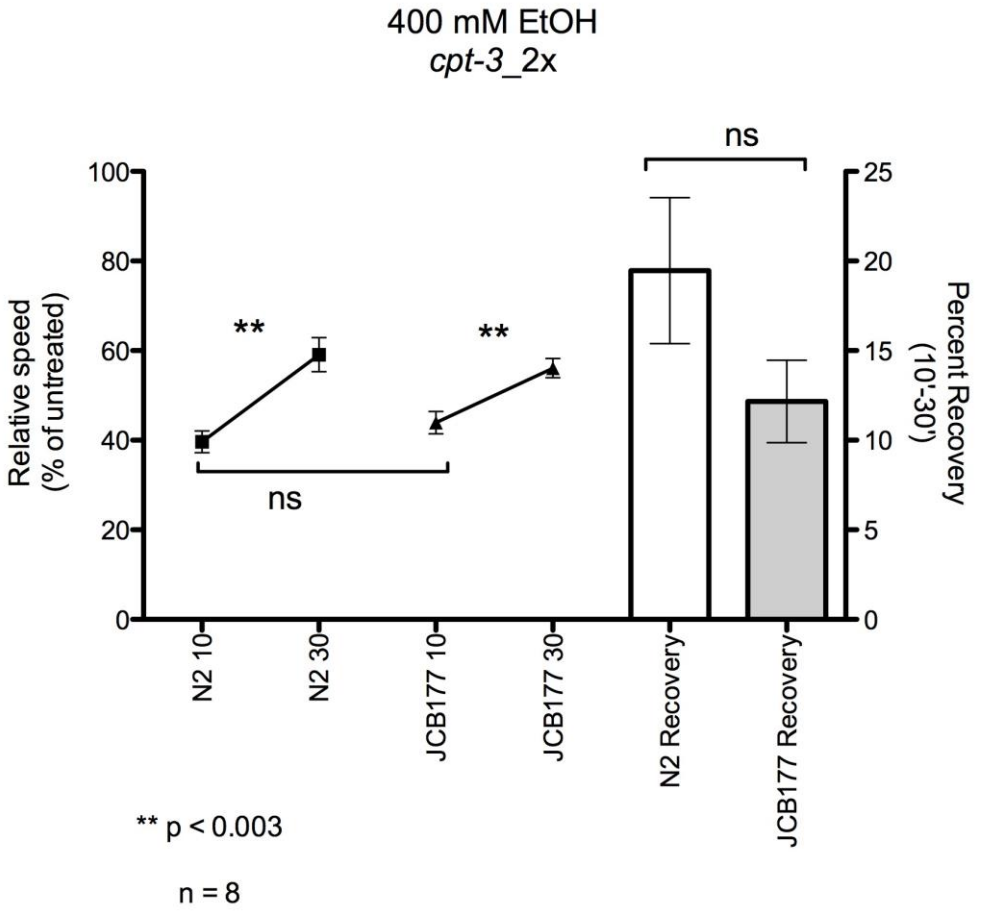

Figure 17. Ethanol sensitivity and acute functional tolerance (AFT) of 2x backcrossed *cpt-3* lf mutant. At 400mM exogenous ethanol these mutants did not differ significantly from N2 in terms of initial sensitivity and AFT development (n = 8)

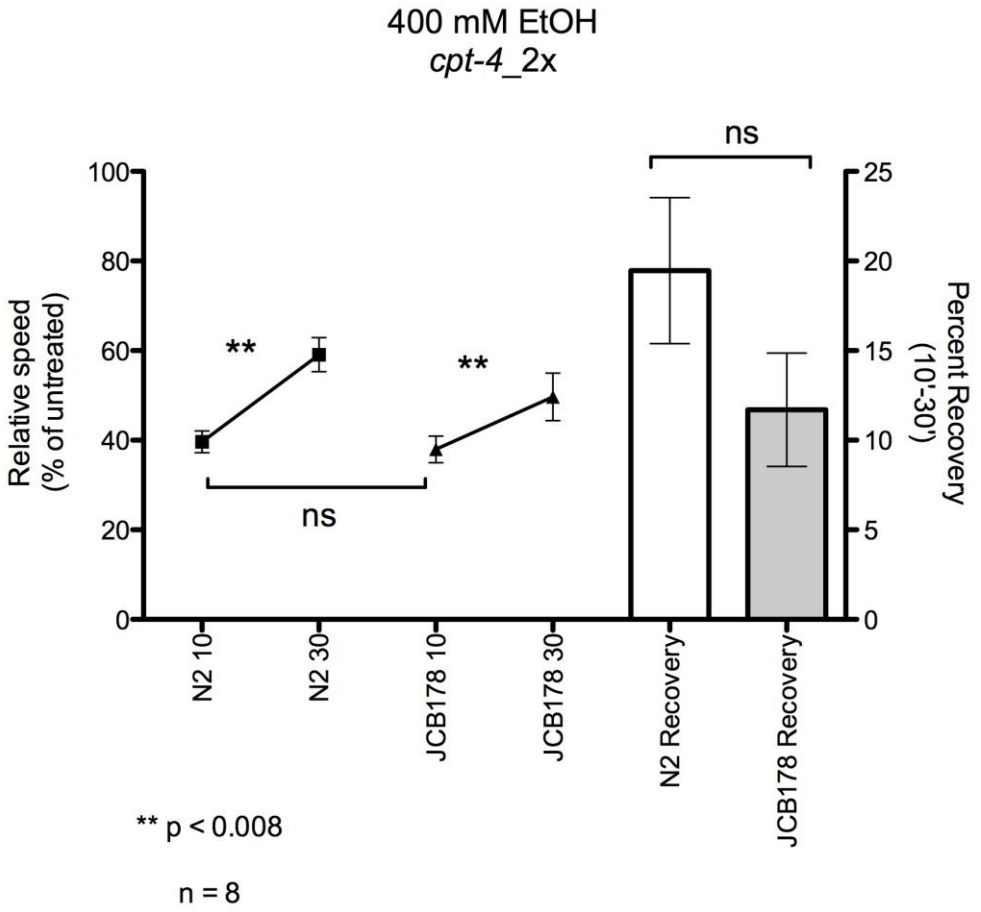

Figure 18. Ethanol sensitivity and acute functional tolerance (AFT) of 2x backcrossed *cpt-4* lf mutant. At 400mM exogenous ethanol these mutants did not differ significantly from N2 in terms of initial sensitivity and AFT development (n = 8)

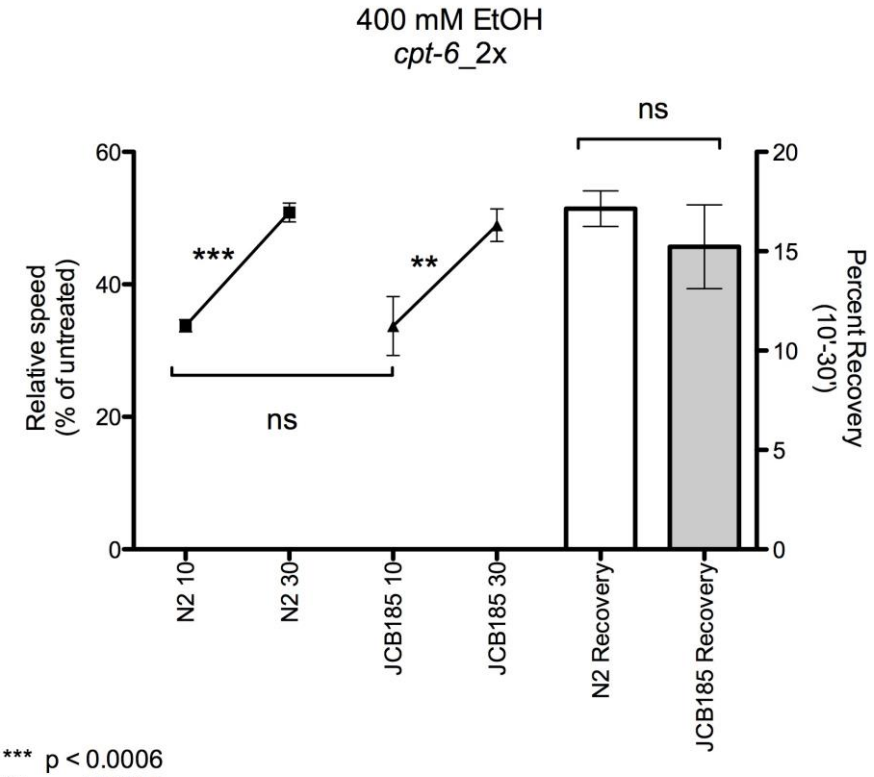

*** p < 0.0006
** p < 0.0015

ns* p = 0.078

n = 4

Figure 19. Ethanol sensitivity and acute functional tolerance (AFT) of 2x backcrossed *cpt-6* lf mutant. At 400mM exogenous ethanol these mutants did not differ significantly from N2 in terms of initial sensitivity and AFT development (n = 4)

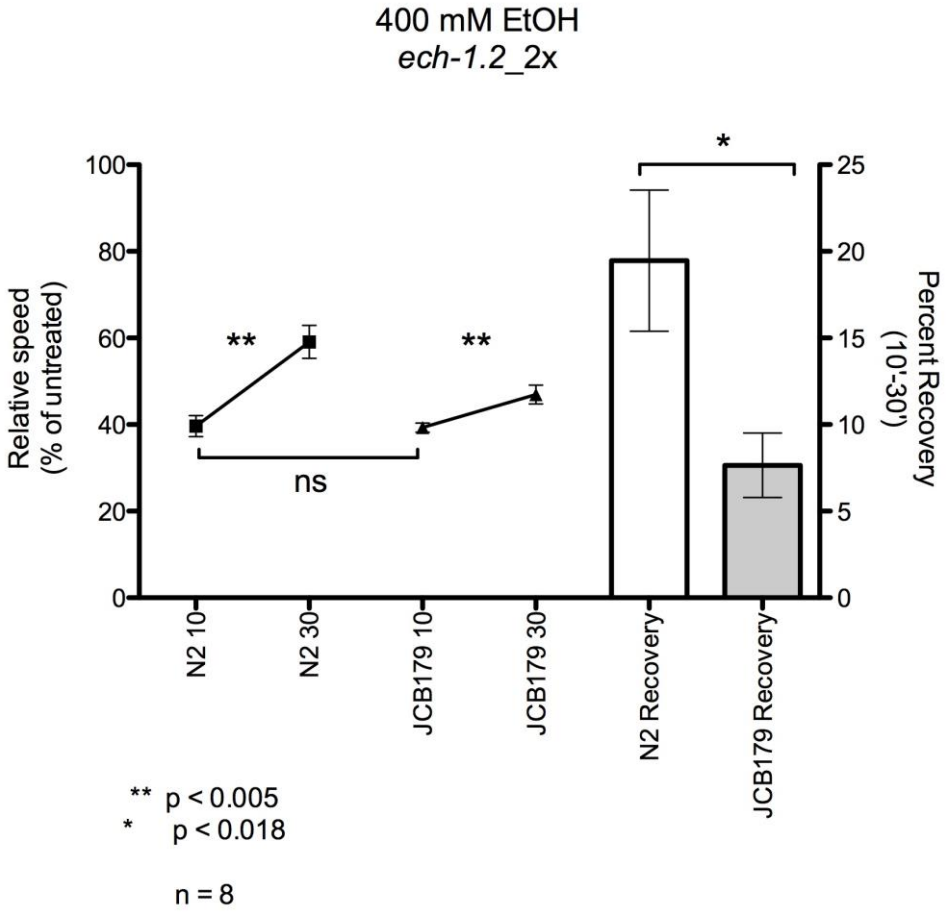

Figure 20. Ethanol sensitivity and acute functional tolerance (AFT) of 2x backcrossed *ech-1.2* lf mutant. At 400mM exogenous ethanol these mutants did not differ significantly from N2 in terms of initial sensitivity but showed reduced development of AFT compared to N2 (n = 8)

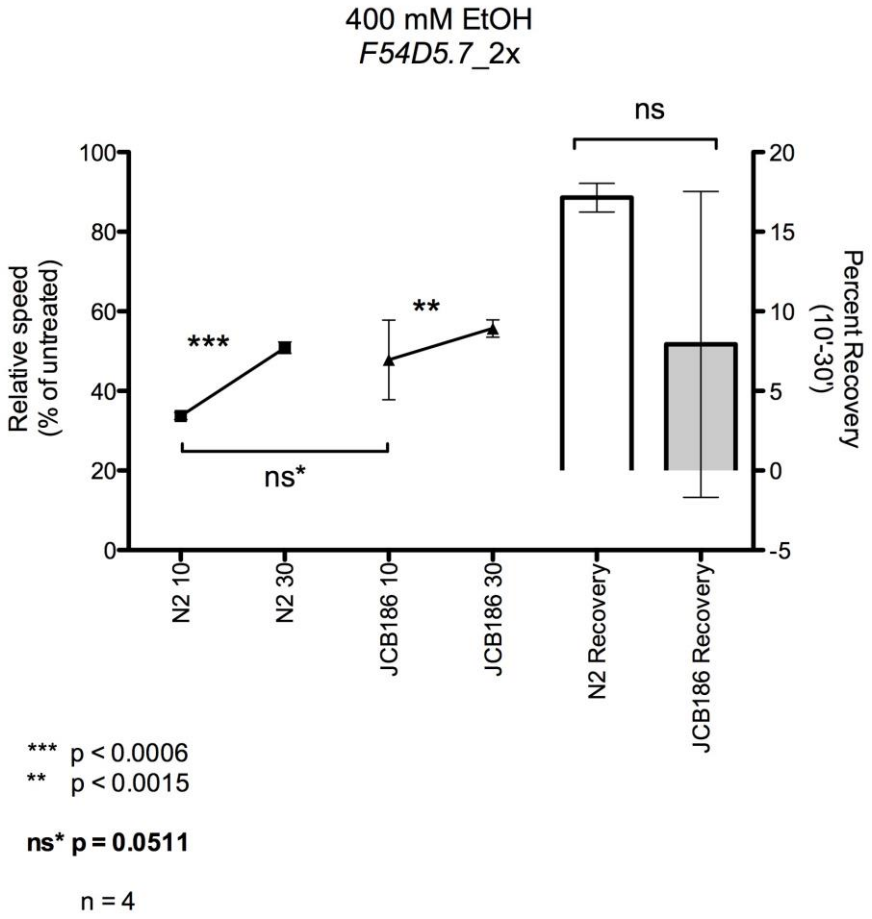

Figure 21. Ethanol sensitivity and acute functional tolerance (AFT) of 2x backcrossed *F54D5.7* lf mutant. At 400mM exogenous ethanol these mutants did not differ significantly from N2 in terms of initial sensitivity and AFT development (n = 4)

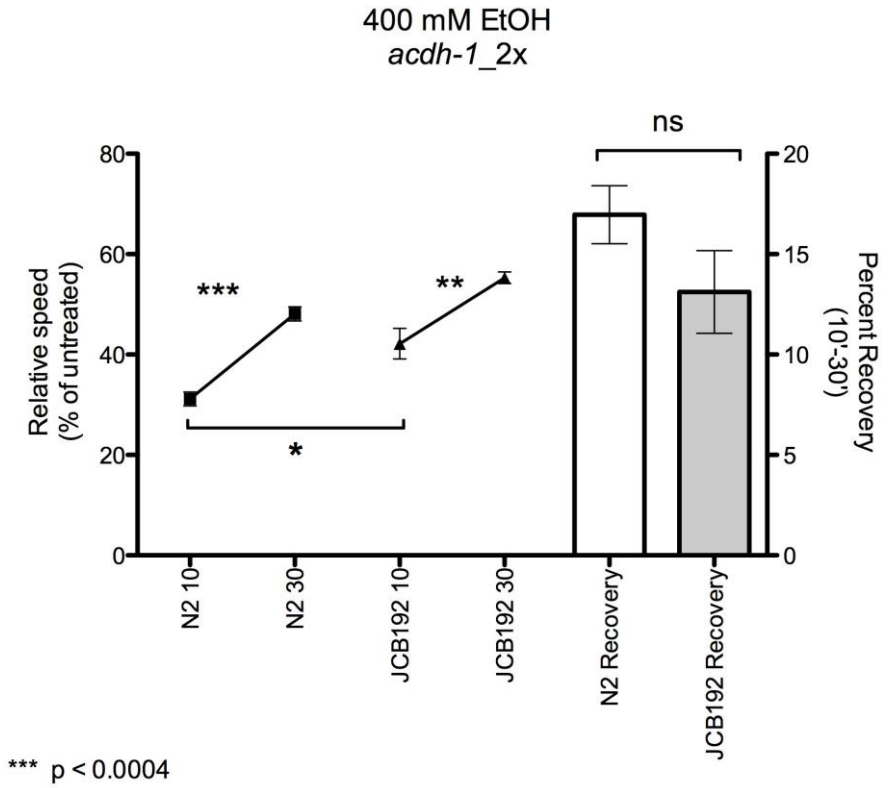

*** p < 0.0004

** p < 0.004

* p < 0.05

n = 5

Figure 22. Ethanol sensitivity and acute functional tolerance (AFT) of 2x backcrossed *acdh-1* lf mutant. At 400mM exogenous ethanol these mutants had significantly increased sensitivity but did not differ significantly from N2 in terms of their AFT development (n = 5)

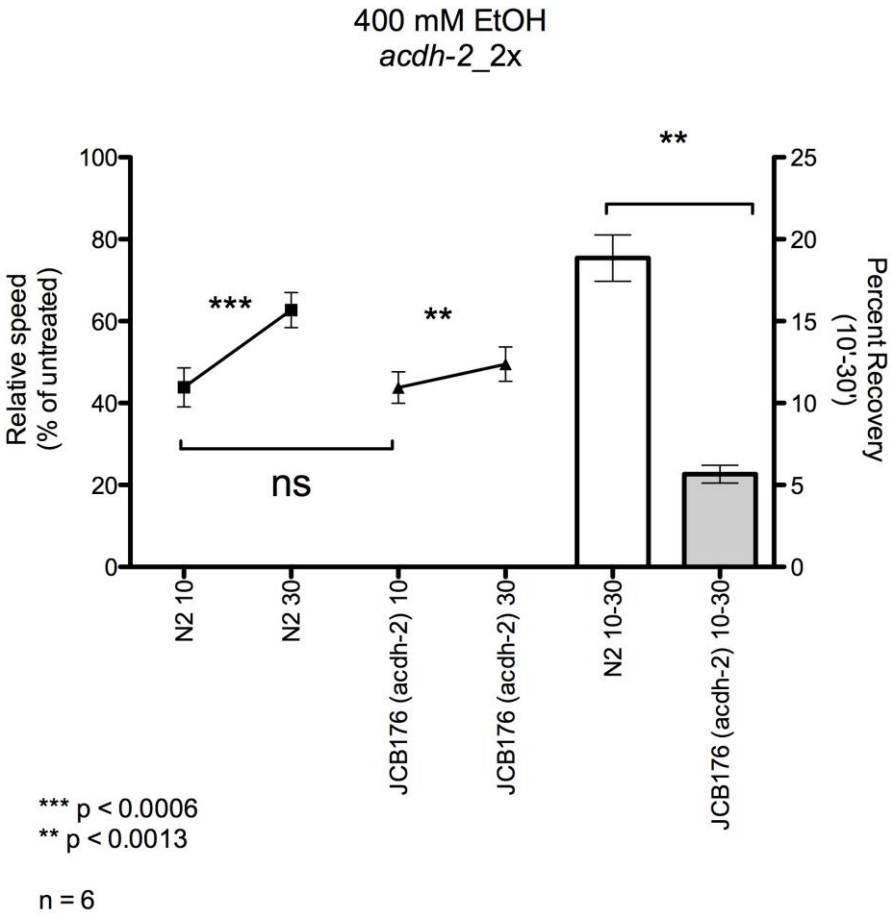

Figure 23. Ethanol sensitivity and acute functional tolerance (AFT) of 2x backcrossed *acdh-2* lf mutant. At 400mM exogenous ethanol these mutants did not differ significantly from N2 in terms of initial sensitivity but displayed significantly reduced AFT development (n = 6)

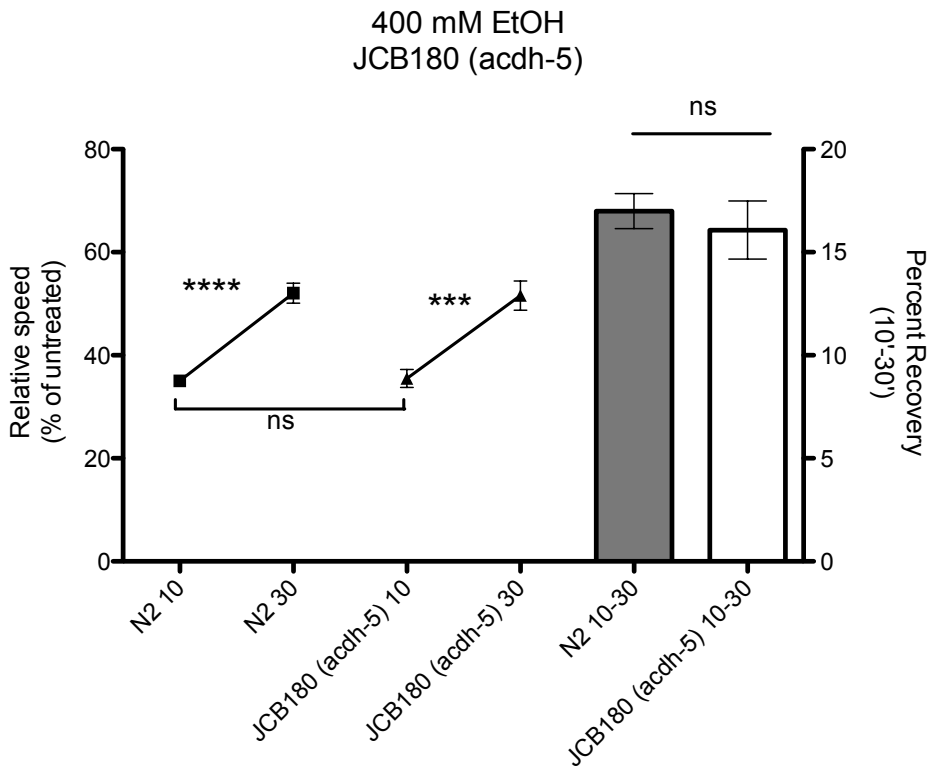

**** p < 0.0001
*** p < 0.0004

n = 5

Figure 24. Ethanol sensitivity and acute functional tolerance (AFT) of 2x backcrossed *acdh-5* lf mutant. At 400mM exogenous ethanol these mutants did not differ significantly from N2 in terms of initial sensitivity and AFT development (n = 5)

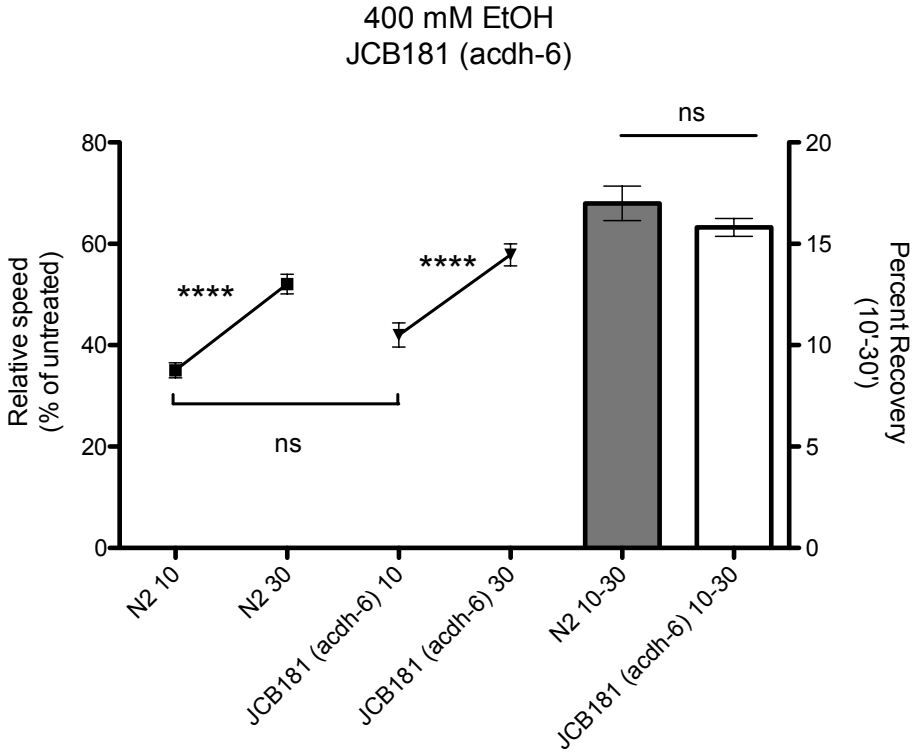

**** $p < 0.0001$

n = 5

Figure 25. Ethanol sensitivity and acute functional tolerance (AFT) of 2x backcrossed *acdh-6* lf mutant. At 400mM exogenous ethanol these mutants did not differ significantly from N2 in terms of initial sensitivity and AFT development (n = 5)

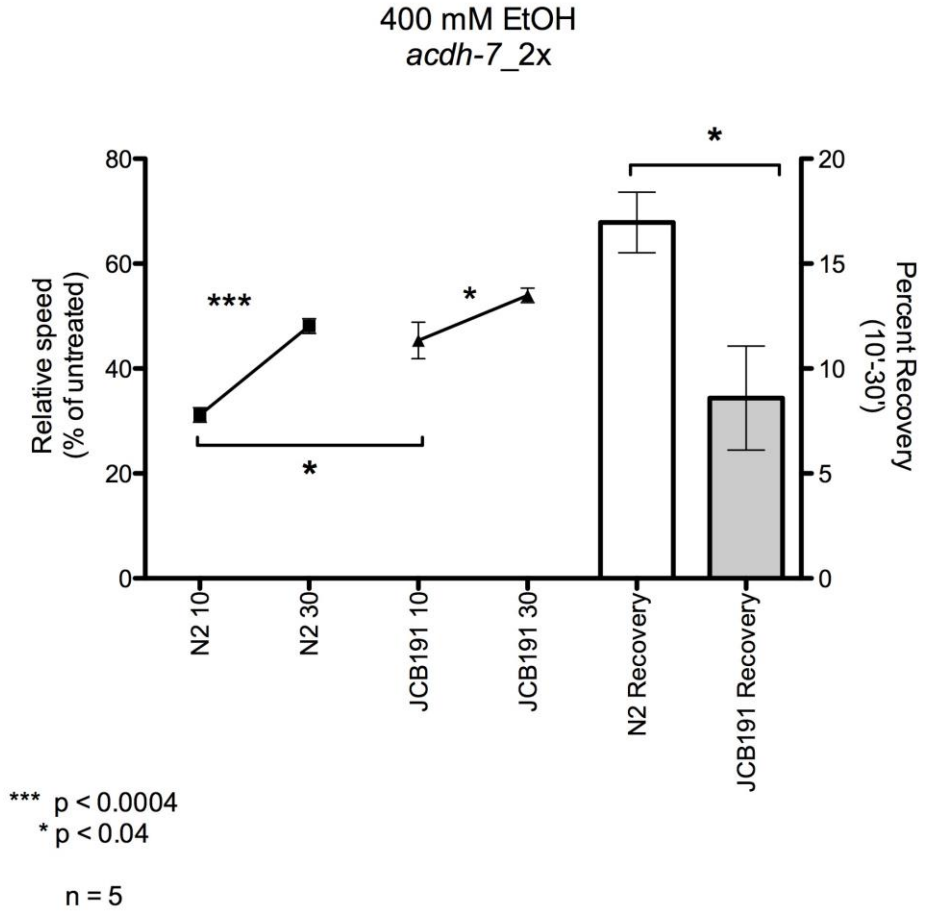

Figure 26. Ethanol sensitivity and acute functional tolerance (AFT) of 2x backcrossed *acdh-7* lf mutant. At 400mM exogenous ethanol these mutants displayed significantly decreased initial sensitivity and had reduced development of AFT relative to N2 (n = 5)

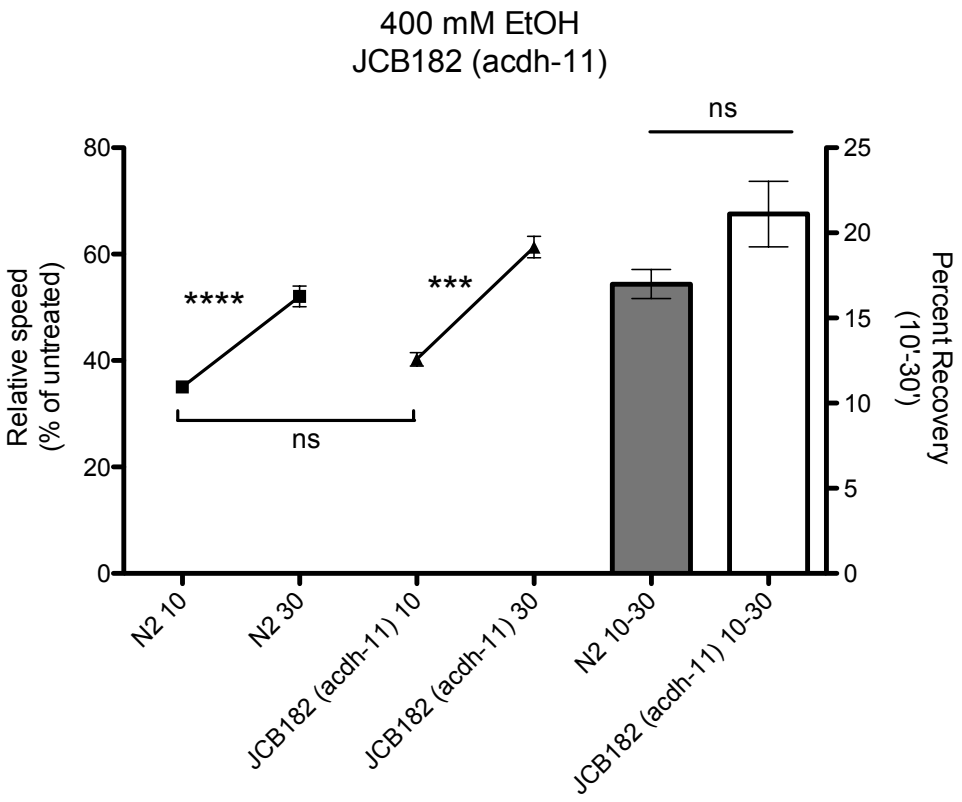

**** p < 0.00001
*** p < 0.0005

n = 5

Figure 27. Ethanol sensitivity and acute functional tolerance (AFT) of 2x backcrossed *acdh-11* lf mutant. At 400mM exogenous ethanol these mutants did not differ significantly from N2 in terms of initial sensitivity and AFT development (n = 5)

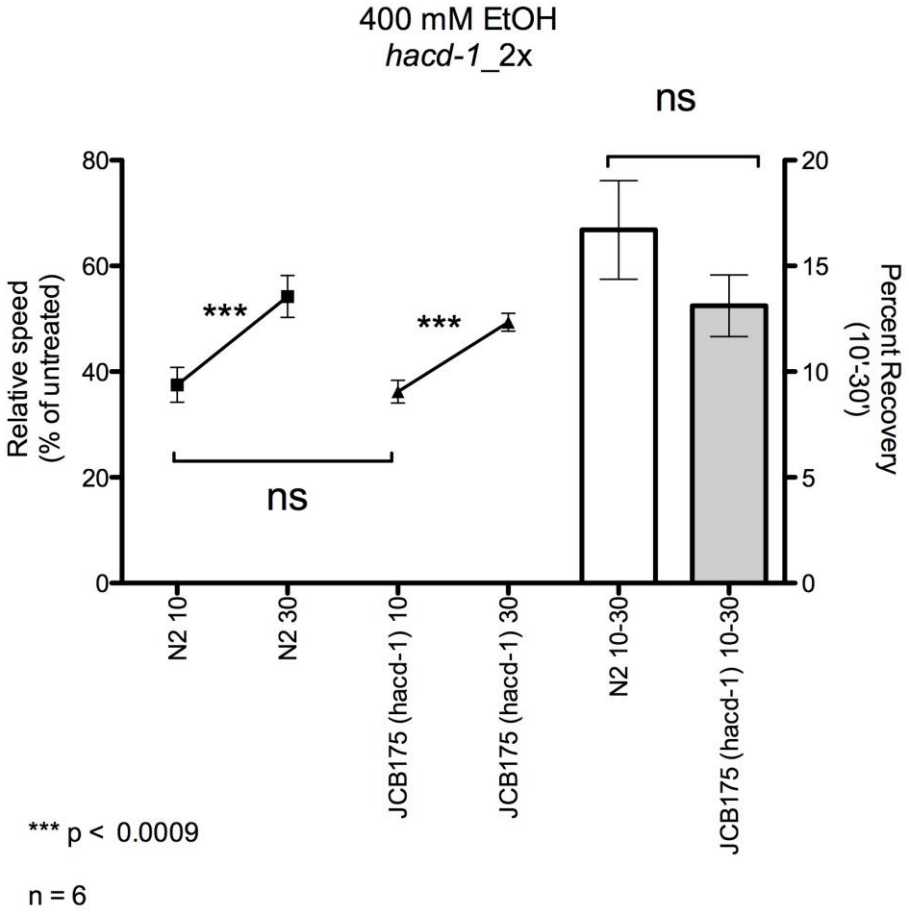

Figure 28. Ethanol sensitivity and acute functional tolerance (AFT) of 2x backcrossed *hacd-1* lf mutant. At 400mM exogenous ethanol these mutants did not differ significantly from N2 in terms of initial sensitivity and AFT development (n = 6)

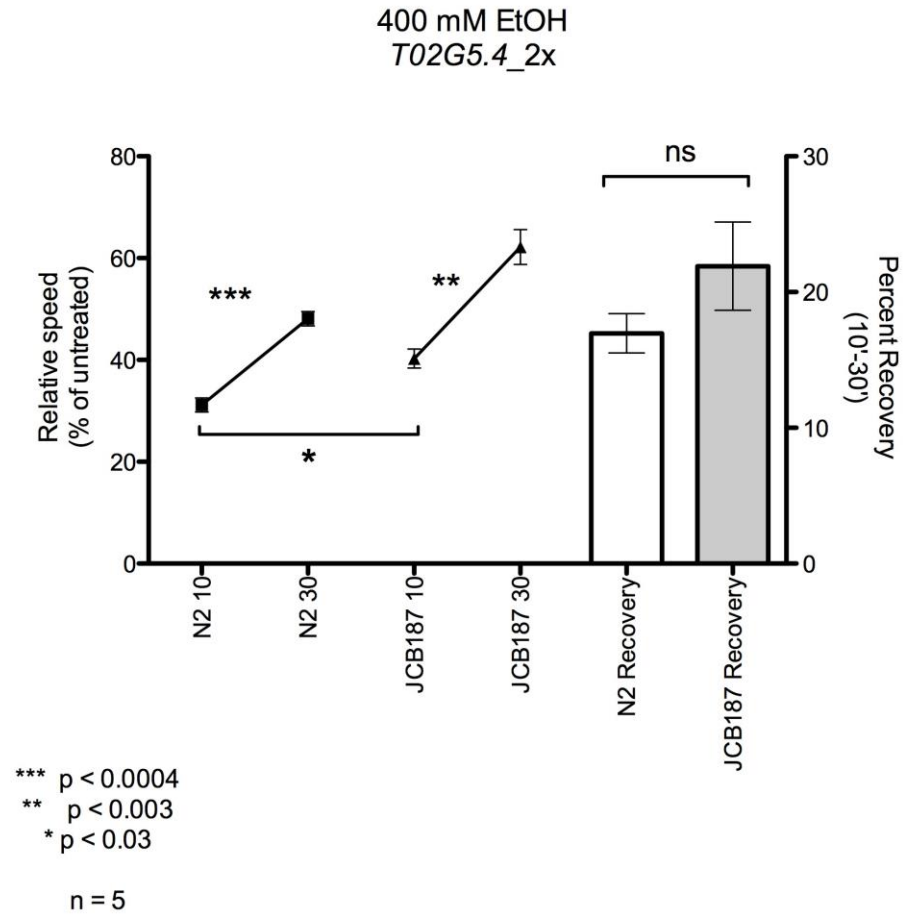

Figure 29. Ethanol sensitivity and acute functional tolerance (AFT) of 2x backcrossed *T02G5.4* lf mutant. At 400mM exogenous ethanol these mutants showed significantly decreased initial sensitivity but they did not differ from N2 in terms of AFT development (n = 5)

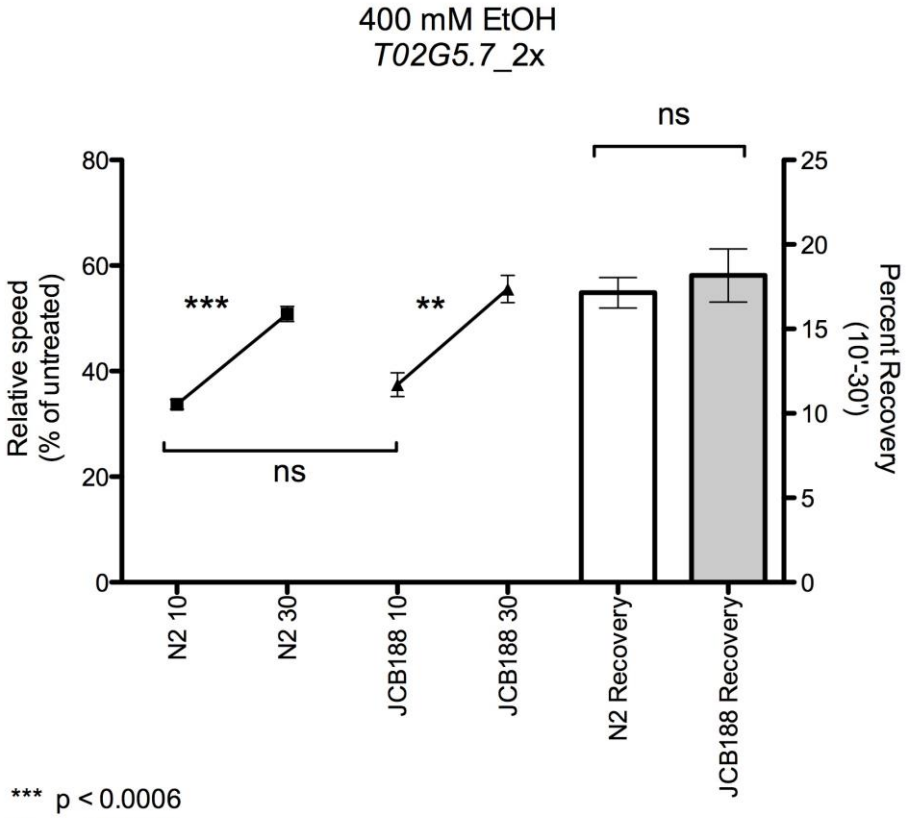

Figure 30. Ethanol sensitivity and acute functional tolerance (AFT) of 2x backcrossed *T02G5.7* lf mutant. At 400mM exogenous ethanol these mutants did not differ significantly from N2 in terms of initial sensitivity and AFT development (n = 6)

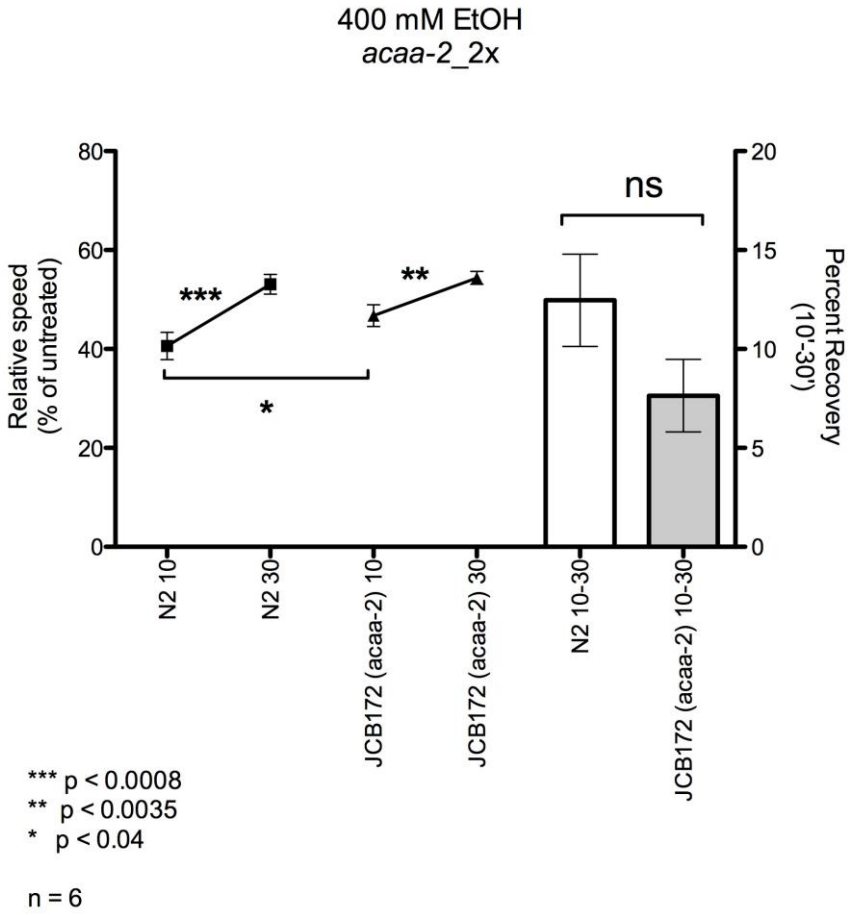

Figure 31. Ethanol sensitivity and acute functional tolerance (AFT) of 2x backcrossed *acaa-2* lf mutant. At 400mM exogenous ethanol these mutants showed a significantly decreased initial sensitivity than N2 but did not differ significantly from N2 in terms of AFT development (n = 6)

2. Graphs of ethanol response phenotypes of 6x backcrossed mutants of candidate genes in the mitochondrial beta-oxidation pathway

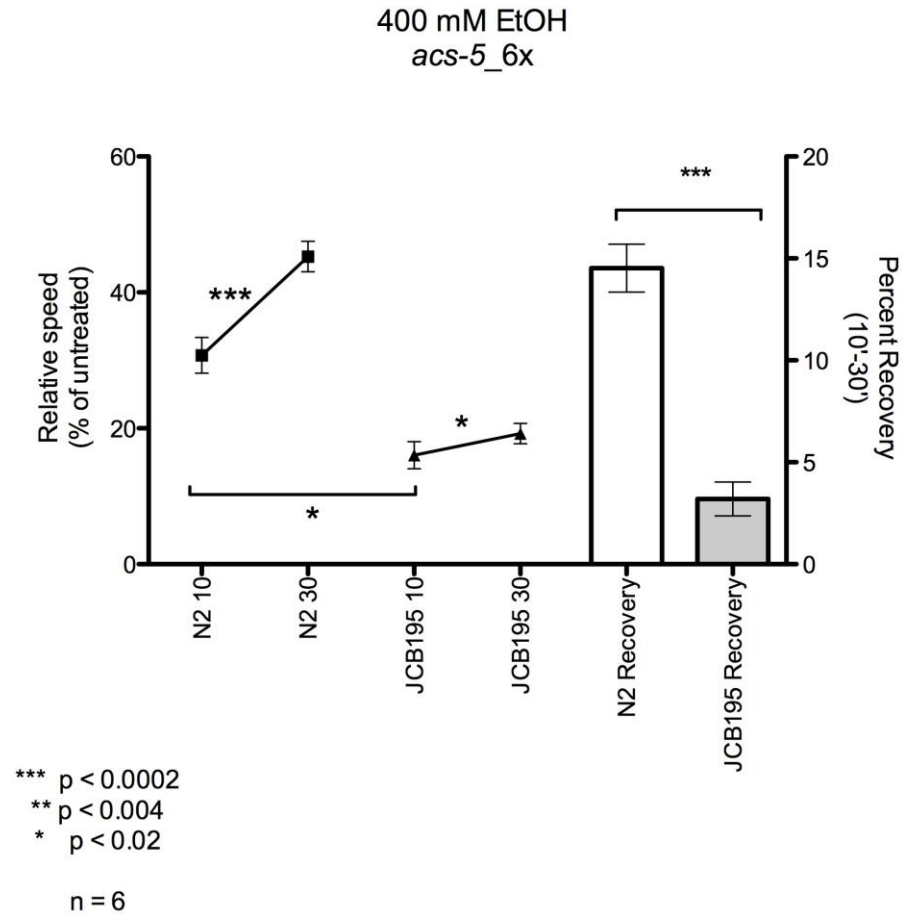

Figure 32. Ethanol sensitivity and acute functional tolerance (AFT) of 6x backcrossed *acs-5* lf mutant. At 400mM exogenous ethanol these mutants displayed increased initial sensitivity and reduced development of AFT relative to N2 (n = 6).

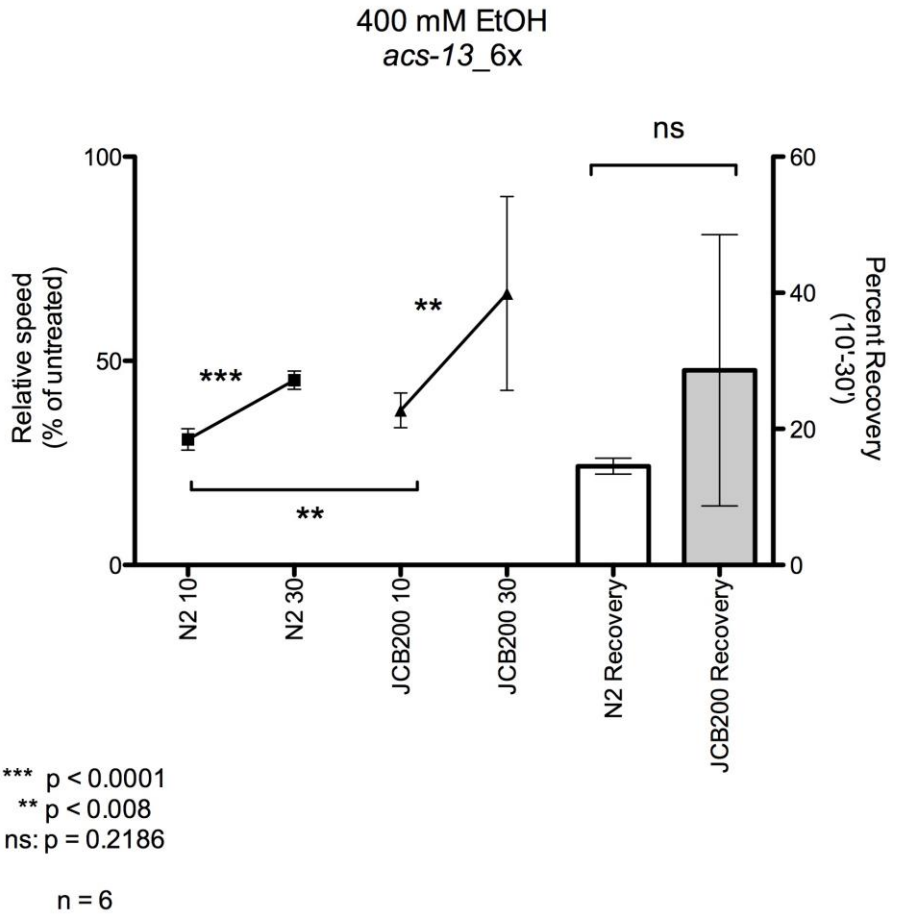

Figure 33. Ethanol sensitivity and acute functional tolerance (AFT) of 6x backcrossed *acs-13* lf mutant. At 400mM exogenous ethanol these mutants displayed decreased initial sensitivity, but no significant difference in the development of AFT relative to N2 (n = 6).

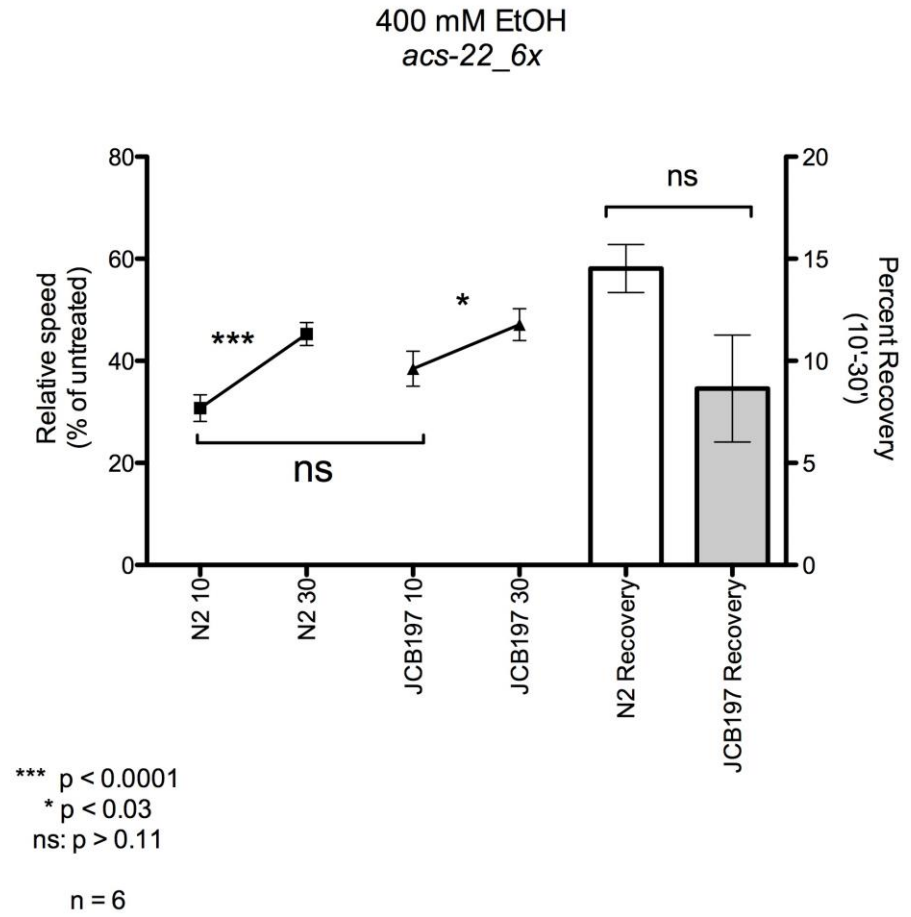

Figure 34. Ethanol sensitivity and acute functional tolerance (AFT) of 6x backcrossed *acs-22* lf mutant. At 400mM exogenous ethanol these mutants did not show any significant difference in terms of initial sensitivity or AFT relative to N2 (n = 6).

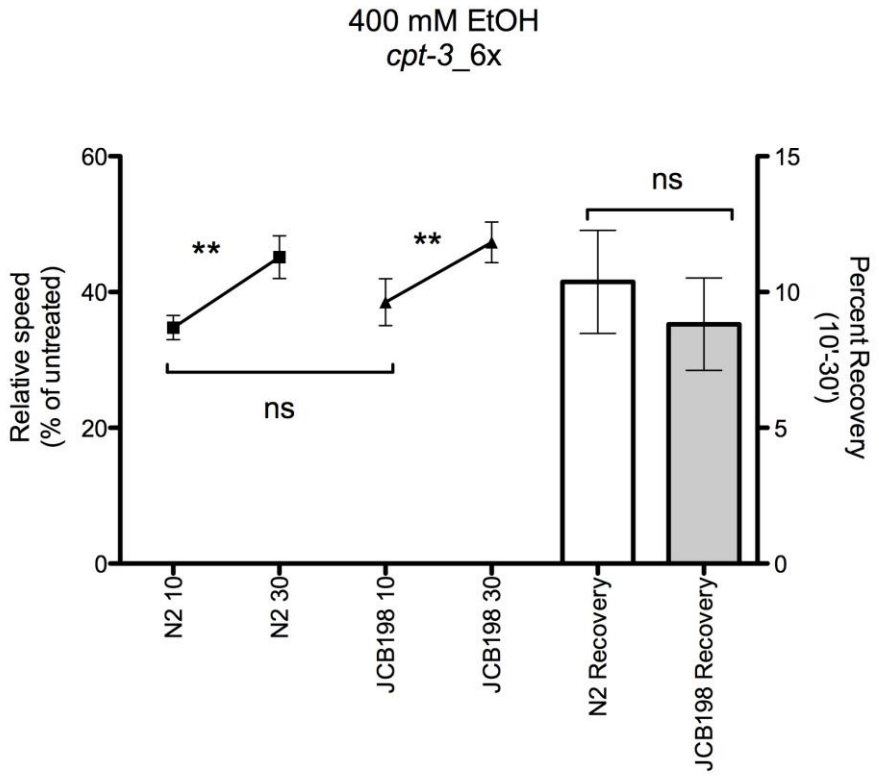

** p < 0.004
ns: p > 0.33

n = 6

Figure 35. Ethanol sensitivity and acute functional tolerance (AFT) of 6x backcrossed *cpt-3* lf mutant. At 400mM exogenous ethanol these mutants did not show any significant difference in terms of initial sensitivity or AFT relative to N2 (n = 6).

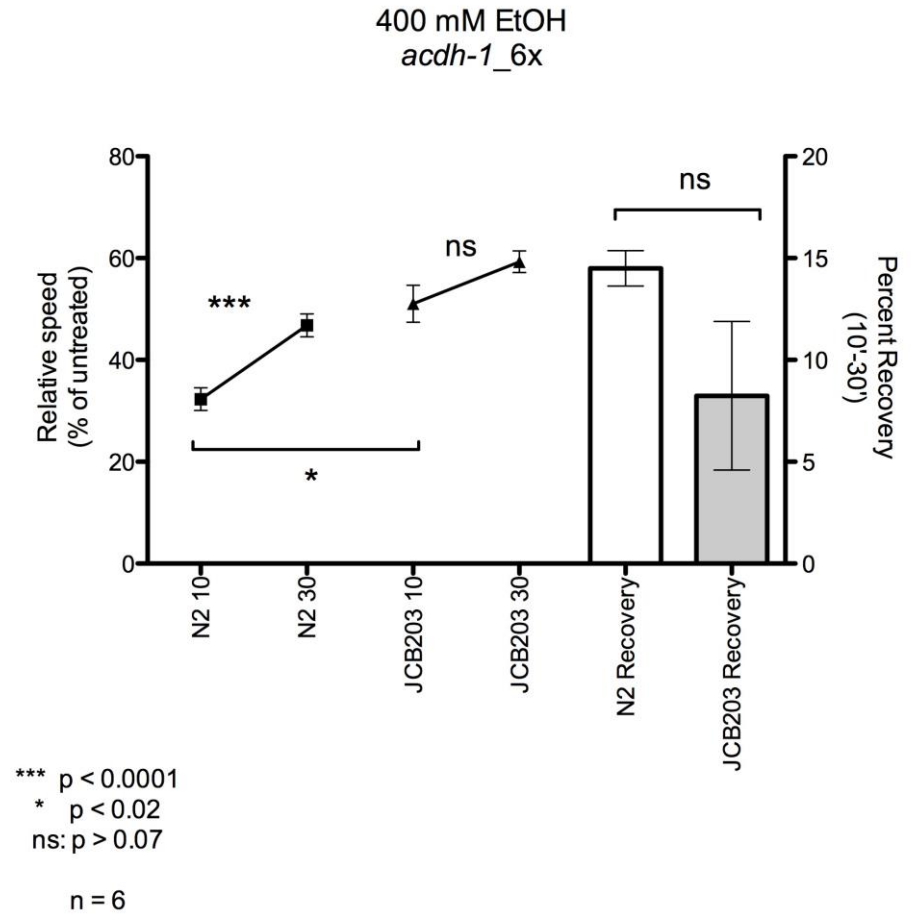

Figure 36. Ethanol sensitivity and acute functional tolerance (AFT) of 6x backcrossed *acdh-1* lf mutant. At 400mM exogenous ethanol these mutants displayed significantly decreased sensitivity compared to N2, but did not show any significant difference in terms of AFT development relative to N2 (n = 6).

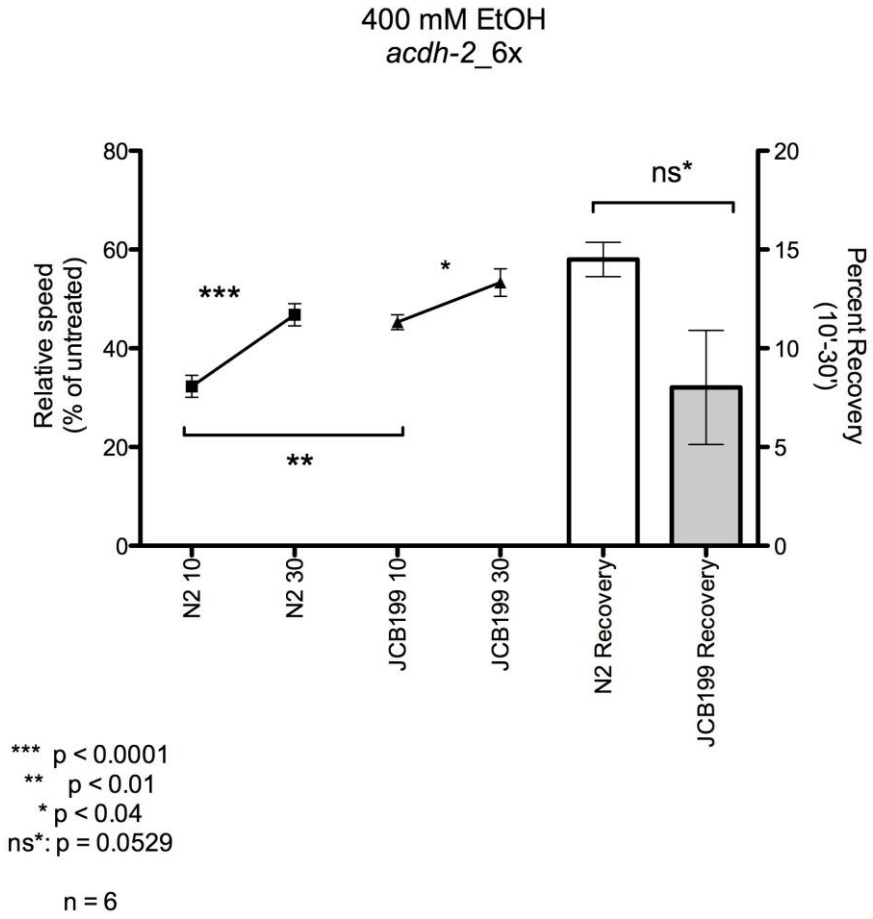

Figure 37. Ethanol sensitivity and acute functional tolerance (AFT) of 6x backcrossed *acdh-2* lf mutant. At 400mM exogenous ethanol these mutants displayed significantly decreased sensitivity compared to N2, but did not show any significant difference in terms of AFT development relative to N2 (n = 6).

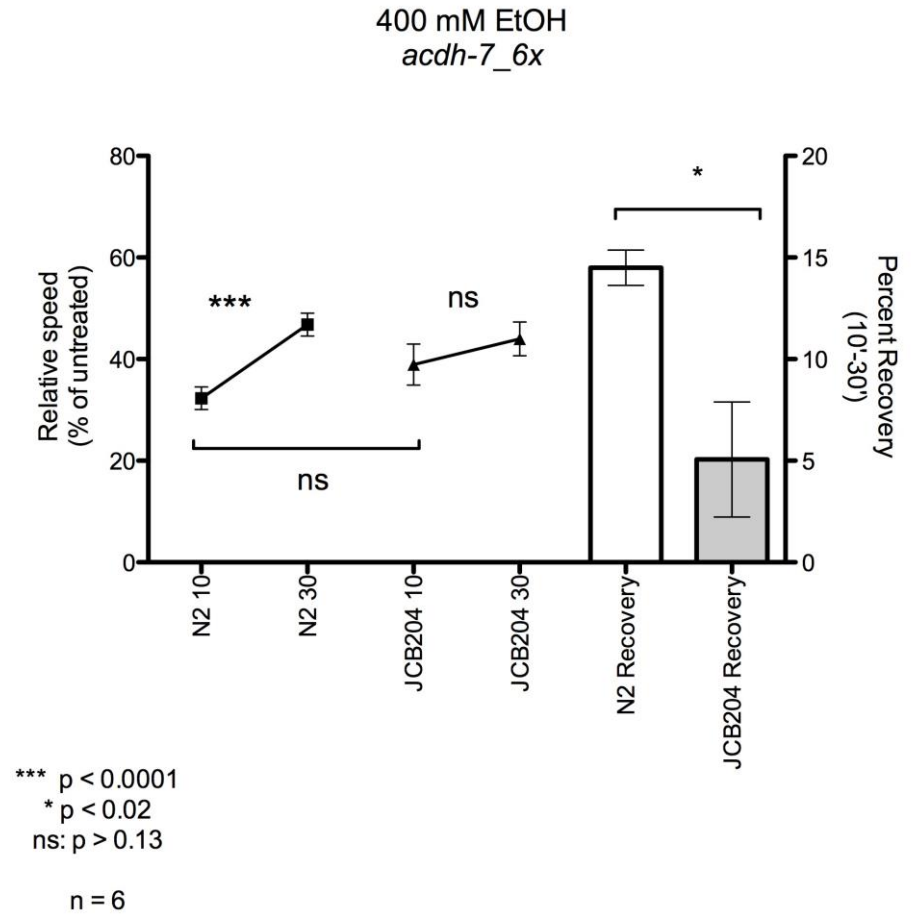

Figure 38. Ethanol sensitivity and acute functional tolerance (AFT) of 6x backcrossed *acdh-7* lf mutant. At 400mM exogenous ethanol these mutants did not show any significant difference in terms of initial sensitivity but displayed significantly reduced AFT development relative to N2 (n = 6).

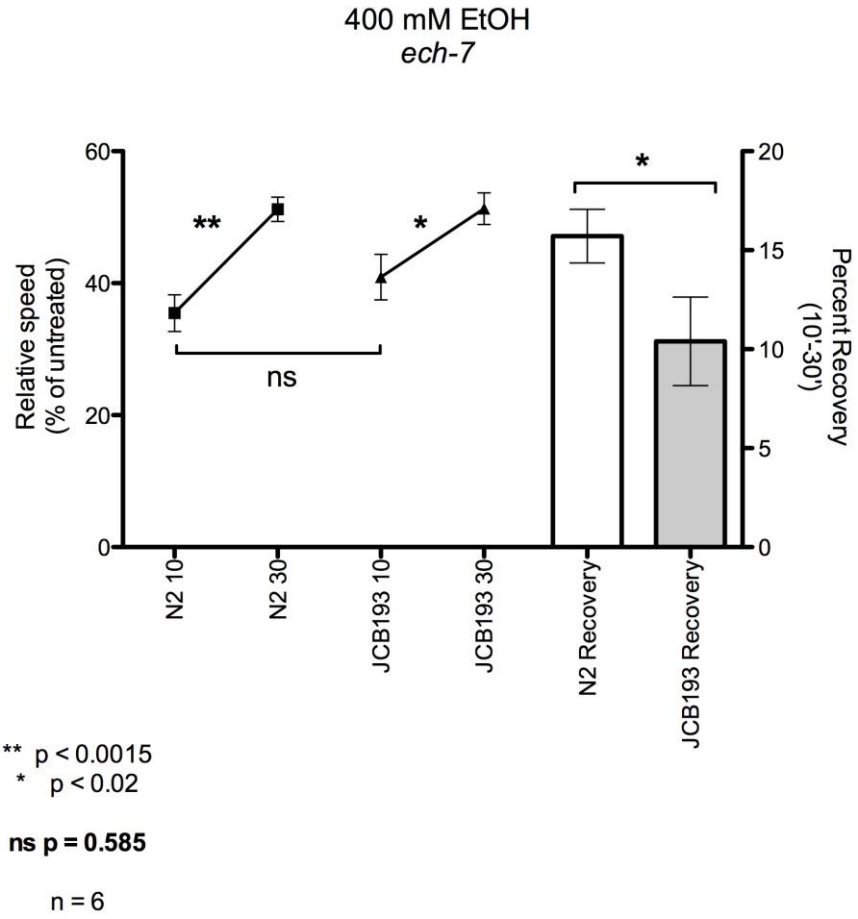

Figure 39. Ethanol sensitivity and acute functional tolerance (AFT) of 10x backcrossed *ech-7* lf mutant (without *paqr-2* deletion). At 400mM exogenous ethanol these mutants did not show any significant difference in terms of initial sensitivity but displayed significantly reduced AFT development relative to N2 (n = 6).

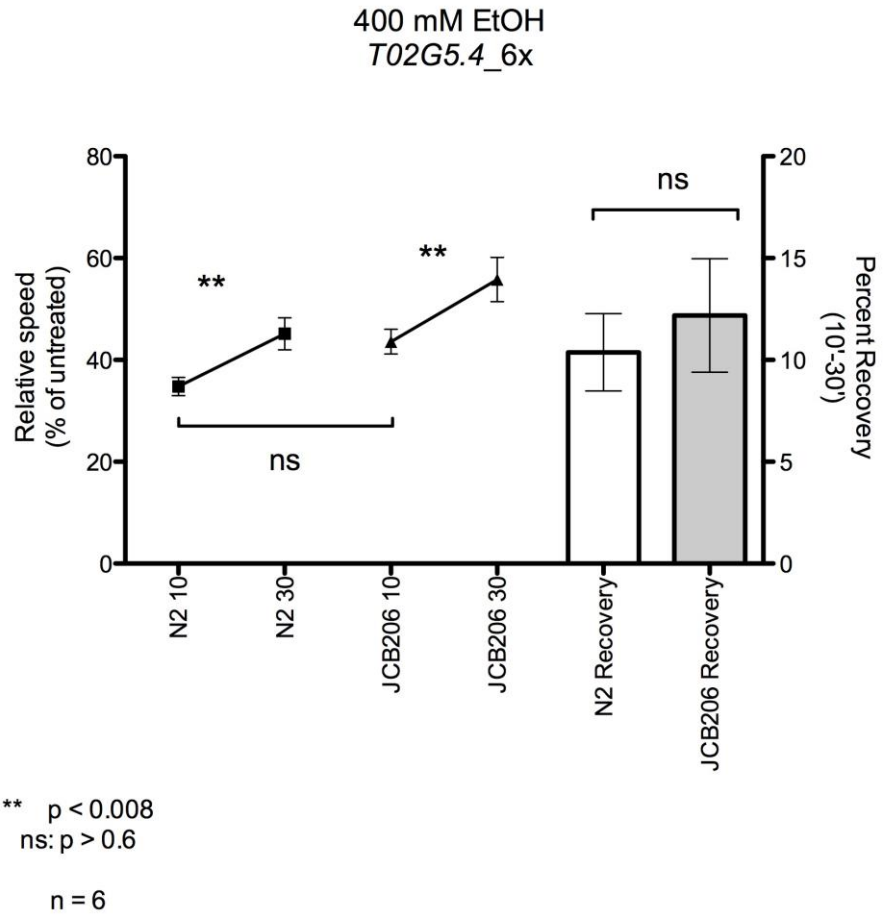

Figure 40. Ethanol sensitivity and acute functional tolerance (AFT) of 6x backcrossed *T02G5.4* lf mutant. At 400mM exogenous ethanol these mutants did not show any significant difference in terms of initial sensitivity or AFT development relative to N2 (n = 6).

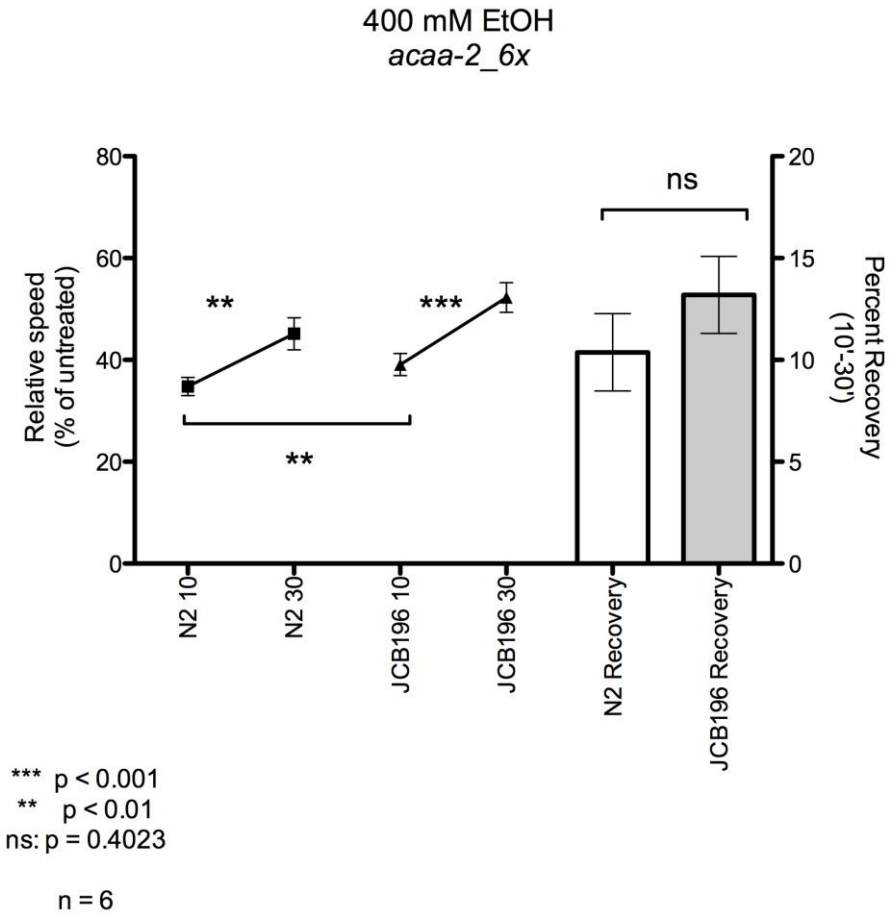

Figure 41. Ethanol sensitivity and acute functional tolerance (AFT) of 6x backcrossed *acaa-2* lf mutant. At 400mM exogenous ethanol these mutants had significantly decreased initial sensitivity compared to N2 but did not show any significant difference in terms of AFT development relative to N2 (n = 6).

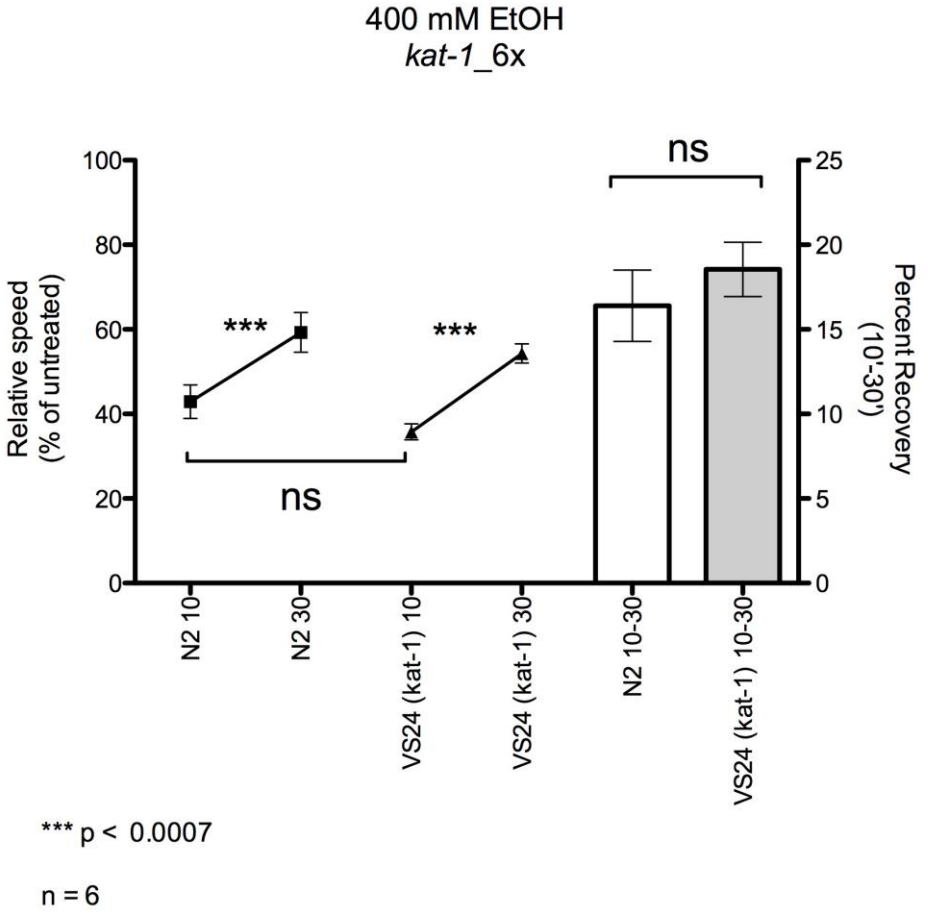

Figure 42. Ethanol sensitivity and acute functional tolerance (AFT) of 6x backcrossed *kat-1* lf mutant. At 400mM exogenous ethanol these mutants did not show any significant difference in terms of initial sensitivity or AFT development relative to N2 (n = 6).

3. Graphs of ethanol response phenotypes of RNAi-mediated knockdown of candidate genes in the mitochondrial beta-oxidation pathway

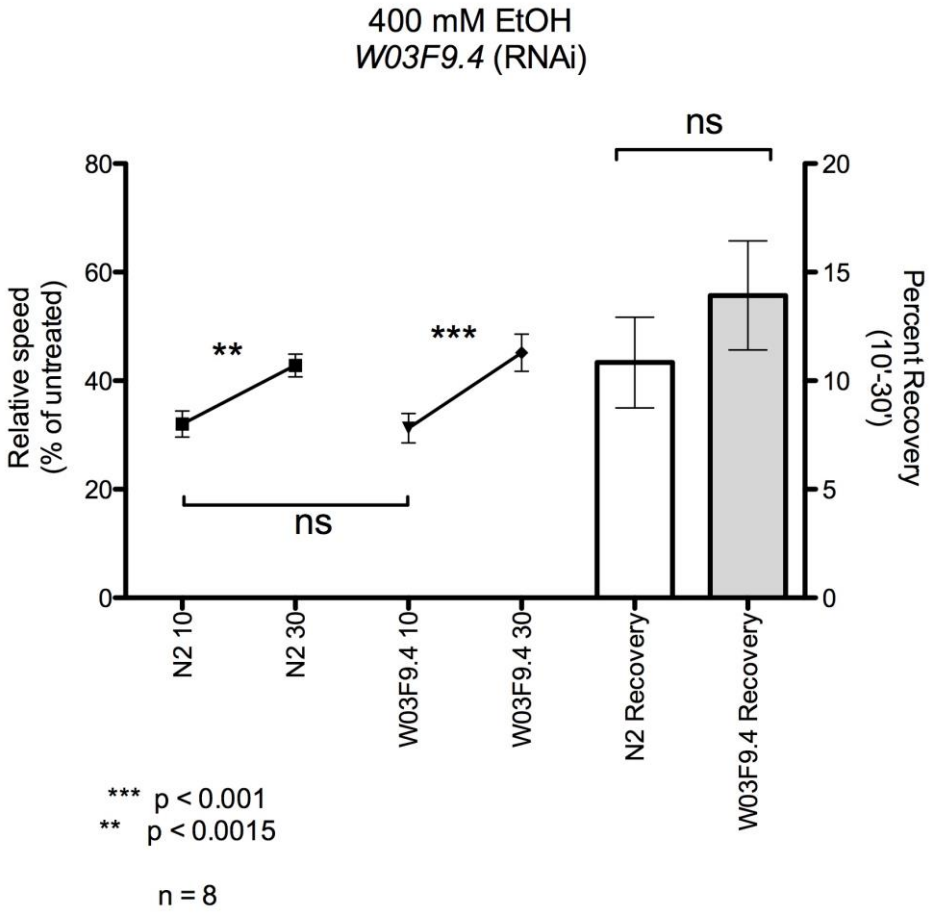

Figure 43. Ethanol sensitivity and acute functional tolerance (AFT) of *W03F9.4* RNAi knockdown of *C. elegans*. At 400mM exogenous ethanol these worms did not show any significant difference in terms of initial sensitivity or AFT development relative to L4440 (n = 8).

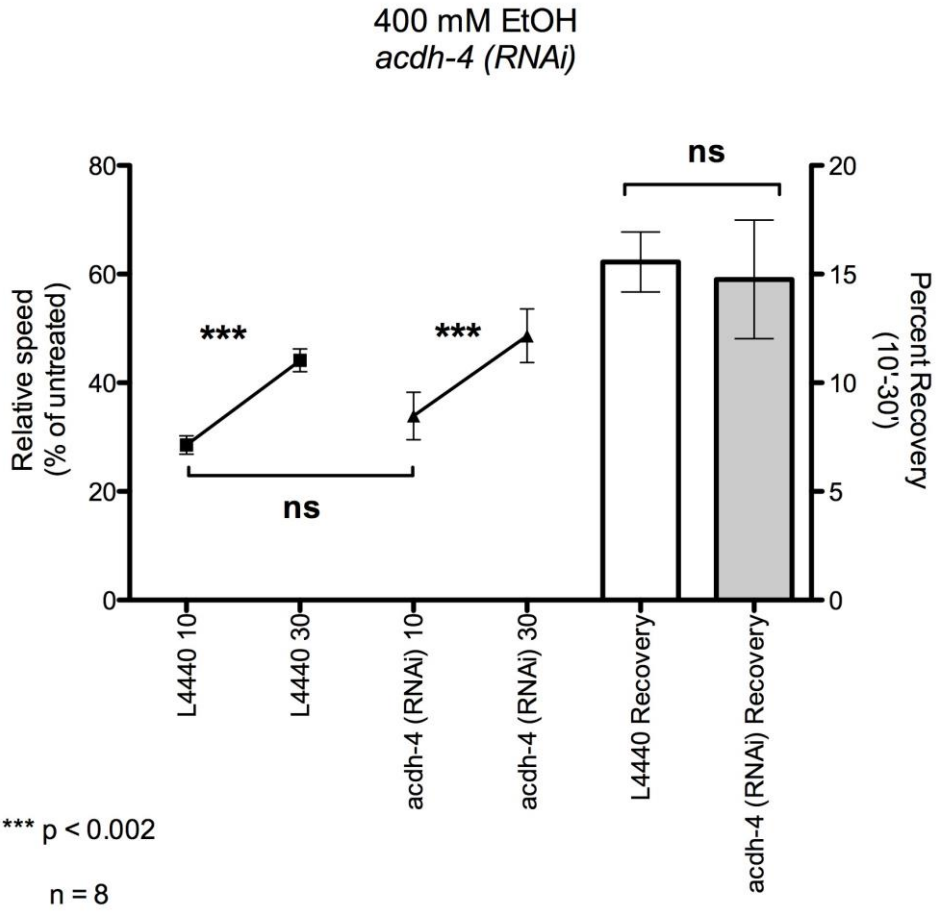

Figure 44. Ethanol sensitivity and acute functional tolerance (AFT) of *acdh-4* RNAi knockdown of *C. elegans*. At 400mM exogenous ethanol these worms did not show any significant difference in terms of initial sensitivity or AFT development relative to L4440 (n = 8).

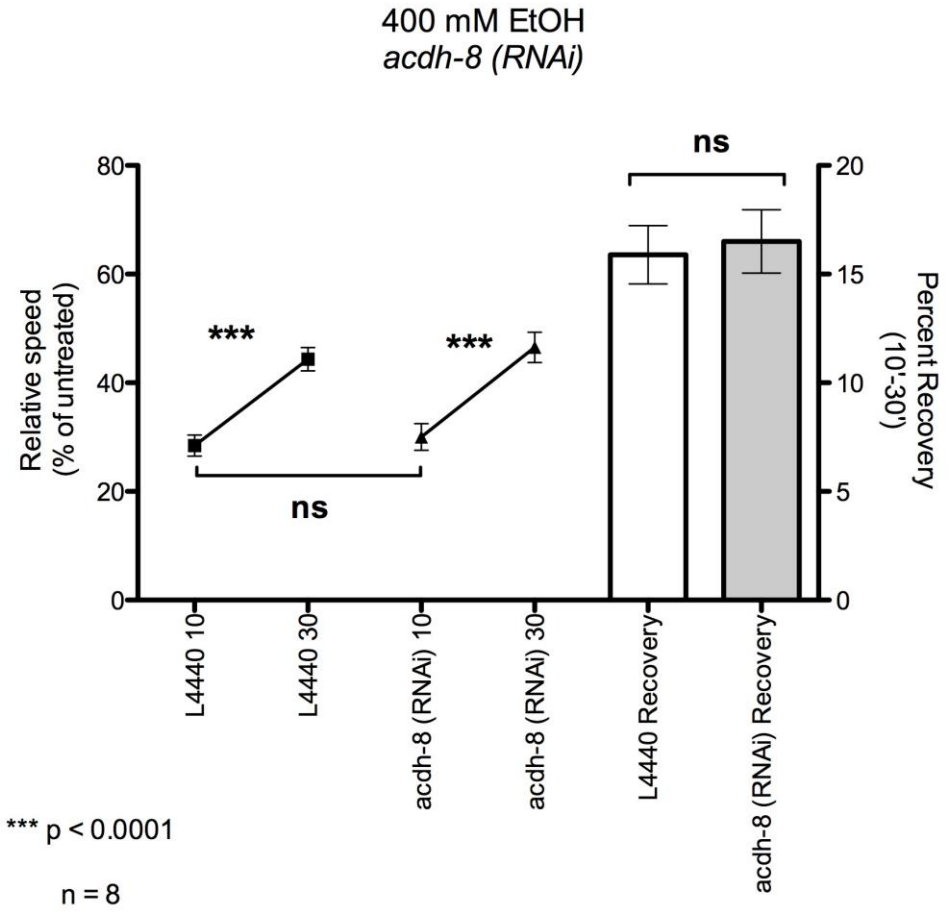

Figure 45. Ethanol sensitivity and acute functional tolerance (AFT) of *acdh-8* RNAi knockdown of *C. elegans*. At 400mM exogenous ethanol these worms did not show any significant difference in terms of initial sensitivity or AFT development relative to L4440 (n = 8).

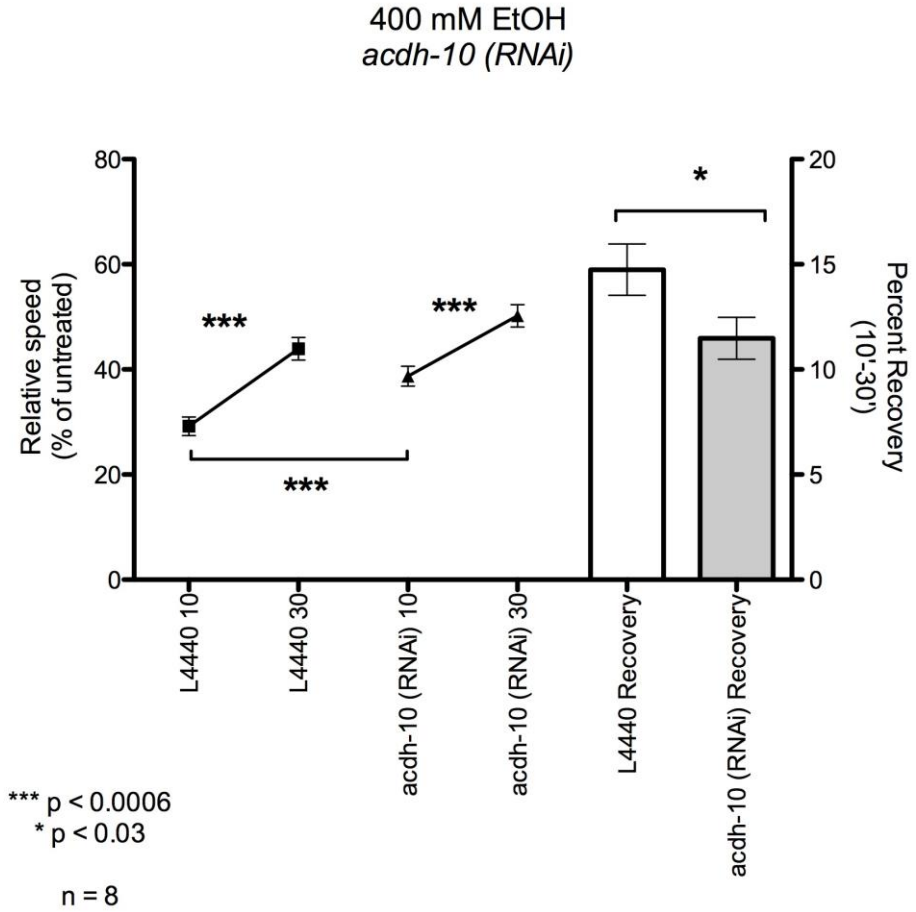

Figure 46. Ethanol sensitivity and acute functional tolerance (AFT) of *acdh-10* RNAi knockdown of *C. elegans*. At 400mM exogenous ethanol these worms showed a significantly decreased sensitivity to ethanol and reduced AFT development compared to L4440 (n = 8).

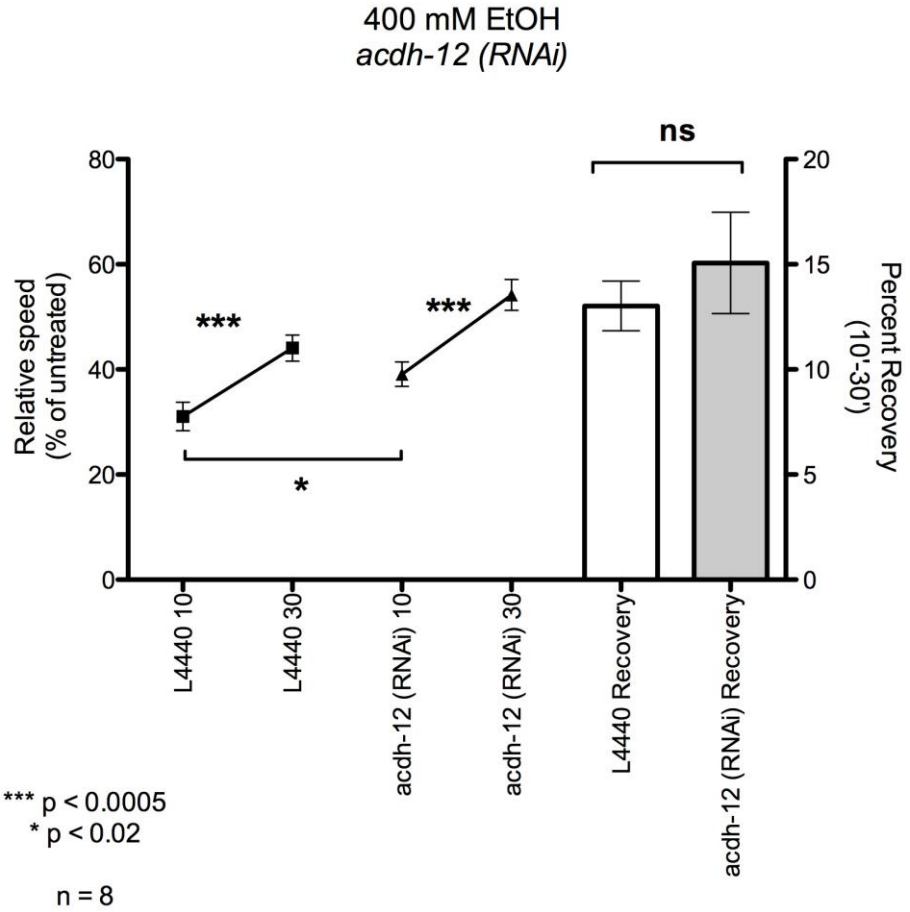

Figure 47. Ethanol sensitivity and acute functional tolerance (AFT) of *acdh-12* RNAi knockdown of *C. elegans*. At 400mM exogenous ethanol these worms showed a significantly decreased sensitivity to ethanol but no significant difference in development of AFT relative to L4440 (n = 8).

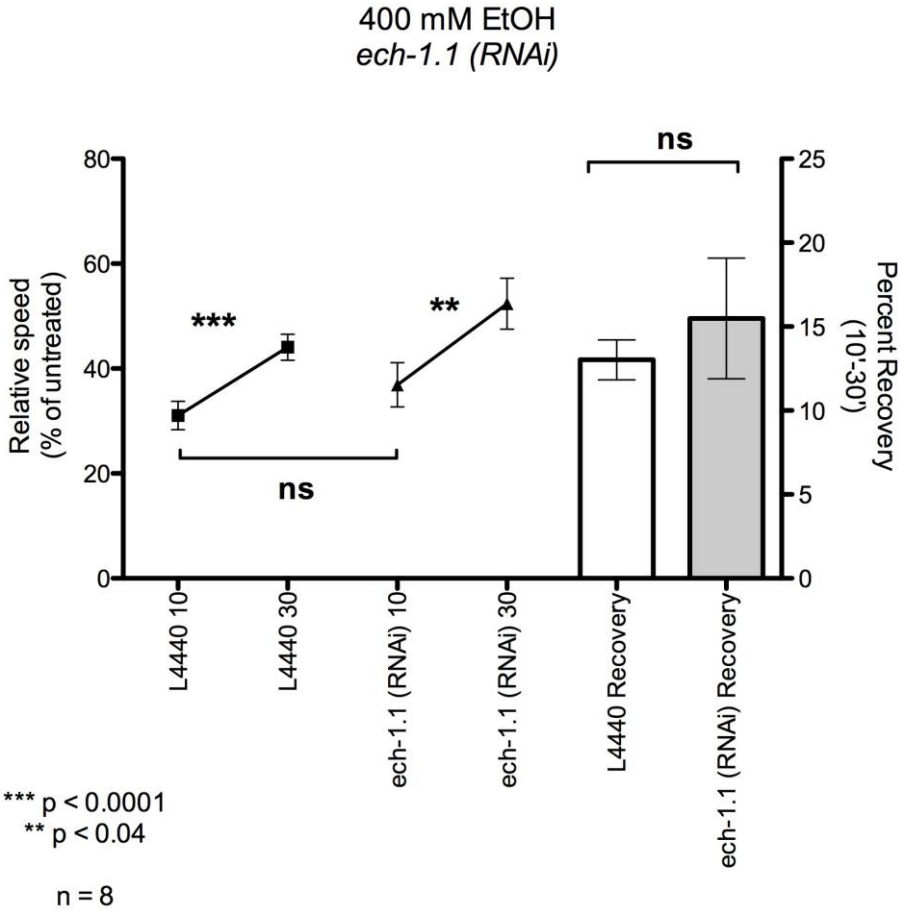

Figure 48. Ethanol sensitivity and acute functional tolerance (AFT) of *ech-1.1* RNAi knockdown of *C. elegans*. At 400mM exogenous ethanol these worms did not show any significant difference in terms of initial sensitivity or AFT development relative to L4440 (n = 8).

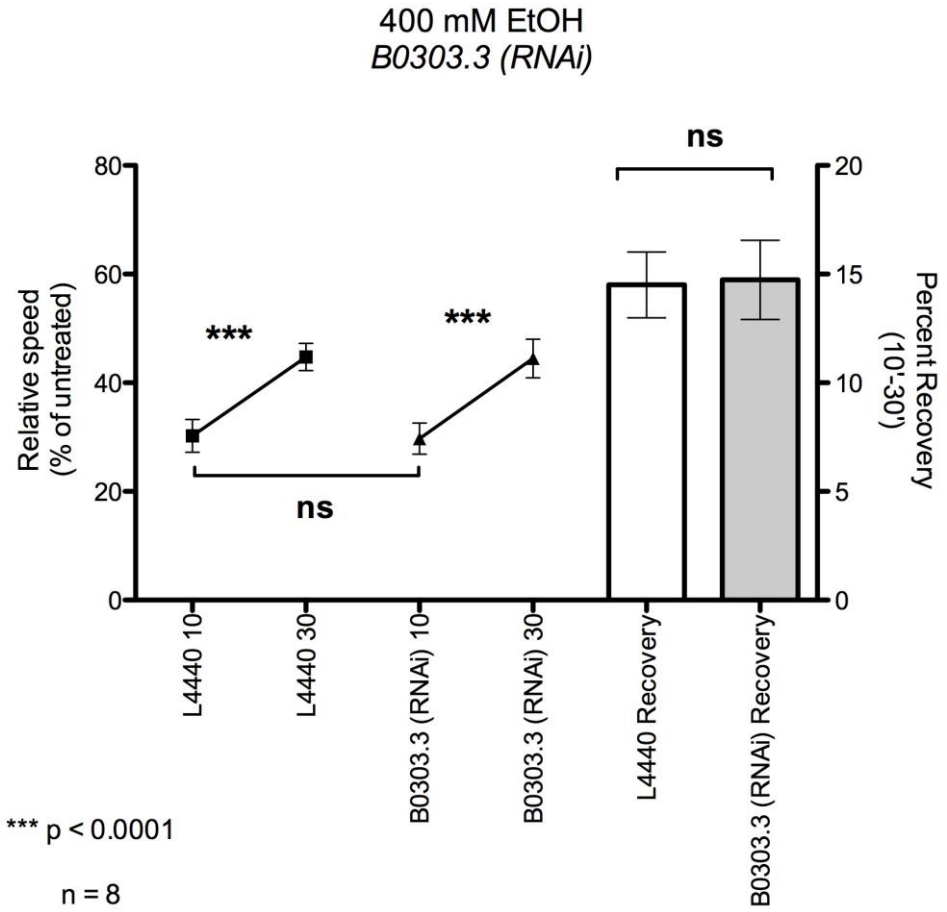

Figure 49. Ethanol sensitivity and acute functional tolerance (AFT) of *B0303.3* RNAi knockdown of *C. elegans*. At 400mM exogenous ethanol these worms did not show any significant difference in terms of initial sensitivity or AFT development relative to L4440 (n = 8).

Vita

Harini Pallikarana Tirumala was born on July 6, 1990 in Tamil Nadu, India. She graduated from Dr. SRK High School in 2005. She received her Bachelors degree in Genetic Engineering from SRM University, Chennai, India in 2011 and went on to do a Masters in the United Kingdom. She graduated with a Masters in DNA Profiling from the University of Central Lancashire, Lancashire, UK in 2012 and worked as a Geneticist at Xcode Life Sciences, Tamil Nadu, India for a year (2014-2015). She joined the Davies-Bettinger lab in August 2015.